CHARACTERIZATION OF THE GRAMILLIN VIRULENCE FACTOR FROM *FUSARIUM GRAMINEARUM* IN BARLEY (*HORDEUM VULGARE* L.)

MONIQUE POWER

Thesis submitted to the University of Ottawa
in partial fulfillment of the requirements for the
Master's degree in Biology

Department of Biology
Faculty of Science
University of Ottawa

© Monique Power, Ottawa, Canada, 2023

Abstract

Fusarium head blight is a devastating fungal disease of cereals caused by the pathogen *Fusarium graminearum* that leads to important economic losses due to diminished yields and grain downgrading. *F. graminearum* deploys several secondary metabolites known as virulence factors to facilitate its invasion of host tissues. These include the gramillins, a group of bicyclic lipopeptide ionophores that cause cell death and increased virulence in *Arabidopsis*, maize, and barley, but not wheat. Ionophores are involved in many plant-microbe interactions, but current knowledge of the molecular mechanisms governing host response to these molecules is limited. Susceptibility to gramillin varies among cultivars of affected species, but the basis for insensitivity has not yet been described, nor has the function of gramillin during infection. Here, we establish ion leakage as a method to survey Canadian barley for sensitivity, demonstrate that insensitivity to gramillin is likely mediated by a plant protease rather than inducible immune responses, and suggest a possible function of gramillin in positively regulating the expression of other fungal virulence factors during infection. This contributes to deepening our understanding of cyclic lipopeptide ionophores and their role during plant-microbe interactions.

Résumé

La fusariose de l'épi est une maladie fongique dévastatrice des céréales causée par le pathogène *Fusarium graminearum*, qui engendre d'importantes pertes économiques dues aux rendements réduits et la dévalorisation du grain. *F. graminearum* déploie plusieurs métabolites secondaires appelés facteurs de virulence pour faciliter son invasion des tissus de l'hôte. Ceci inclut les gramillines, un groupe de lipopeptides bicycliques ionophores qui causent la mort cellulaire et la virulence accrue dans l'*Arabidopsis*, le maïs, et l'orge mais pas le blé. Les ionophores sont impliqués dans plusieurs interactions plante-microbe, mais les connaissances présentes sur mécanismes moléculaires gouvernant la réponse de l'hôte à ces molécules demeure limitée. La susceptibilité à la gramilline varie entre les cultivars des espèces affectées, mais la base de cette insensibilité n'a pas encore été décrite, ni la fonction de la gramilline pendant l'infection. Ici, nous établissons la fuite d'ions comme méthode pour sonder l'orge canadienne pour la sensibilité, nous démontrons que l'insensibilité à la gramilline est vraisemblablement médiée par une protéase végétale plutôt que des réponses immunitaires induites, et nous suggérons une fonction possible de la gramilline en régulant positivement l'expression d'autres facteurs de virulence fongiques pendant l'infection. Ceci contribue à approfondir nos connaissances des lipopeptides cycliques ionophores et leur rôle dans les interactions plante-microbe.

Acknowledgements

I would like to thank Dr. Elizabeth Brauer for her constant guidance and support, as well as my committee members, Dr. Allyson MacLean and Dr. Tim Xing.

This project would not have been possible without the assistance of others at the ORDC. I wish to convey my appreciation to all the Brauer Lab technicians who supported my project – Whynn Bosnich, Mirko Tabori Ortiz, Kirsten Holy, Danielle Wolfe, and Arezo Pattang, as well as Julia Desbiens-St. Amand. A special thank you goes out to Moatter Syed, who completed the staining and microscopy for my callose assays. In particular, the greenhouse team at the ORDC deserves huge recognition for the watering and care of my experimental plants, especially Matt Linsdell, Dat Cotter-Buajitti, and Dan Casselman. I would not have completed this project without them. Further thanks to Linda Harris for developing the gramillin knock-out fungal strains used during this project, Kerin Hudson for showing me how to do a pathology assay, and Hannah Morrison and Matthew Davidson from the Khanal Lab for their help with the field trials. I am grateful Dr. Barbara Blackwell and members of the Blackwell lab, notably Indira Thapa for producing the gramillin used in all assays and for quantifying the gramillin in my apoplastic degradation assays, Sally Buffam for performing all DON quantification, and Denise Chabot for assistance with microscopy. I wish to thank all members of the Subramaniam Lab, particularly Chris Blackman and Margaret Balcerzak, for their support in experimental design and the loan of so many reagents.

I'm extremely grateful to my family for their unwavering support and encouragement throughout my entire academic career, and especially this degree. I'm also grateful for the moral support of the other students around me during this time, namely Pomona Osmers, Dominique Daniels, and especially Lochlen Farquharson – I could not have done this without you.

Table of Contents

List of tables

List of figures

List of abbreviations

ADON: Acetyldeoxynivalenol

BAK1: BRI1 associated receptor kinase

BIK1: Botrytis induced kinase 1

CBP: Calmodulin-binding protein

CDR1: Constitutive disease resistance 1

CEBiP: Chitin Elicitor Binding Protein

CERK: Chitin elicitor receptor kinase

CWDE: Cell wall degrading enzyme

DON: Deoxynivalenol

Dpi: Days post-inoculation

DPI: Diphenyleneiodonium

ETI: Effector triggered immunity

FGL: *Fusarium graminearum* lipase

Fgr: *Fusarium graminearum*

FHB: Fusarium head blight

GSL: Glucan synthase-like

Hpi: Hours post-inoculation

HR: Hypersensitive response

HSD: Honest significant difference

ICS: Isochorismate sythase

LOX: Lipoxygenase

LYK: Lysin motif receptor kinase

MAMP: Microbe-associated molecular pattern

MAPK: Mitogen-activated protein kinase

MAPKK: MAPK kinase

MAPKKK: MAPK kinase kinase

MLOC: Morex locus

MPK: Mitogen-activated protein kinase

MR: Moderately resistant

MTI: MAMP-triggered immunity

NADPH: Reduced nicotinamide adenine dinucleotide phosphate

NIV: Nivalenol

NLP: Necrotic and ethylene-inducing peptide-like protein 1

NLR: Nucleotide-binding leucine rich repeat

NPR: Non-expressor of pathogenesis-related genes

NRPS: Non-ribosomal peptide synthase

PAL: Phenylalanine ammonia lyase

PAMP: Pathogen-associated molecular pattern

PBL: PBS-like protein

PIP1: *Phytophthora*-inhibited protein 1

POX: Peroxidase

PR2A-2: Pathogenesis related

PRR: Pattern recognition receptor

PUB23: Plant U-Box 23

qPCR: Quantitative polymerase chain reaction

QTL : Quantitative trait locus

RBOHD: Respiratory burst oxidase homolog D

RLK: Receptor-like kinase

ROS: Reactive oxygen species

SA: Salicylic acid

SAR: Systemic acquired resistance

SARD: SAR deficient

SHAM: Salicylhydroxamic acid

TRI: Trichothecene biosynthetic gene

ZEA: Zearalenone

Introduction

Plant-microbe interactions

Plants and fungi have been intertwined since the evolution of terrestrial plants, over 400 million years ago (Selosse et al., 2015). The relationship between these two kingdoms can take many forms, from mutualism, to commensalism, to parasitism (Wu et al., 2009). These interactions are highly relevant to society due to their impact on food production. Beneficial symbiotic fungi, such as arbuscular mycorrhizal fungi, help plants acquire nutrients and water from the soil, increasing crop yields and offering protection from drought (Wu et al., 2022). While these microbes can preserve plants from abiotic stress, pathogenic ones are among the primary causes of biotic stress (Chaudhary et al., 2022). Indeed, fungal disease causes global losses of up to 23% of crop yields annually, spoiling enough food to sustain over 600 million people each year (Steinberg and Gurr, 2020; Stukenbrock and Gurr, 2023). Over the course of evolution, plants have developed complex defense mechanisms that allow them to be resistant to the majority of microbes (Panstruga and Moscou, 2020). Pathogens, however, can also evolve to overcome this resistance (Rimbaud et al., 2018). The field of plant-pathogen interactions has been studied for some time as researchers seek to understand the molecular basics of pathogenicity and immunity in plants as well as to develop more disease-resistant crop varieties (Andersen et al., 2018). Here, we seek to deepen our understanding of the function of gramillin, a recently described cyclic lipopeptide virulence factor from *Fusarium graminearum* (Bahadoor et al., 2018), as well as the basis of sensitivity to it in Canadian barley.

Plant immunity

Plants possess a two-tiered inducible immune system that allows them to defend themselves against pathogens (Hückelhoven and Seidl, 2016). The first layer is initiated in the cell membrane via pattern recognition receptors (PRRs) and is known as microbe-associated molecular pattern (MAMP)-triggered immunity (MTI), while the second is initiated in the cytosol via nucleotide-binding leucine-rich repeat containing receptors (NLRs) and is known as effector-triggered immunity (ETI) (Yuan et al., 2021). There is cross-talk between these two layers, and many of their downstream effects are convergent (Yuan et al., 2021). However, while MTI induces a small and transient activation of signaling responses, ETI induces a long and sustained signaling response which is frequently associated with programmed cell death and long-distance signaling (Cui et al., 2015). MTI is triggered by plant sensing of molecules that are highly conserved across microbial lineages and are typically an integral part of the microbes' physiology (Bigeard et al., 2015). For bacteria, these include flagellin, a component of flagella (Hajam et al., 2017); bacterial elongation factor EF-Tu, which is involved in protein translation (Harvey et al., 2019); and lipooligosaccharides, a component of the cell membrane (Shang-Guan et al., 2018). For fungi, these include chitin, a key component of the fungal cell wall, and chitosan, a derivative of chitin (Guo and Cheng, 2022). As a whole, these molecules are known as microbe-associated molecular patterns, or MAMPs.

MAMPs are detected upon their binding with pattern recognition receptors (PRRs) found in the plant plasma membrane (Jones and Dangl, 2006). For example, a conserved peptide of flagellin, flg22, binds to the FLS2 receptor in *Arabidopsis*, prompting its heterodimerization with the membrane-bound receptor-like kinase BAK1 (Bentham et al., 2020). BAK1 will activate and phosphorylate the receptor-like cytoplasmic kinase BIK1, which initiates downstream responses

(Bentham et al., 2020). In *Arabidopsis*, chitin binds to the AtLYK5 lysin motif receptor kinase homodimer, which then dimerizes with AtCERK1, whose kinase activity induces downstream responses (Cao et al., 2014). In some monocots, including rice and barley, the plasma membrane glycoprotein CEBiP is required to interact with CERK1 for chitin-induced signalling (Tanaka et al., 2010). The downstream signalling cascades induced by these MAMPs cause responses including calcium signalling, reactive oxygen species (ROS) production, mitogen-associated protein kinase (MAPK) phosphorylation, salicylic acid (SA) signaling, expression of defense related genes, defense compound production and callose deposition (Meng and Zhang, 2013). This MAMP-triggered immunity, or MTI, is the first layer of inducible immunity against pathogens (Jones and Dangl, 2006). MTI can be supported by the production of damage-associated molecular patterns (DAMPs), which are plant-derived compounds either released from the cytosol, membrane or wall of pathogen-damaged cells, or secreted by untouched cells in response to infection (Hou et al., 2019). The signalling pathways induced by these molecules overlap with and reinforce MTI (Hou et al., 2019).

The earliest events in MTI occur within seconds or minutes of PRR recognition of MAMPs and include calcium spiking, membrane depolarization, ROS production and MAPK signaling (Blume et al., 2000). Calcium spiking occurs due to the opening of calcium channels within the plasma membrane including cyclic gated nucleotide channels (CNGCs) and glutamate receptors (GLRs) (Köster et al., 2022) and is associated with membrane depolarization and fluxes of chloride and potassium ions (Jeworutzki et al., 2010). Calcium spiking differs between MAMPs and is particularly important to activate subsequent signaling steps in the immune response including MAPK signaling and ROS production (Ranf et al., 2011). Calcium spiking is sensed by several cytosolic proteins, including calmodulins, calcium-dependent protein kinases, and calcineurin B-

like proteins (CBLs) which interact with CBL-interacting protein kinases to phosphorylate signaling proteins (Ranf et al., 2014). Calcium spiking also helps to trigger an apoplastic ROS burst within minutes of PRR activation in conjunction with PRR-triggered phosphorylation of receptor-like cytosolic kinases (RLCK) including BIK1 and PBL1 (Rao et al., 2018). The RLCKs directly phosphorylate RBOHD, a NADPH oxidase that produces extracellular hydrogen peroxide (Yuan et al., 2021). Approximately half of the ROS burst is generated by cell wall peroxidases, though the mechanism of their activation during MTI remains unknown (O'Brien et al., 2012). ROS has several functions in defense and can directly inhibit pathogens by creating an environment that is toxic to them (Huang et al., 2011). They can also act to strengthen cell walls by oxidative cross-linking and inducing callose deposition (Jwa and Hwang, 2017). Finally, they can transduce the signal for further immune responses, such as differential gene expression in the nucleus, activating MAPKs through a feedback loop with calcium, hormonal signaling, or other pathways (Tripathy and Oelmüller, 2012). The MAPK signaling cascade occurs within minutes of PRR activation and involves sequential phosphorylation of protein kinases culminating in altered gene expression (Yamada et al., 2016). For example, during chitin-induced MAMP signalling in *Arabidopsis*, activated AtCERK1 phosphorylates its associated RLCK PBL27, which forms a membrane-bound complex with AtMKKK5 (MAP kinase kinase kinase) (Yamada et al., 2016). PBL27 phosphorylates AtMKKK5, which dissociates into the cytosol where it phosphorylates AtMKK4/5 (MAP kinase kinase), which activates AtMPK3/6 (MAP kinase) (Kawasaki et al., 2017). The MAPKs play a role in plant defense by interacting with many signalling pathways, including regulation of gene expression, cellular component re-compartmentalization, secondary metabolite biosynthesis, and further downstream signalling (Lassowskat et al., 2014; Lee et al., 2015).

The later events in MTI are characterized by signaling and defense responses which occur within an hour to days of PRR activation (Alhoraibi et al., 2019). These include transcriptional reprogramming, hormonal signaling, callose production and defensive compound production (Alhoraibi et al., 2019). In most pathosystems, it remains unclear exactly which combinations of these responses are required to generate resistance, but as a whole, they are essential to provide broad-spectrum basal resistance to microbes (Muthamilarasan and Prasad, 2013). Transcriptional reprogramming typically begins approximately 30 minutes after MAMP sensing and is primarily regulated by the MAPK and calcium-based signaling cascades (De Torres et al., 2003). The induced genes have functions related to ROS, ethylene, SA, DAMPs, and callose deposition. Many of these responses ensure stable positive feedback loops (Li et al., 2016). An important class of transcription factors activated by MPK3/MPK6 is the WRKY class transcription factors. WRKY33 has been well-studied and has roles in inducing the defense phytoalexin camalexin (Mao et al., 2011) and repressing ABA, a negative regulator of plant defense (Liu et al., 2015). These transcription factors are usually induced within one to six hours of MAMP sensing (Kalde et al., 2003). Within a similar time frame, SA is produced through the isochorismate pathway as a result of induction of biosynthetic genes including isochorismate synthase (ICS1) (Wildermuth et al., 2001; Shine et al., 2019). SA contributes to reinforcing the MTI response by upregulating genes encoding both MAMP receptors and their downstream components including callose production (Zhang and Li, 2019). Callose is a β-(1,3)-glucan polymer that is deposited below the cell wall to form papillae, appositions to the cell wall that reinforce it against fungal attack by slowing its spread and preventing hyphal entry (Voigt, 2014). The primary callose synthase responsible for its production is GSL5 (first described as PMR4) (Ellinger and Voigt, 2014). This member of the glucan synthase-like family is regulated by the SA receptor NPR1 (non-expressor of pathogenesis-

related genes 1) and is strongly upregulated in the presence of SA (Ellinger and Voigt, 2014). Callose is also deposited at the neck of plasmodesmata, where it can narrow or close these channels to prevent intercellular movement of pathogens (Wang et al., 2021). These are considered a late MTI response, as they typically occur several hours after MAMP elicitation (Ellinger and Voigt, 2014).

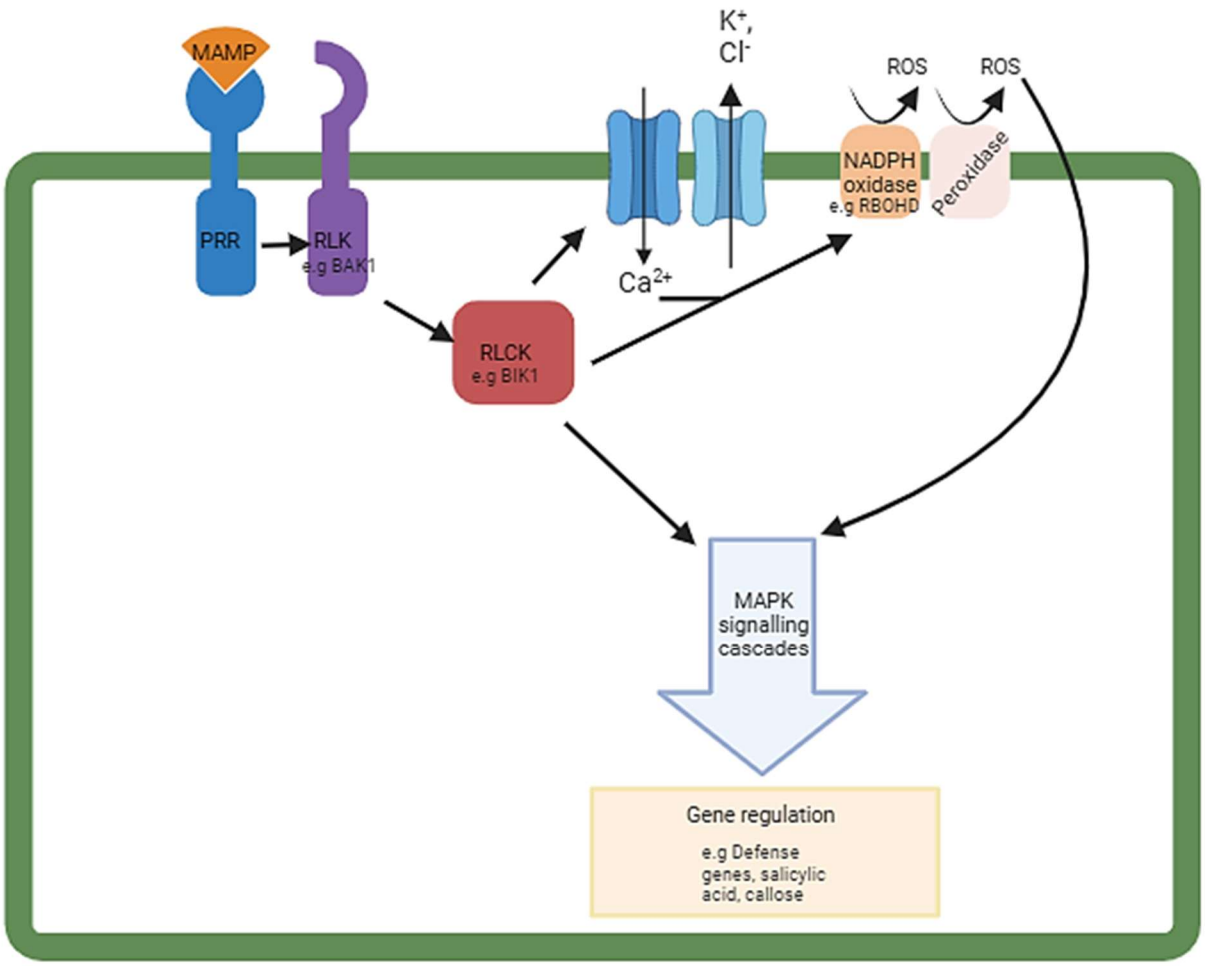

Figure 1: Simplified model of inducible immune responses during MTI. Microbe-associated molecular patterns (MAMPs) are sensed by pattern recognition receptors (PRRs). These interact with receptor-like kinases (RLKs) and receptor-like cytoplasmic kinases (RLCKs) to activate inducible immunity. This includes calcium (Ca^{2+}) spiking and ion fluxes (K^+, Cl^-) leading to membrane depolarisation. Together with signalling from the RLCKs, these activate production or reactive oxygen species (ROS) from nicotinamide adenine dinucleotide phosphate (NADPH)

oxidases and cell wall peroxidases. This leads to downstream activation of mitogen-activated protein kinase (MAPK) signalling cascades, which eventually cause differential gene regulation, inducing later immune responses such as transcription of defense-associated genes, salicylic acid and other hormonal signalling, and callose deposition. *Figure produced with Biorender.com.*

While our understanding of MTI is mostly derived from studies on *Arabidopsis*, the same temporal induction of similar signaling pathways has been observed in cereals (Hückelhoven and Seidl, 2016). There is increasing evidence that members of the *Triticeae* tribe possess most described basal immune responses. Barley has been shown to have similar chitin-sensing PRRs to rice, as HvCEBiP has been characterized and shown as necessary for immunity to *Magnaporthe oryzae* (Tanaka et al., 2010). This is homologous to OsCEBiP, whose interaction with OsCERK1 is required for chitin-induced MTI signalling (Yamaguchi et al., 2013). Calcium spiking after infection has been described in barley (Felle et al., 2004), though little is known about the transporters or the fluxes of other ions (Hao et al., 2022). Interestingly, chitin can induce a ROS burst in barley leaves, but this response is not detectable in wheat (Hao et al., 2022). From the barley genome, 20 HvMAPKs, 6 HvMAPKKs, and 156 HvMAPKKKs have been identified, but few have been functionally characterized (Cui et al., 2019). The barley MAPK PWMK1 seems to be involved in general stress response, while HvMPK4 negatively regulates SA after infection (Eckey et al., 2004; Abass and Morris, 2013). In general, barley MAPKs have been shown to be activated within five minutes of chitin or flg22 elicitation (Scheler et al., 2016). GeneChip assays have shown that infection of barley with *Fusarium graminearum* leads to defense gene induction including pathogenesis related proteins, ROS enzymes, and phenylpropanoid pathway enzymes (Boddu et al., 2006). However, many of the particular mechanisms and genes involved in these facets of MTI still need to be elucidated in barley and other cereals, as homologous proteins to *Arabidopsis* do not always share their described immune function (Hückelhoven and Seidl, 2016).

In addition to localized immune responses, microbe-derived molecules can also trigger increased resistance in distal tissues. This can be induced by both pathogenic and non-pathogenic microbes and can be due to host sensing of molecules including cyclic lipopeptides (Nadarajah, 2016). First isolated over 60 years ago from bacteria in the *Bacillus* genus (Jacques, 2011), cyclic lipopeptides (CLPs) are metabolites characterized by short peptide chains that form lactone or lactam rings, and are linked to fatty acids (Raaijmakers et al., 2006). They are produced by non-ribosomal peptide synthetases (Jacques, 2011). CLPs have a wide range of structures, as there is variability in the number, type and configuration of the amino acids forming the oligopeptide, as well as length and composition of the fatty acid tail (Schneider et al., 2014). They are produced by microbes such as bacteria, cyanobacteria, eubacteria, and fungi (Schneider et al., 2014). These molecules act as surfactants and have a variety of roles in microbial survival including promoting biofilm formation, motility, virulence factors during pathogenesis, and antimicrobial activity (Raaijmakers et al., 2006). Several cyclic lipopeptides, including those in the surfactin and iturin families, have ionophore activity (Thimon et al., 1993; Maget-Dana and Peypoux, 1994). Ionophores are molecules that typically have a hydrophilic ion-binding site, while the exterior of the compound is hydrophobic (Freedman, 2012). Carrier ionophores selectively bind to an ion and directly facilitate its passage across lipid membranes, while channel-forming ionophores create pores in membranes through which ions can pass (Freedman, 2012).

CLP production contributes to the ability of some beneficial bacteria to enhance host resistance by triggering induced systemic resistance (ISR) (Omoboye et al., 2019). Once the plant senses beneficial bacteria, jasmonic acid and ethylene signalling lead to priming of distal tissues, where they are able to respond more quickly and strongly to pathogen invasion (Pieterse et al., 2014). Changes during ISR include up-regulation of defense genes, callose deposition, and

stomatal closure (Pieterse et al., 2014). One of the better characterized CLPs is the ionophore surfactin. Elicitation by surfactin induces a calcium influx and potassium efflux in tobacco cells (Jourdan et al., 2009). The resulting K^+/H^+ exchange across the membrane leads to extracellular alkalinization, while calcium influx leads to an oxidative burst. Downstream effects of surfactin elicitation include upregulation of phenylalanine ammonia lyase (PAL) and lipoxygenase (LOX) (Jourdan et al., 2009). The PAL enzyme is the entry point to the phenylpropanoid pathway, which is necessary for the production of lignin, flavonoids, and coumarin (Fraser and Chapple, 2011). LOX catalyzes the addition on oxygen into polyunsaturated acids to form fatty acid hydroperoxides that are converted into oxylipins, which are involved in defense and include the important phytohormone jasmonic acid (Vellosillo et al., 2013). Different CLPs have different abilities to induce resistance, and the plants' response may vary between species (Jourdan et al., 2009).

Recently, a mechanism for CLP-induced ISR has been elucidated, as Pršić et al. (2023) demonstrated that surfactin can bind to sphingolipid-rich domains in the *Arabidopsis* plasma membrane, which causes deformations and tension. This affects the gating of ion channels, allowing their influx into the cell and provoking downstream immune responses, though the signalling events between initial sensing and induced immunity remain elusive. The diverse structure of different CLPs may individualize their interaction with the membranes of various hosts, which would explain why, while many CLPs induce beneficial immunity, some act as virulence factors – a phenomenon that is as yet not well described (Girard et al., 2020; Pršić et al., 2023).

Plant defense against *Fusarium graminearum*

The *Fusarium* genus contains at least 300 species of filamentous ascomycete fungi (Sordariomycetes: Hypocreales: Nectriaceae) that are found all over the world (Ma et al., 2013; Summerell, 2019). There are many non-pathogenic species found in the genus, and some are opportunistic pathogens of humans, but it is most known for containing several species that cause devastating disease in agricultural crops (Leslie and Summerell, 2013). These include vascular wilts, head blights, canker diseases, and stem, root, and crown rots (Leslie and Summerell, 2013). *Fusarium* species also produce a vast array of secondary metabolites that enhance their growth and reproduction under certain circumstances, several of which are toxic to plants, humans, and animals (Nishiuchi, 2013). These are known as mycotoxins.

One particular disease of concern is Fusarium head blight (FHB), also known as scab (McMullen et al., 1997). This disease affects maize and small-grain cereal crops including wheat, barley, and oats (Valverde-Bogantes et al., 2019). It is characterized by bleaching and early senescence in the head, where spike and peduncle tissues turn brown prematurely (Osborne and Stein, 2007). It results in shriveled and discoloured grains known as “tombstone” kernels which are unsuitable for uses in milling or malting (Wegulo et al., 2015). This disease causes yield losses, but more critically, leads to deposition of toxins detrimental to human health in the grain including deoxynivalenol (DON), zearalenone (ZEA), fumonisins, and HT-2/T-2 toxin (Karlsson et al., 2021), the first two of which whose levels in grain destined for consumption by humans or animals are tightly regulated in Canada and internationally (European Commission, 2006; Charmley and Treholm, 2017). The presence of toxins is also detrimental in grain destined for malt, not only due to the risk of toxicity, but also because DON contamination in beer severely reduces quality by causing “gushing”, or excessive foaming upon opening (Piacentini et al., 2015). Between yield

loss and grain downgrading, epidemics of this disease can cause economic losses of over 1 billion dollars in the United States alone (McMullen et al., 2012).

FHB can be caused by many species from the *Fusarium* genus, including *F. culmorum*, *F. avenaceum*, and *F. poae*, but the most globally important is *F. graminearum* (Karlsson et al., 2021). *F. graminearum* Schwabe (teleomorph *Gibberella zeae* (Schwein.) Petch) is able to live saprophytically in soil and on plant residues (Leplat et al., 2013). Unlike some other species in the *Fusarium* genus, *F. graminearum* (*Fgr*) is homothallic and can reproduce sexually (Valverde-Bogantes et al., 2019). It will overwinter on plant residues, and when more suitable environmental conditions arrive, the fungus discharges ascospores from perithecia (Wegulo et al., 2015) which are carried by wind over extensive distances (Schmale et al., 2006). It infects cereals most often at anthesis due to abundant nutrients and possibly stimulators of fugal growth in floral structures (Osborne and Stein, 2007), but infection can occur until the soft dough stage (Windels, 2000).

Fgr has been described as a hemibiotrophic pathogen – which have a short biotrophic stage where the hyphae progress asymptomatically through the plant, before switching to a necrotrophic lifestyle and causing cell death (Perfect and Green, 2001). *Fgr* has been said to be simultaneously a biotroph at the infection front and a necrotroph at the infection centre (Brown et al., 2010). In wheat, it enters through the spikelet and then moves through the rachis node into the rachis towards the rest of the spike (Dweba et al., 2017). In barley, spread within the rachis is more limited, and it tends to move over the surface of the head toward other spikelets (Bai and Shaner, 2004). Resistance to FHB in cereal has been classified into various types. Type I and Type II resistance, first described by Schroeder and Christensen, denote resistance to initial entry of the pathogen into plant tissues, and resistance to spread within the plant, respectively (Schroeder and Christensen, 1963). Barley naturally has strong Type II resistance while the partial resistance bred into wheat

primarily enhances type II resistance (Langevin et al., 2004; Hales et al., 2020). In addition to these forms of resistance, Mesterházy (1995) describes a Type III resistance which prevents damage to the kernels themselves while Type IV maintains overall yield. Type V resistance involves the degradation of mycotoxins or the prevention of their deposition within tissues (Mesterházy, 1995). Together, the scientific community has attempted to capture as much FHB resistance as possible through breeding but wheat, maize and barley remain only partially resistant at best (Chamarthi et al., 2014). In addition, the mechanisms underlying the observed quantitative resistance are only partially understood (Buerstmayr et al., 2021). They include the currently uncharacterized major quantitative trait loci (QTLs) *Fhb1* and *Qfhs.ifa-5A*, flowering traits including shape and cleistogamy, mycotoxin detoxification, and MAMP and DAMP signalling (Kluger et al., 2015; Buerstmayr et al., 2021; Manes et al., 2021).

F. graminearum infection strategies

Pathogens have co-evolved with plants over millions of years to overcome the basal immune system and constitutive defenses (Anderson et al., 2010). The molecules that pathogens produce during infection to specifically overcome host defenses and resistance are called virulence factors and can include proteinaceous effectors, small metabolite toxins or cell wall modifying enzymes (Cross, 2008; Zhang et al., 2022). Over time, some plant species are able to recognize virulence factors to evade their negative effects on defense and develop resistance. For example, effector proteins derived from biotrophic and hemibiotrophic pathogens can be sensed through nucleotide-binding leucine-rich repeat proteins (NLRs) to elicit effector-triggered immunity, or ETI, which typically results in hypersensitive response and long-distance signalling (Boller and He, 2009; Cui et al., 2015). ETI frequently leads to complete (qualitative) resistance, whereas resistance to *F. graminearum* is quantitative, suggesting ETI may not be implicated in this

interaction. *F. graminearum* produces and secretes enzymes and a suite of structurally unusual small metabolites to overcome plant defense and promote infection (Sieber et al., 2014). The most important and most well-researched virulence factors from *Fgr* are the trichothecenes due to their negative impact on grain quality (Foroud et al., 2019). These molecules are heterocyclic sesquiterpenoid secondary metabolites and the B-type trichothecenes have been shown to be virulence factors in wheat (Hao et al., 2023a). *Fgr* species can be distinguished by chemotypes depending on which B-type trichothecene they produce: nivalenol (NIV), 3-acetyldeoxynivalenol (3-ADON), and 15-acetyldeoxynivalenol (15-ADON) (Chen et al., 2019). The latter two are deacetylated by fungal or plant esterases, yielding deoxynivalenol (DON) (Alexander et al., 2011). Fifteen *TRI* genes spread across three loci are involved in DON biosynthesis (Alexander et al., 2009). *TRI5*, *TRI6*, and *TRI10* have been shown to be required for full pathogenicity of *Fgr* (Xu et al., 2022a). TRI6 and TRI10 are both transcription factors; TRI10 is specific to the *TRI* cluster while TRI6 is a global regulator (Seong et al., 2009). The *TRI5* gene encodes trichodiene synthase, the first step in the DON biosynthesis pathway (Chen et al., 2019). *TRI5* expression is required for *Fgr* infection to progress beyond the initially inoculated spikelet in wheat; that is, the hyphae cannot pass through the rachis node into the rest of the spike without DON (Maier et al., 2006). However, trichothecene-disrupted strains were found to have intact virulence in barley, which is consistent with its strong Type II resistance, as the DON-producing strains were also inhibited at the rachis node (Maier et al., 2006). In addition to DON, the *FGL1* gene encodes a secreted lipase virulence factor (Voigt et al., 2005). *FGL1* is upregulated in the presence of lipids such as free fatty acids and diacetyleglycerol, and is induced within 24 hours of infecting a host plant (Voigt et al., 2005). Its activity creates the free fatty acids linoleic and α-linoleic acid, which inhibit the synthesis of callose (Blümke et al., 2014). This prevents cell wall thickening in the phloem of the spikelet,

and allows hyphae to travel from cell to cell (Blümke et al., 2014). Without *FGL1*, *Fgr* cannot spread into the wheat spike beyond the spikelet into which it is inoculated (Voigt et al., 2005).

Cell-to-cell movement is also impacted by fusaoctaxin A and B, which are two recently characterized non-ribosomal octapeptides that act as virulence factors for *Fgr* in wheat (Jia et al., 2019; Tang et al., 2021). They are linear peptides composed of eight amino acid residues synthesized by two non-ribosomal peptide synthases (NRPS), NRPS5 and NRPS9 (Jia et al., 2019). Fusaoctaxin synthesis begins in NRPS9 and the remaining amino acids are sequentially added by NRPS5. Invasion of wheat requires fusaoctaxins in a dose-dependent manner. These molecules suppress the formation of cell wall depositions and plasmodesmata closure, allowing the hyphae to travel between cells. The mode of action for this function remains unclear (Jia et al., 2019). Though they are similar, plant cell response differs between the two, as fusaoctaxin A treatment depolarizes chloroplast distribution to a greater extent than fusaoctaxin B (Tang et al., 2021).

The importance of the cell wall structure for plant resistance to *Fgr* is further indicated by the role of the cell wall degrading enzymes (CWDE) in promoting virulence in wheat and *Arabidopsis* (Ferrari et al., 2012; Tundo et al., 2016). Other virulence factors include orphan protein OSP24, which mediates proteasomal degradation of TaSnRK1α (Jiang et al., 2020); FgNahG, a salicylate hydroxylase that metabolises host SA (Qi et al., 2019); Fg12, a ribonuclease that degrades RNA and promotes host cell death (Yang et al., 2021); FgNls1, an effector that interacts with a wheat histone to promote virulence (Hao et al., 2023b); extracellular protein Fg62 (Wang et al., 2023); Fg02685, a small secreted protein upregulated during infection that causes cell death and triggers plant basal immunity (Xu et al., 2022b); and gramillin A and B, two non-

ribosomal peptides (NRP) which are toxic and promote virulence in maize but not in wheat (Bahadoor et al., 2018).

The gramillins are bicyclic lipopeptides comprised of seven amino acids (Bahadoor et al., 2018). They are encoded by the *GRA1* biosynthetic gene found within the *NRPS8* gene cluster, which is upregulated in low-nutrient conditions. This cluster is co-expressed alongside the *TRI* gene cluster involved in DON biosynthesis, but neither Δ*gra1* nor Δ*tri* mutants were impaired in production of DON or gramillin, respectively, meaning the fungus can deploy these secondary metabolites individually. It is not however possible to separate these two forms of gramillin, as gramillin B differs from A by the addition of a sole -CH_2 group (Bahadoor et al., 2018), and therefore a mixture of the two forms is referred to simply as gramillin.

Purified gramillin causes cell death in maize leaves but not in wheat, indicating that gramillin sensitivity differs across the grasses (Bahadoor et al., 2018). Recent work indicates that gramillin is only toxic in plant species and that barley and all tested dicots are gramillin-sensitive species (Brauer et al., 2023). Tissue collapse in the context of pathogenesis can be due to uncontrolled cell death (necrosis) or programmed cell death (hypersensitive response, induced by ETI) (Van Doorn et al., 2011). In gramillin's case, the damage conforms to necrosis, as the plasma membrane shrinks rapidly within an hour of gramillin exposure, indicating that gramillin does not activate the ETI pathways (Brauer et al., 2023). Furthermore, inhibition of active cell metabolism such as ROS production, photosynthesis, and translation did not affect gramillin-induced cell death, indicating that phytotoxicity does not depend on host cell metabolism. Aside from necrosis, purified gramillin triggers immune responses in maize and *Arabidopsis* including a calcium burst, ROS production, MAPK phosphorylation, defense gene induction, and callose deposition (Brauer et al., 2023).

To assess gramillin's purpose during *Fgr* infection, knock-out strains have been generated. The *GRA1* gene was disrupted by *Agrobacterium*-mediated insertion of a hygromycin resistance gene to create a *Δgra1-1* strain that produced no gramillin (Bahadoor et al., 2018). A transformation control (TC) strain was also generated by ectopic insertion. The disruption mutant is not affected in its capacity to reproduce or to form infection structures like infection cushions. However, virulence is reduced in *Δgra1-1 F. graminearum* during infection of maize silks, barley spikelets, and *Arabidopsis* seedlings (Bahadoor et al., 2018; Brauer et al., 2023). In contrast, the virulence of *Δgra1-1* is intact in wheat (Bahadoor et al., 2018). The quantity of gramillin released by *Fgr* during infection is not currently known (Brauer et al., 2023). While the virulence function of gramillin in plants remains unclear, electrophysiology experiments indicate that they are ionophores in gramillin-sensitive plant species, creating pores in cell membranes through which ions and cellular contents can leak into the apoplast. This direct interaction with the membrane causes depolarization in sensitive plants, but is not observed in wheat, suggesting cellular pores are not formed (Brauer et al., 2023). However, the gramillin molecules are unstable and will linearize in conditions such as a high pH (Bahadoor et al., 2018). The toxicity of gramillin depends on its structure, as linearized, denatured, or reduced forms cause significantly less necrosis (Brauer et al., 2023). Whether gramillin contributes to virulence through increasing nutrition during infection for the pathogen, disrupting plant defense responses or inducing cell death remains unclear.

What is more, the mechanism of the observed gramillin resistance in wheat and its contribution to FHB resistance is not yet known. Preliminary work has shown that gramillin appears to be degraded or modified in the apoplast of insensitive wheat, as these molecules are virtually undetectable 30 minutes after infiltration, while they remain partially intact in gramillin-

sensitive barley leaves (Brauer et al., unpublished data). In the apoplast, several molecules with the potential to disrupt gramillin's structure and toxicity are present. These include proteases which degrade pathogen peptides, reductase enzymes that can reduce disulfide bonds, and lipid transfer proteins, which can bind to lipids (Farvardin et al., 2020). On the other hand, insensitivity could be mediated by inducible immune responses, as genes regulating this process (*BIK1*, *ILK1*, *RBOHD*) are required for the gramillin-induced ROS burst in *Arabidopsis* and knocking them out increases cell death in response to gramillin (Brauer et al., 2023). Variation in sensitivity to this virulence factor also exists across 20 genotypes of barley and maize, where the majority of genotypes display some level of sensitivity when injected with purified gramillin (Brauer et al., unpublished data). In barley, the FHB resistant Lowe variety has a uniquely high level of insensitivity to purified gramillin (Brauer et al., unpublished data).

Barley (*Hordeum vulgare* subsp. *vulgare* L.) is a cereal within the tribe Triticeae in the Poaceae family (Blattner, 2018). While the majority of barley (75-80%) is destined for animal feed, 20-25% serves as malt for the brewing industry and approximately 6% is for human consumption (Tricase et al., 2018). In 2022, 149.53 million metric tons of barley was produced globally (USDA, 2023). Russia is the lead barley producing country with 13% of global volume, followed by Australia and Canada (both 7%) (USDA, 2023) . Lowe is a two-row hulled spring malt barley bred with moderate resistance to FHB and low DON accumulation (Juskiw et al., 2019). Lowe is taller and matures slightly later than other cultivated varieties AC Metcalfe and Chevron, traits which are both linked to superior FHB resistance (Ogrodowicz et al., 2020). In addition to FHB, Lowe has moderate resistance to scald and spot form of net blotch, while being fully resistant to both surface-borne and loose smuts (Juskiw et al., 2019). Lowe was bred from a cross between Ponoka, a general purpose spring barley (Juskiw et al., 2005), and the breeding line

H92017203Z. The latter originates from a cross between AC Oxbow and Leo (Fig 2). AC Oxbow was registered in 1994 and has contributed genetics to many lines in the Canadian germplasm developed since then (CFIA, 2015). Leo is a malting variety from Chile known for early maturity, good malting quality, and moderate resistance to scald (Beratto M., 1990). The basis for Lowe's high level of insensitivity to gramillin is not known, nor is the sensitivity of the lines from which it is derived. In order for breeders to develop barley lines that are resistant to gramillin through marker-assisted selection, the molecular markers associated with resistance need to be identified. Several bi-parental mapping populations are currently under development by researchers at Olds College in Alberta using Lowe as a parent. However, the gramillin resistance of the other parental lines used in these bi-parental crosses is unknown.

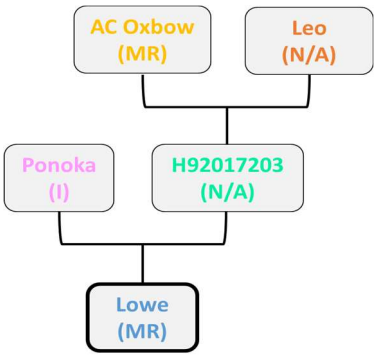

Figure 2: Lowe barley parental lines. The FHB resistance rating of each line is shown in parentheses, where MR indicates moderate resistance and I indicates intermediate resistance. N/A indicates that a resistance rating is not available.

Research objectives

To advance our understanding of plant-*Fgr* interactions, the goal of this work was to investigate the nature of gramillin sensitivity in barley and further our understanding of its role during infection. Towards this goal, the objectives of this research were to:

1. Establish methods to rapidly survey Canadian barley genotypes for gramillin sensitivity.
2. Determine if the basis of gramillin insensitivity in barley is linked to induced signaling responses or degradation of the toxin.
3. Evaluate the contribution of gramillin to FHB severity and DON deposition during infection.

Characterizing the molecular mechanisms involved in gramillin resistance in barley will further our understanding of host defense against ionophores and the contribution of gramillin resistance to general FHB resistance. Together, this this information will improve our understanding of plant-microbe interactions and plant responses to CLP toxins. Leveraging gramillin resistance may improve FHB resistance which would reduce economic losses for Canadian barley farmers and lower the risks to human and livestock health from mycotoxin contamination.

Methods

Plant growth

Plants used in pathology assays were planted in a 75 Promix:24 black earth:1 lime soil mix in five-inch pots and were watered twice daily and fertilized with 20-20-20 (N-P-K) twice a week. Seedlings used in all other assays were grown in the same soil in 1.75-inch plug trays with the same soil and watering regimen. All plants were grown in growth cabinets with a 20°C daytime temperature, 15°C nighttime temperature, and 16-hour daylength.

Gramillin purification

A purified mixture of gramillin A and B (approximately 50:50 ratio of A and B) was prepared by Indira Thapa from fungal extracts according to the method described by Bahadoor et al. (2018). The concentration of cyclic gramillin was verified by HPLC by Indira Thapa for every batch of aliquots prepared.

Ion leakage

The youngest fully expanded leaf of a three to four-week-old barley plant was syringe-infiltrated with a 10 μM gramillin solution or a water control. Ten 4 mm disks are cut from the infiltrated area and placed in 1 mL of MilliQ water in a 24-well plate. The water was removed and replaced with fresh water, at which point the time 0 measurement is taken. The conductivity of the liquid is measured with a LaquaTwin Compact Conductivity Meter (Horiba Scientific, #EC-11). The plate was placed on a shaker at 60 rpm under illumination (two 13W lightbulbs 12 cm above the plate), and measurements on the water's conductivity are taken at 2, 4, 6, and 24 hours. There were four replicate wells per barley line for the gramillin treatment and two wells for the water treatment. For inhibitor studies, 2 mM SHAM (Sigma-Aldrich, S607), 25 μM DPI (Sigma-Aldrich, D2926),

or Pierce™ Protease Inhibitor (EDTA-Free, Thermo-Fisher Scientific™, A32965, prepared in water according to the manufacturer's methods – approximately 2.5 mg/mL (w/v)) were co-infiltrated with gramillin. The protease inhibitor is designed to inhibit serine proteases, cysteine proteases, aspartic acid proteases, and aminopeptidases. SHAM, DPI, protease inhibitor and water were included as controls. These ion leakage trials were conducted according to the same methods, except that only three 4 mm disks were cut from the infiltrated areas and were placed in 300 µL MilliQ water in a 96-well plate, and six replicate wells were measured for each treatment.

Peroxidase activity

The protocol for peroxidase measurements was adapted from a pre-existing method (Mott et al., 2018). Briefly, the cotyledon of a two-week-old barley seedling was infiltrated with solution containing water or an elicitor and three 4 mm disks were cut and placed in 300 µL of water in a 96-well plate. The water was removed once all the leaf disks had been cut and replaced with fresh water. To measure the peroxidase production from these leaf disks, 50 µL of the incubation water was combined with 50 µL of 1 mg/ mL 5-aminosalicylic acid (Sigma-Aldrich, #A79809) and 0.01% hydrogen peroxide (Sigma-Aldrich, #216763) and incubated for three minutes. The reaction was stopped with 20 µL of 2N NaOH (Anachemia, #83076-380) and the oxidation measured with a Tecan Infinite F Plex plate reader at 595 nm.

ROS assay

Four-millimetre leaf disks were cut from the youngest fully expanded leaf of three to four-week-old barley seedlings, and one disk was placed per well into 100 µL of water in a 96-well plate. Eight leaf disks from four different plants were used per treatment, with the duplicate disks from each plant split between water controls and elicitor treatments. Disks were allowed to rest in darkness for 16 to 18 hours prior to removing the water and replacing it with detection buffer

(elicitor, 0.08 mg/mL of L-012 (Sigma Aldrich, #SML2236), 0.04 mg/mL horseradish peroxidase (Sigma Aldrich, #P8375)). The relative luminescence was measured by a microplate reader and quantifies the amount of ROS produced over 45 time points spaced 90 seconds apart. The elicitors used during these experiments were flg22 (1 μM) (AnaSpec Inc., #AS-62633), chitin (100 μg/mL) (Sigma-Aldrich, #C9752), and a mixture of chitin and gramillin (100 μg/mL and 10 μM, respectively).

Lesion assay

The cotyledon of a two-week-old barley seedling was syringe-infiltrated with a 5 μM gramillin solution and a water control (each over a length of approximately 1 inch). The infiltrated area was circled, and the seedlings were returned to their growth cabinet. After 24 hours, the percentage of the infiltrated area that showed necrotic lesions was scored. A score of 0 indicates no lesions; 1 indicates 1-25% of the infiltrated area has lesioned; 2 indicates 26-50% lesions; 3 indicates 51-75% lesions; and 4 indicates 76-100% lesions (Fig 3). For inhibitor studies, 2 mM SHAM (Sigma-Aldrich, S607), 25 μM DPI (Sigma-Aldrich, D2926), or Pierce™ Protease Inhibitor (EDTA-Free, Thermo-Fisher Scientific™, A32965, prepared in water according to the manufacturer's methods – approximately 2.5 mg/mL (w/v)) were co-infiltrated with gramillin. The protease inhibitor is designed to inhibit serine proteases, cysteine proteases, aspartic acid proteases, and aminopeptidases. SHAM, DPI, protease inhibitor and water were included as controls. Five seedlings from each barley line were infiltrated with both the gramillin treatment and the water control.

FHB nursery trial

Fifteen lines of barley were planted in a Fusarium head blight nursery in May of 2022. The FHB nursery is a field in which conditions for an FHB epidemic have been optimized – the field has

previously been infected with *Fusarium*, it is irrigated daily to ensure high humidity, and it is newly inoculated with *Fusarium* once the plants begin to head (Legge et al., 2004). The lines were sown in two-row plots and randomly distributed, with two replicate plots of each line. In July of 2022, the field was inoculated twice, 1 week apart, with solid inoculum at a rate of 30g/m^2. Two weeks post-inoculation, infection was measured on a weekly basis for four weeks, using a 0-5 scale that incorporates both incidence and severity (Table 1).

Table 1: Description of the Fusarium head blight symptom rating scale.

0	No infection
1	Incidence low, up to 5% of spikes infected; Severity low, up to 7% of head affected
2	Incidence moderate to low, 5-15% spikes infected; Severity low to moderate, up to 15% of head affected
3	Incidence moderate, 15-30% of spikes infected; Severity moderate, up to 25% of head affected
4	Incidence moderate to high, 30-50% of spikes infected; Severity moderate to high, up to 40% of head affected
5	Incidence high, 50% of more of spikes infected; Severity high, up to 50+% of head infected

Once the grain was mature, each plot was harvested with a hand sickle and placed in a paper bag at approximately 65ºC until dry. Samples were ground and analyzed for DON content by the Blackwell Lab (see DON content section below).

Pathology assays

Spore preparation

A plug was taken from an SNA stock plate and placed in the centre of a ½ concentration PDA plate (12 g/L of potato dextrose (Sigma-Aldrich, #P6685) and 20 g/L of bacto-agar (BD, #214010) in

dH_2O). The plate is placed face-up in an incubator with UV light at 25°C, with a 16-hour daylength, for 5-7 days until confluence. These seed plates are then stored face-down at 4°C until use. To obtain spores, 5 mL of sterile water is poured on to a seed plate, and the mycelia is scraped off the media with a sterile microscope slide. The fluid on the plate is then filtered through two layers of cheesecloth (VWR, #21910). One mL of this filtrate is pipetted on to a ½ PDA plate and spread to cover the whole plate evenly to create a 40-hour plate. Generally, three 40-hour plates are made from a seed plate. The 40-hour plates are placed face-up in an incubator under the same conditions as the seed plates described above. After 40 hours of incubation, the plates are retrieved. To collect the spores, 5 mL of sterile water is poured onto each plate and the mycelia are scraped off the media with a sterile microscope slide. This fluid is filtered through two layers of cheesecloth into a 50 mL Falcon tube. The fluid is then centrifuged for 10 minutes at 4200 rpm at 4°C to pellet the spores. This pellet is then washed and additional two times in 15 mL of cool sterile water. After the final wash, the pellet is resuspended in 5-10 mL of sterile MilliQ water. A 10x dilution of the spores is taken to quantify the spore concentration with a hemacytometer. Subsequently, 75 mL of a 5.0 x 10^4 spore/mL solution is prepared in MilliQ water in a Nalgene aerosol spray bottle (Thermo Fisher, #2430-0200).

Inoculation

Plants were grown in individual 5” pots in a growth cabinet. Heading dates were monitored, and tillers were tagged as headed when 75% of the head had emerged from the flag leaf sheath (Zadoks stage 57) (Zadoks et al., 1974). Heads were infected 14 days after heading by spray-inoculation in a plexiglass box (Hudson, 2023). All heads other than the target were temporarily covered by a plastic bag to protect them from infection, while the target head was sprayed from a distance of approximately 5 cm on all sides to the point of run-off. The head and flag leaf were then covered

with a resealable 9" x 12" plastic bag which was affixed to the pot stake to ensure the tiller remained upright and plants were returned to the growth cabinet. Heads were monitored for infection at two, three, and four days post-inoculation. The level of infection was quantified by the proportion of the spikelets showing brown or purple *Fgr*-induced discolouration. At the final time point, the heads were cut from the plant and flash frozen in liquid nitrogen to be stored at -80ºC before further analysis. Additional heads were infected for microscopy. For callose staining, the lemma and palea of the third spikelet from the top of the head were removed with tweezers and destained for 32 hours in 1:3 acetic acid:ethanol (acetic acid: Anachemia, #AC-135; ethanol: Greenfield Global, # P016EA95), then incubated in 0.01% (w/v) aniline blue stain (Sigma-Aldrich, #415049) for 16 hours before being fixed in 50% glycerol (Schenk and Schikora, 2015).

RNA extraction

Heads were ground in liquid nitrogen using a mortar and pestle until a flour-like consistency was obtained. Approximately 100 µL of this tissue was placed in 800 µL of Trizol (Ambion, #15596018), and allowed to incubate at room temperature for 10-20 minutes. The samples were then centrifuged at 4ºC for 15 minutes at 12000*x*g to precipitate carbohydrates. The supernatant was placed in a Phaselock tube (Quantabio, #2302830) with 200 µL of chloroform (Anachemia, #23510) and mixed by inversion, then centrifuged for 9 minutes at 12000*x*g at room temperature. The aqueous phase was added into 400 µL of -20ºC isopropanol (Sigma-Aldrich, #278475) and placed at -20ºC overnight. This fluid was subsequently run through a Plant RNEasy Mini Kit (Qiagen, #74904), starting at step 5 of the protocol. The following modifications were made – before the final elution, the 44 uL of water was allowed to incubate at room temperature for 5 minutes. The extracted RNA was DNAse treated with Turbo™ DNAse (Invitrogen, #AM2238). The RNA concentration was verified with a NanoDrop™ One/OneC Microvolume UV-Vis

Spectrophotometer (Thermo Scientific), and then cDNA was prepared using a High-Capacity cDNA Reverse Transcription Kit (Applied Biosystems, #4368813). RNA and cDNA were stored frozen until use.

Quantitative PCR (qPCR) analysis

Gene expression was measured by qPCR according to the manufacturer's instructions for PowerUp SYBR Green Mastermix (Applied Biosystems, #A25742) where 0.5 µL of cDNA was used per reaction except in the case of *NRPS8* where 1 µL of cDNA was used. Results were analyzed using the Pfaffl method to determine relative expression of target genes (Pfaffl, 2001). *HvCyclophilin* and *HvActin* were used as reference genes for barley-specific primers, while *FgEF1a* and *FgGAPDH* were used as reference genes for fungal-specific primers (Table S3).

DON content

Barley heads harvested at 3 days post-infection were individually ground roughly in liquid nitrogen, then dried in a drying oven (LabLine Imperial V, #3478M) at 65°C for 3 days and finely ground in a grain grinder for approximately 1 minute (PerkinElmer, #LM 3610). For the final replicate, four heads were combined from two plants and ground together in liquid nitrogen with a mortar and pestle to a fine powder, then lyophilized for 96 hours. Samples were stored at 4°C until DON analysis was performed by the Blackwell Lab using an enzyme-linked immunosorbent assay (ELISA) according to previously published methods (Sinha et al., 1995).

Callose

The cotelydon of a two-week-old barley seedling was syringe-infiltrated over approximately one inch of leaf surface with a 5 µM gramillin solution, a water negative control, or a 10 µM flg22 (AnaSpec Inc., #AS-62633) solution positive control. After 24 hours, the infiltrated segments of leaf were cut and destained for 32 hours in a 1:3 acetic acid:ethanol solution (acetic acid:

Anachemia, #AC-135; ethanol: Greenfield Global, # P016EA95). They were then rinsed with 150 mM K_2HPO_4 and incubated overnight in a 0.01% (w/v) aniline blue solution (Sigma-Aldrich, #415049), before being fixed in 50% (v/v) glycerol (Thermo Fisher Scientific, #G33), according to the methods described in Schenk and Schikora (2015). Samples were observed under fluorescence microscopy using the DAPI filter and the callose depositions in the area visible under 200x microscopy (1.25 mm^2) were counted. This was done for five samples per treatment.

Gramillin degradation in extracted apoplastic fluid

Apoplastic fluid was extracted from barley using centrifugation. The two youngest fully expanded leaves from three four-week-old barley seedlings were cut into 40 mm sections and infiltrated with water before incubation at room temperature for four hours. The leaf segments were centrifuged at 1560 rpm for 10 minutes at room temperature. The extracted apoplastic fluid was centrifuged again twice for 5 minutes at 1000 rpm to remove debris. Gramillin was added to this fluid to a total concentration of 20 μM, along with protease inhibitor or a water control, and the samples are incubated at room temperature for 30 minutes before flash freezing. Gramillin content was measured by HPLC by members of the Blackwell lab.

Statistics

The data for the ROS, POX, callose, and ion leakage assays was analyzed with two-tailed Student's t-tests. The lesion assays done for the inhibitor studies were analyzed with one-tailed Student's t-tests. All other data was analyzed by ANOVA in R with post-hoc Tukey's test. All experiments were conducted a minimum of three times with similar results. Significant differences are noted using *, †, α, or β for $p < 0.05$.

Results

Gramillin sensitivity across the Canadian germplasm

Gramillin induces necrotic lesions in a light- and humidity-dependent manner and thus previous evaluation of gramillin sensitivity across barley genotypes may be influenced by environmental variation (Brauer et al., unpublished data). To establish gramillin sensitivity and quantification methods in barley genotypes of interest, we infiltrated the cotyledons of 19 genotypes (Table S1) and monitored necrotic lesion formation after 24 hours. As previously observed, Lowe barley demonstrated a uniquely high level of insensitivity to gramillin, as it did not form any lesions when infiltrated with 5 μM gramillin (Fig 4 a). However, Lowe did form lesions when infiltrated with 10 μM gramillin indicating that insensitivity was dose-dependent (Fig S1). Six of the genotypes were significantly more sensitive than Lowe including Xena, Gadsby, Sirish, Radegast, Lowe's direct parent H92017203Z and its parent Leo (Fig 4 a). AC Oxbow, the other parental line to H92017203Z, as well as Lowe's other direct parent Ponoka did not differ significantly from Lowe. To obtain an objective numerical measure of gramillin-induced necrosis, we optimized ion leakage assays on infiltrated leaf disks (Fig 4 b). Time course assays revealed that ion leakage begins immediately and plateaus around six hours post-infiltration prior to decreasing slightly by 24 hours post-infiltration (Fig 4 c). We next used this approach to quantify ion leakage in Lowe and its parental genotypes and observed similar trends as the lesion-based approach (Fig 4 b). Though Lowe showed a slight increase in conductivity at the six-hour time point, it did not differ significantly from the water control. Gramillin treatment induced ion leakage in AC Oxbow, Leo, and Ponoka that was significantly higher than in Lowe. AC Oxbow and Leo also differed significantly from their water controls, though Ponoka did not, which is consistent with its low lesioning response. This suggests that our observed ranking of gramillin sensitivity is

not a result of environmental conditions, since leaf disks were exposed to the same water, humidity, and light during this test. The ion leakage responses to gramillin of AC Oxbow, Leo, and Ponoka did not differ significantly from one another (Fig 4 b). Taken together, these results highlight Lowe's uniquely high insensitivity to gramillin-induced cell death, and suggest the genetic origin is from Ponoka, which displays a low level of sensitivity.

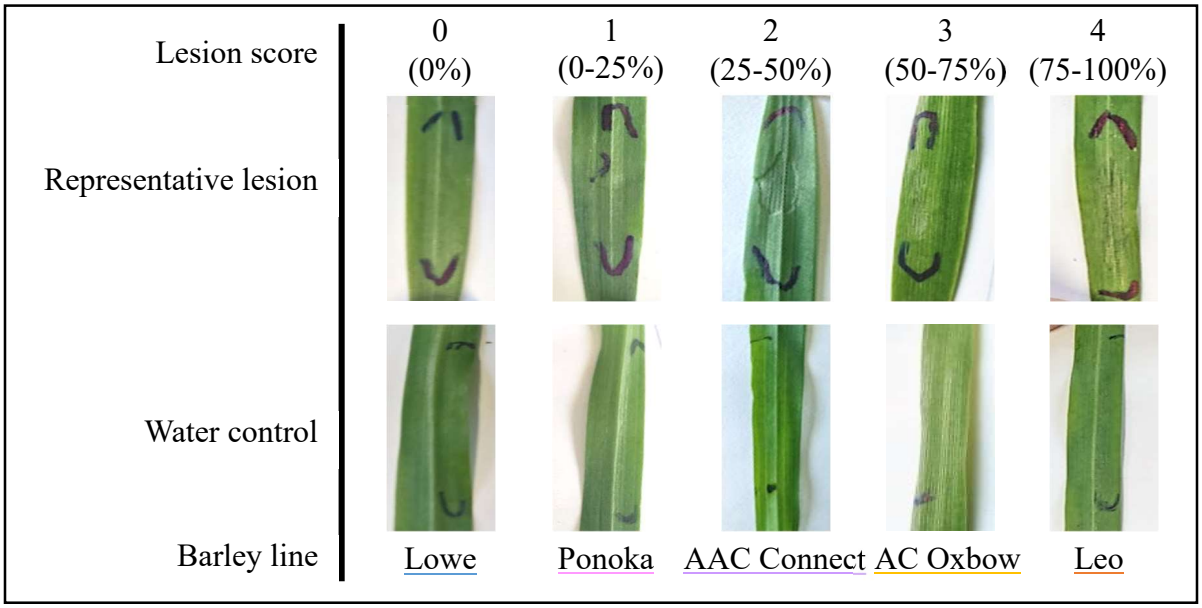

Figure 3: Lesion scoring scale. Representative images of the lesions formed on different barley lines for each point on the scoring scale used to evaluate gramillin-induced lesion severity. The images depict the second true leaf of a two-week-old seedling infiltrated with 5 µM purified gramillin. Lesions are scored after 24 hours on a 0-4 scale where 4 represents that 75-100% of the infiltrated area has lesioned.

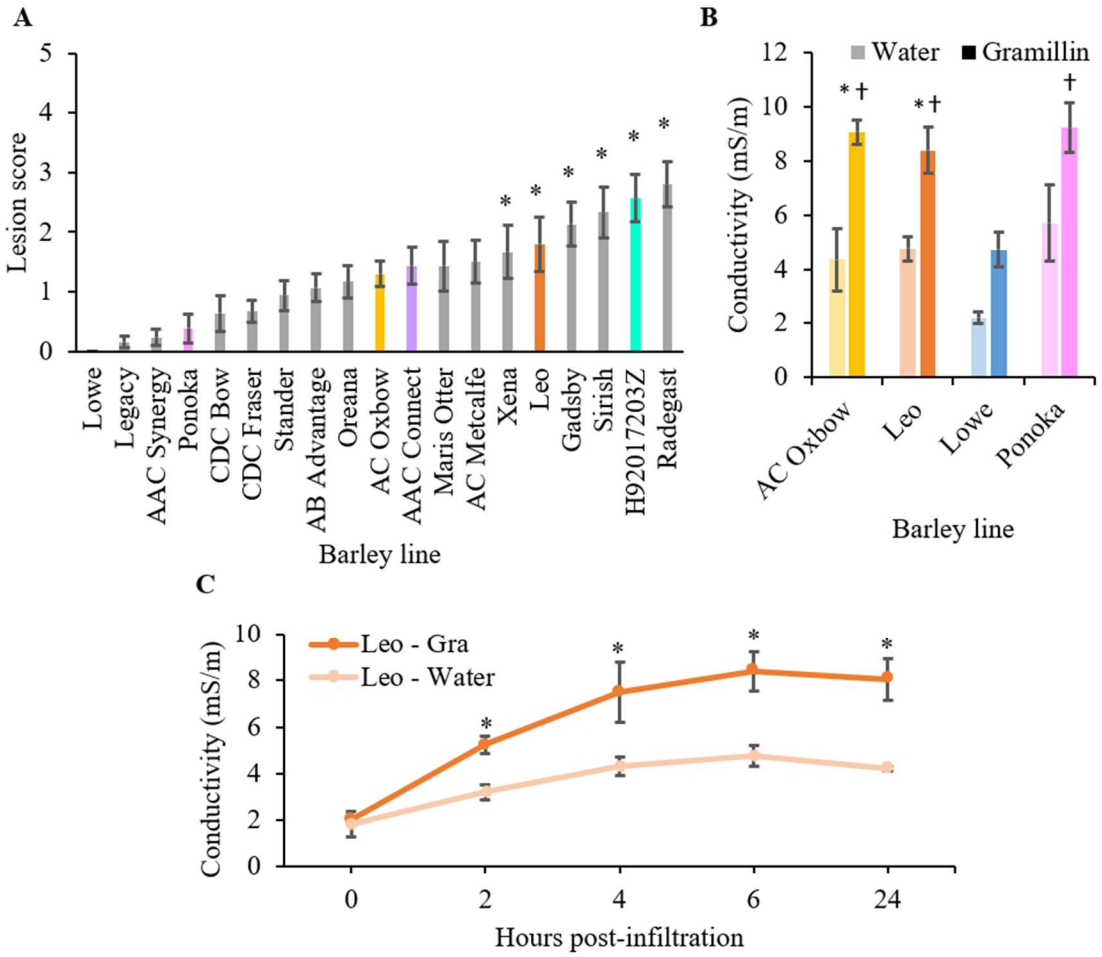

Figure 4: Gramillin sensitivity varies among barley genotypes. A) Gramillin-induced lesion severity in cotyledons infiltrated with 5 µM purified gramillin. Lesions are scored after 24 hours on a 0-4 scale. An asterisk denotes a line that varied significantly from Lowe, and Lowe's parental lines are shown in colour. This data is the average pooled from three replicates experiments (n=15) and SEM is indicated. Significance was determined by ANOVA with post-hoc Tukey's HSD test ($p<0.05$). **B)** Ion leakage from leaf disks 6 hours after water or 10 µM gramillin infiltration. The average from four samples per line and SEM is presented (n=4) from a single experiment. An asterisk denotes significant difference from the respective water control while a cross denotes significant difference from Lowe treated with gramillin. **C)** Ion leakage in the Leo genotype infiltrated with 10 µM gramillin or a water control. The average of four samples and SEM is presented from a single experiment (n=4). An asterisk denotes significant difference from the water control at its respective timepoint. In panels B) and C), significance was determined by two-tailed t-test ($p<0.05$) and three replicate experiments were conducted with similar results.

Gramillin sensitivity is independent of inducible signaling responses

In order to determine if Lowe's lack of response to gramillin is due to insufficient immune responses, we evaluated its ROS response to the MAMPs chitin and flg22 as well as to gramillin. These assays were done on Lowe and its parental lines, in addition to CIMMYT-6, which was used as a benchmark since previous assays had shown it to have moderate ROS responses (Brauer et al., unpublished data). Chitin and flg22 both induced a ROS burst that differed significantly ($p<0.05$) from the water control in all of the lines, suggesting that MTI is intact in Lowe (Fig 5). With the exception of a stronger chitin-induced ROS burst in AC Oxbow relative to Lowe (Fig 5 a), none of lines' responses differed from Lowe's (Fig 5 b).

In *Arabidopsis*, purified gramillin alone can induce a small ROS burst which is dependent on the NADPH oxidase *RBOHD* (Brauer et al., 2023; Fig S2), and gramillin acts to downregulate the chitin-induced ROS burst (Brauer et al., 2023). However, there is no perceptible burst triggered in barley at similar gramillin concentrations (2 μM; Brauer et al., unpublished data). Furthermore, when gramillin was combined with chitin and applied to barley, it did not significantly modulate the oxidative burst in any of the lines tested (Fig 5 c). This suggests that Lowe's insensitivity to gramillin is not due to defective ROS responses, and its virulence function in barley is not to modulate the chitin-induced oxidative burst.

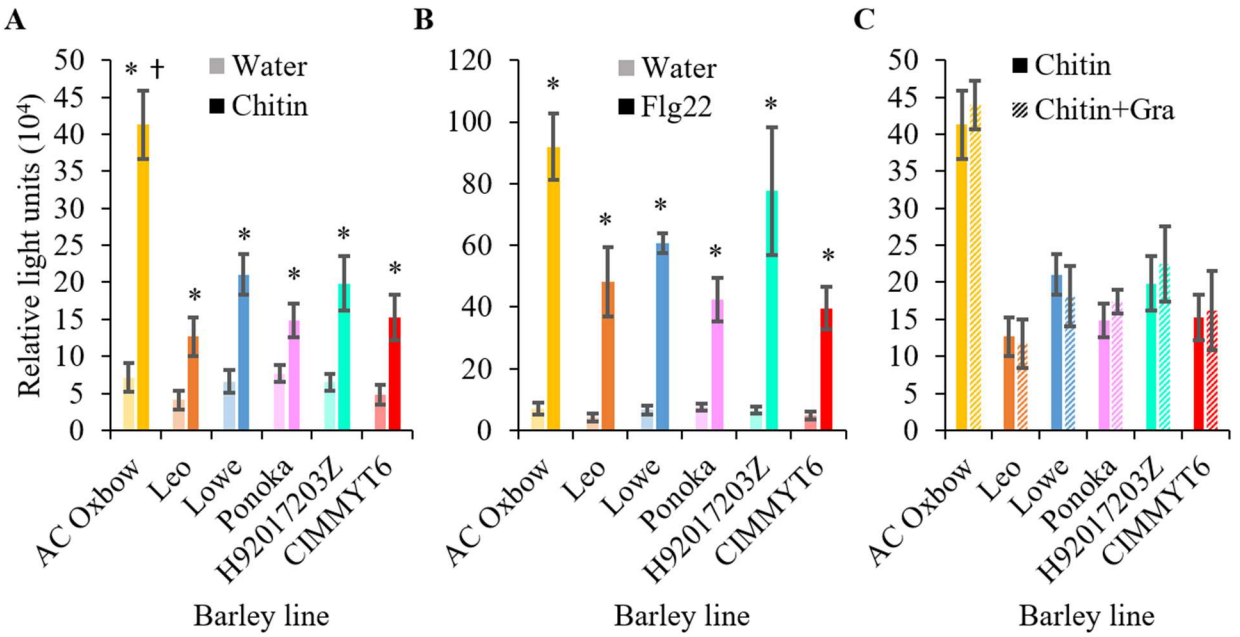

Figure 5: Lowe displays functional immune responses to MAMPs. Sum of luminescence values caused by ROS production at all time points during the first 30 minutes after exposure to **A)** water or 10 µg/mL chitin, **B)** water or 1 µM flg22, or **C)** chitin or chitin combined with 10 µM gramillin (Gra). Each value is the average and SEM of measurements from four leaf disks (n=4). An asterisk denotes a line that is significantly different from its own water control ($p<0.05$), while a cross denotes a line that differs significantly from Lowe. Significance was determined by ANOVA analysis with post-hoc Tukey's HSD test. The data presented is from a single experiment; the experiment was replicated three times with similar trends.

To compare the late inducible immune responses to gramillin, we focused on gramillin-induced callose production between Lowe and Leo, Lowe's most sensitive parental line. Gramillin did induce callose deposition in both lines at a significantly ($p<0.05$) higher level than the water control, but the response did not differ between Lowe and Leo (Fig 6). Lowe also responded to chitin challenge with a similar amount of callose to Leo, and interestingly responded to flg22 with significantly more callose than Leo. Together, this suggests that Lowe is indeed able to sense and respond to gramillin, indicating that insensitivity to gramillin toxicity is not due to a lack of gramillin interaction with cellular components or due to an inability to induce cellular responses.

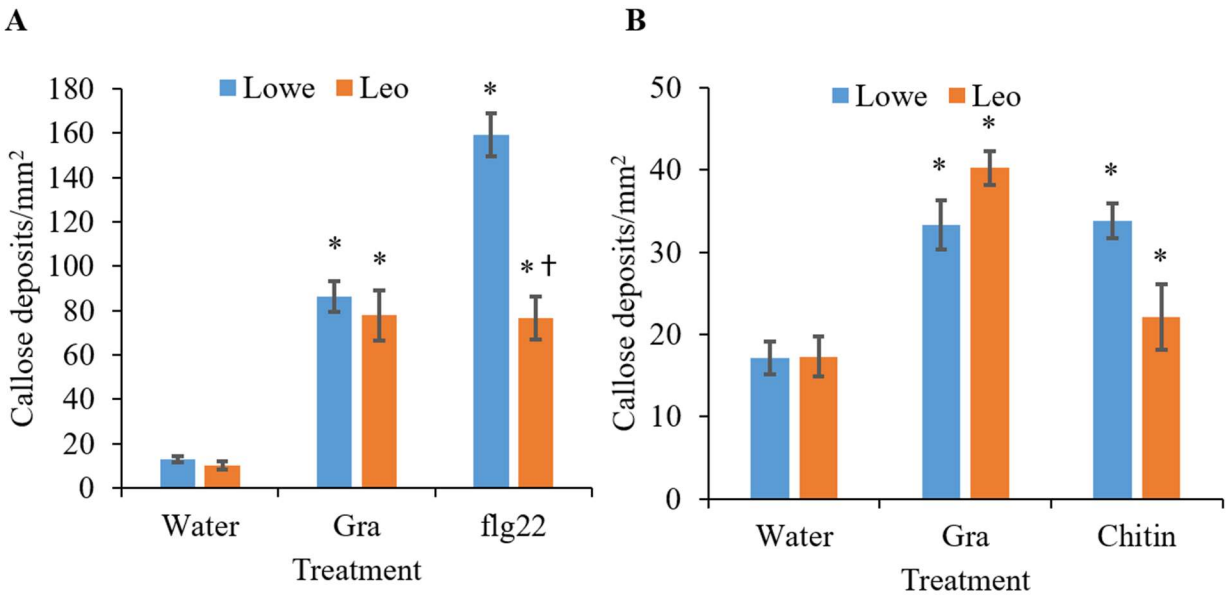

Figure 6: Gramillin induces callose deposition in barley. Callose deposits per square millimetre 24 hours after infiltration of water, 5 µM gramillin (Gra), **A)** 10 µM flg22 or **B)** 10 µg/mL chitin into two-week old barley cotyledons. Tissues were stained with aniline blue to be visualised with a DAPI filter. The average (n=5) and SEM are presented. An asterisk denotes a treatment where there was a significant difference to the respective water control, while a cross denotes where Leo differed to Lowe for the same treatment. Statistical significance ($p<0.05$) was determined by two-tailed Student's t-tests. The data presented is from a single experiment; three replicate experiments were conducted with similar trends. *Data generated by Moatter Syed.*

To determine if inducible immune responses were required for gramillin toxicity, we used chemical inhibitors to disrupt several gramillin-induced signaling responses and observed the impact on cell death. Salicylhydroxamic acid (SHAM) can inhibit peroxidase activity, which leads to decreased ROS activity, but has also been shown to repress the alternative oxidase (AOX) pathway which can lead to increased ROS accumulation (Khokon et al., 2010; Zhang et al., 2011; Hoque et al., 2012; Dinakar et al., 2016; Singh et al., 2017; Liu et al., 2021). SHAM did not significantly affect the response to gramillin in Lowe nor in Leo, either in terms of the formation of foliar lesions (Fig 7 a) or of ion leakage (Fig 7 b). Diphenyleneiodonium chloride (DPI)

application reduces ROS levels in plant tissue (Andronis et al., 2014), as it inhibits NADPH oxidases such as the respiratory burst oxidative homolog (RBOH) family of enzymes (Castro et al., 2022). DPI exacerbated gramillin-induced foliar lesions in Lowe barley, but did not increase cell death as quantified by ion leakage. It further did not significantly affect the gramillin response of Leo for either lesioning or leakage. Calcium channels are opened as an early response to ROS accumulation. Lanthanum acts as a calcium channel blocker and has been shown to reduce gramillin-induced ROS bursts and cell death in *Arabidopsis* (Brauer et al., 2023). However, the addition of lanthanum chloride did not have a significant effect on gramillin-induced cell death in either Lowe or Leo barley. Together, this suggests that gramillin toxicity is independent or upstream of the inducible signaling responses.

In *Arabidopsis*, gramillin induces peroxidase activity which are involved in producing ROS during defense, and are implicated in a variety of defense responses against biotrophs and necrotrophs, including ROS production, cell wall strengthening, and secondary metabolite production (Almagro et al., 2009). In barley, no induced peroxidase activity was observed up to six hours after infiltration with gramillin in Lowe or Leo (Fig S3). Furthermore, the addition of a general protease inhibitor, an alternative oxidase (AOX) inhibitor (SHAM), an NADPH oxidase inhibitor (DPI) (Fig S4 a), or a calcium channel blocker (lanthanum) (Fig S4 b) did not cause significant differences to peroxidase activity observed in either the gramillin or water treatment. In addition, there were no significant differences in peroxidase activity between Lowe and Leo for any treatment, though peroxidase activity was present in all treatments (Fig S3 c and d).

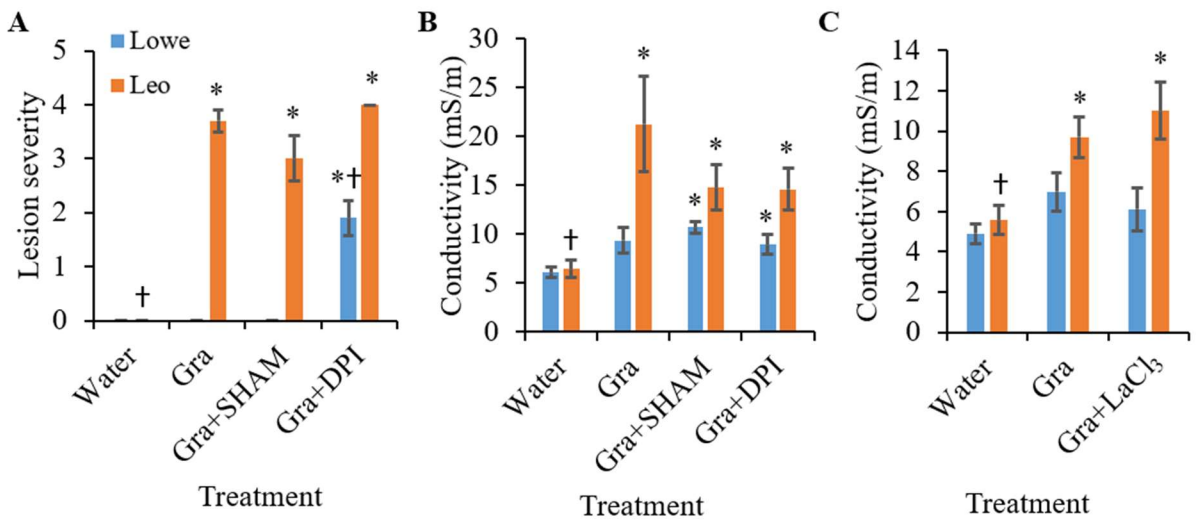

Figure 7: Inducible immune responses are not required for gramillin toxicity. A) Lesion severity is evaluated by monitoring necrosis in barley cotyledons infiltrated with water, 5 µM purified gramillin, gramillin combined with ROS inhibitors 2 mM salicylhydroxamic acid (SHAM), or 25 µM diphenyleneiodonium chloride (DPI). Lesions are scored after 24 hours on a 0-4 scale where 4 represents that 75-100% of the infiltrated area has lesioned. **B)** Ion leakage from barley leaf disks six hours after infiltration with water, 5 µM purified gramillin (Gra), gramillin combined with 2 mM SHAM, or 25 µM DPI. **C)** Ion leakage from barley leaf disks six hours after infiltration with water, 5 µM purified gramillin (Gra), or gramillin combined with 1.5 mM $LaCl_3$. For panel A), the average (n=5) and SEM are shown. For B) and C), the average (n=6) and SEM are shown. For all panels, the data from one experiment is presented; three replicate experiments were conducted with similar trends. An asterisk denotes a treatment that differs significantly from its own water control while a cross denotes a treatment that differs significantly from its own gramillin response. Statistical significance ($p<0.05$) was determined by a one-tailed Student's t-test (A) or a two-tailed Student's t-test (B and C). Controls for the SHAM, DPI and $LaCl_3$ were included and did not differ from the water control (Fig S4).

Gramillin insensitivity is influenced by apoplastic conditions

Since gramillin-induced signaling responses are similar in gramillin sensitive and insensitive barley genotypes, we hypothesized that gramillin insensitivity may be linked to differences in cellular conditions that influence gramillin stability or interaction with plant membranes. Gramillin's cyclic structure is essential to its function, and its immunogenic properties are reduced when it is degraded to a linear form (Brauer et al., 2023). To establish if proteases may play a role in gramillin sensitivity, a protease inhibitor was co-infiltrated with gramillin into Lowe and Leo barley leaves. The addition of the protease inhibitor significantly increased foliar lesions in Lowe by an average of 1.300±0.058 (SEM) (Fig 8 a). This effect was not significant in Leo, where the application of gramillin alone frequently resulted in the maximum lesion score (Fig 8 a). However, application of the protease inhibitor did significantly increase gramillin-induced ion leakage in Leo, though interestingly it did not do so for Lowe (Fig 8 b). To assess whether the protease inhibitor was targeting a protease found in the apoplast or in the plant cell, we extracted apoplastic fluid from Lowe and Leo and measured the degradation of gramillin in it with or without the protease inhibitor. The results from this assay are extremely preliminary and not replicated, but show slightly less degradation when the protease inhibitor is present (Fig S5). These results suggest the function of one or more apoplastic proteases in mediating gramillin sensitivity in barley.

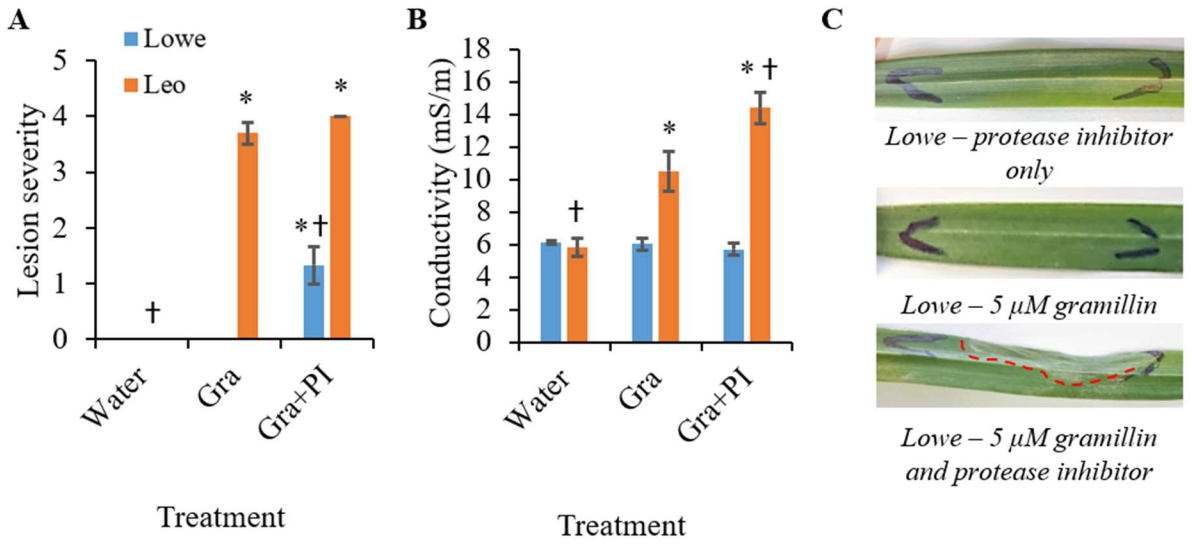

Figure 8: Gramillin insensitivity may be dependent on proteases. A) Lesion severity is evaluated by monitoring necrosis in barley cotyledons infiltrated with water, 5 μM purified gramillin, or gramillin combined with protease inhibitor (PI). Lesions are scored after 24 hours on a 0-4 scale where 4 represents that 75-100% of the infiltrated area has lesioned. **B)** Ion leakage from barley leaf disks six hours after infiltration with water, 5 μM purified gramillin, gramillin combined with protease inhibitor (PI). **C)** Representative images of lesions on Lowe barley cotyledons after treatment with the protease inhibitor, gramillin, or a combination thereof. Lesions are indicated by a red dotted line. For panel A), the average (n=5) and SEM are shown. For B), the average (n=6) and SEM are shown. For all panels, this data is representative of three replicated experiments. An asterisk denotes a treatment that differs significantly from its own water control while a cross denotes a treatment that differs significantly from its own gramillin response. Statistical significance ($p<0.05$) was determined by one-tailed Student's t-tests (A) or two-tailed Student's t-tests (B). A control for the PI was included and did not differ from the water control (Fig S4).

Fungal gramillin production does not influence virulence in spray-inoculated barley

Previous work comparing infection with a gramillin-producing transformation control (TC) or gramillin-non-producing (*Δgra1-1*) strain of *Fusarium graminearum* indicates that gramillin production is required for full virulence in barley (Brauer et al., 2023). While this work was done using point inoculation of a single spikelet within a spike, we sought to determine the relative contribution of gramillin production to fungal virulence *in planta* during spray-inoculation, which Geddes et al. (2008) found to be more representative of infection in the field and more reproducible for the evaluation of phenotypic symptoms. The disease progression was monitored until three days post-inoculation, which is when the highest variability in symptoms was present (Fig S6), at which time the heads were harvested and flash-frozen for RNA extraction. In terms of visual assessment of disease (Fig 9 a), all lines had significantly ($p<0.05$) more symptoms (discoloration, shrivelling of kernels, presence of hyphae on the grain) when inoculated with either fungal strain than when mock-inoculated with water. Furthermore, the *Δgra1-1* strain was overall significantly more virulent ($p=0.001$), though within individual lines only AC Oxbow had a difference between its TC and *Δgra1-1* treatment that was near significance ($p=0.067$). Lowe's visual infection rates did not differ significantly from the infection rate in any other line with the TC strain, though when taking into account both fungal strains, AC Oxbow and Leo both had significantly higher rates of infection than Lowe, indicating Lowe has stronger FHB resistance. Quantification of infection within the same plants by qPCR in Lowe, Leo, and AAC Connect revealed no differences in infection rates between the different barley lines, neither for the TC treatment nor overall (Fig 9 b). All lines' *Δgra1-1* treatments showed significantly more infection than the water control, but only Leo's TC treatment also differed from the water control. Overall, the virulence of the *Δgra1-1* strain was nearly significantly higher than that of the TC ($p=0.072$), but no individual lines had

differences between the two strains. DON content within these plants revealed significantly more DON in Leo than in Lowe overall. There was also more DON deposited by the TC *Fgr* in both Leo and AAC Connect than in Lowe (Fig 9 c). Both Leo and AAC Connect had more DON content when infected with either fungal strain than when with water, as opposed to Lowe which did not differ significantly from its water control. There was no apparent difference in the amount of DON deposited by either the *Δgra1-1* or TC fungal strains.

Despite some statistical discrepancies between the visual and qPCR virulence assessment and DON deposition, the values for each of these metrics correlate significantly ($p<0.001$) (Fig S7). This validates these methods as a consistent approximation of disease. When FHB is evaluated under these inoculation conditions, it does not seem to be possible to detect a virulence-enhancing function of gramillin.

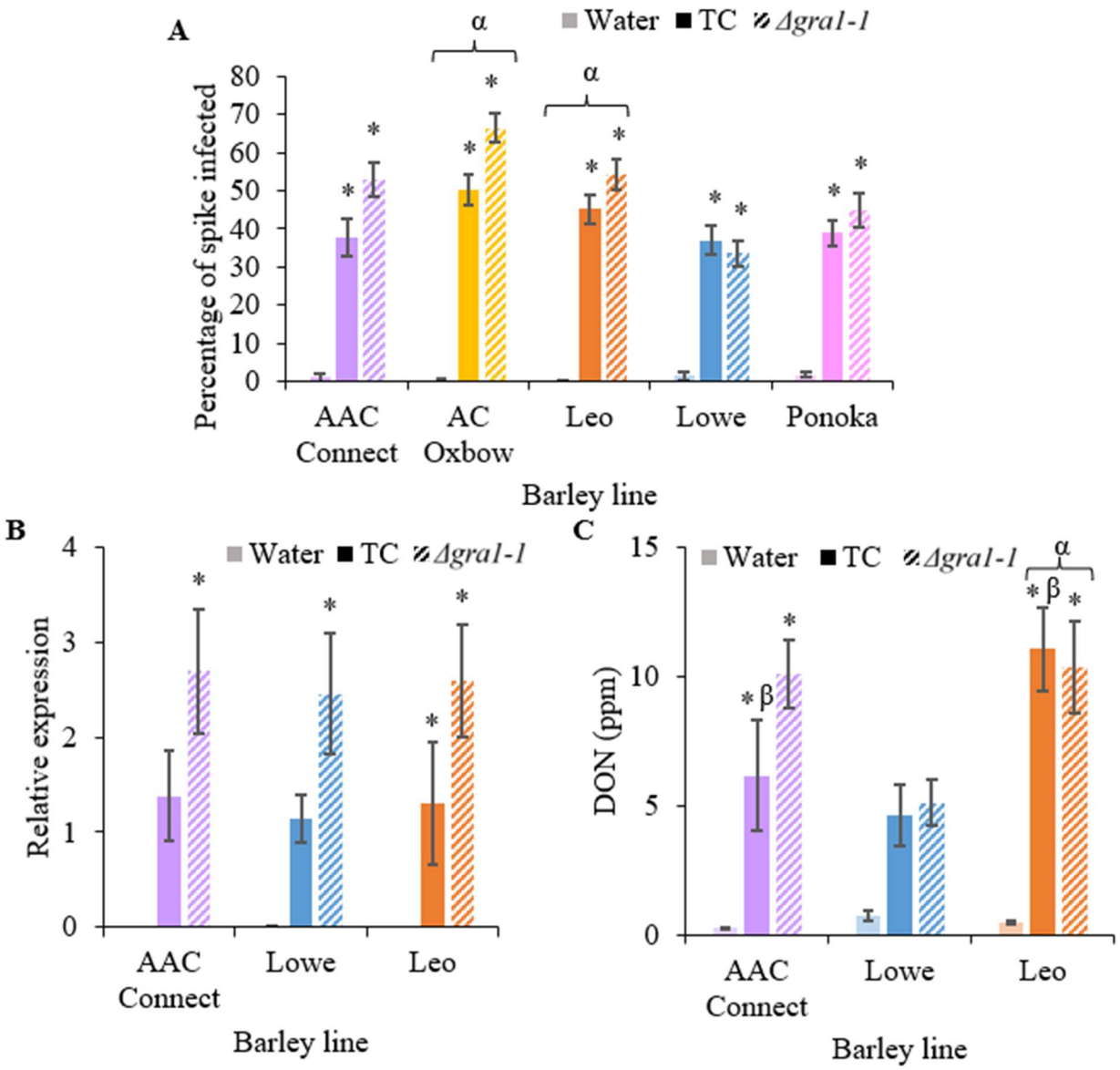

Figure 9: Fungal gramillin production does not enhance virulence in spray-inoculated barley. **A)** Percentage of spikelets on a barley spike visually showing symptoms of FHB at 3 days post-inoculation (dpi). Barley heads were spray-inoculated at 14 days post-emergence with gramillin-producing transformation control (TC) *Fgr* spores or gramillin-non-producing (*Δgra1-1*) spores, or a water control. The average values and SEM pooled from three replicate assays are shown (n=18-44). **B)** Fungal colonization at 3 dpi is quantified by qPCR. The average expression of two Fgr housekeeping genes, *FgGAPDH* and *FgEF1α*, is normalized to the average expression of two barley housekeeping genes, *HvCyclophilin* and *HvActin*. Two barley heads were combined into each sample. The average values and SEM pooled from three replicate assays are presented (n=7-

13). **C)** DON content at 3 dpi. Two barley heads were combined into each sample. The average values and SEM pooled from three replicate assays are presented (n=11-18). In all panels, an asterisk denotes treatment that differed significantly from its own water control, and an α denotes a line that differed significantly from Lowe overall, while a β denotes a TC value that differed significantly from Lowe's TC value. Statistical significance ($p<0.05$) was determined by ANOVA with post-hoc Tukey's honest significant difference analysis.

To further understand the role of gramillin during infection and determine how it impacts plant defense or fungal survival, we first measured the relative gene expression of ten barley genes linked to pathogen defense. Putative orthologs of MTI signaling genes *BAK1*, *BIK1*, and *SOBIR1* and defense response genes *PR2A-2*, *PUB23-like*, and *WRKY23* were identified by preliminary experiments as induced in leaf tissue by purified gramillin. Meanwhile, *MLOC_3110, MLOC_18474, MLOC_58734*, *MLOC_68201* were identified as being in the top 10 most upregulated genes in barley following inoculation with *Fgr* (Huang et al., 2016). In these pathology assays, only *MLOC_18474*, *MLOC_58734*, and *MLOC_68201* were significantly upregulated during infection in comparison to their expression in the control heads inoculated with water (see Table S2 for full expression data). Furthermore, none of the genes tested were differentially expressed in heads inoculated with TC *Fgr* in comparison to those inoculated with *Δgra1-1*. Similarly, their expression did not differ significantly between any of the three barley lines tested (AAC Connect, Leo, and Lowe). This suggests that gramillin does not have a role in modulating inducible defense during infection. However, it is important to note that only a very small portion of the genes involved in pathogen response were measured here.

We assessed the expression of *F. graminearum* virulence factor genes which are induced during infection (Voigt et al., 2005; Harris et al., 2016; Jia et al., 2019) to evaluate a potential role for gramillin in modulating the production of other aspects of the fungal infection strategy (Fig S8; Table S3). To begin, we confirmed that the TC fungus was expressing *NRPS8*, and indeed the

relative expression of this gene in TC-inoculated samples was significantly higher than that in water- or *Δgra1-1*-inoculated samples across all lines (Fig S9). However, no individual line had TC samples that were significantly higher than *Δgra1-1* or water consistently across all three replicates. The *TRI5*, *TRI6*, *NRPS9*, and *FGL1* genes which encode the virulence factors DON, fusaoctaxin, and lipase (respectively) were not differentially expressed in the presence or absence of gramillin nor in different barley lines (Fig S8). However, when the average *FGL1* and *NRPS8* expression values from heads inoculated with TC *Fgr* were correlated, there is a significant ($p=0.023$) positive correlation with an R^2 value of 0.571, suggesting there may possibly be a relationship between the expression of these two genes (Fig S8 e). The *TRI5*, *TRI6*, *NRPS9* and *FGL1* expression when normalized to barley housekeeping genes positively correlated with the level of infection as determined by qPCR, but *NRPS8* did not (Fig S10). We also assessed the resistance to disease in an FHB nursery of the same 19 lines used to evaluate gramillin sensitivity, and did not find a correlation between gramillin sensitivity and disease progression or DON content, though these results must be considered preliminary due to small sample size and lack of replication (Fig S11). This suggests that gramillin does not play a role in modulating the expression *Fgr*'s described virulence factors DON or fusaoctaxin.

Discussion

Lesion assessment and ion leakage are effective assessment methods for gramillin sensitivity in barley

We used two methods to evaluate variation in sensitivity to gramillin in barley varieties from the Canadian germplasm. We tested 19 varieties through a lesion assay and found that the cultivar Lowe exhibited a particularly high level of insensitivity, suggesting a possible quantitative genetic basis for gramillin resistance in barley. Interestingly, Lowe's parental varieties all showed a certain degree of sensitivity, though only Leo was significantly more so. We also used ion leakage from leaf disks as an objective quantitative measure of gramillin-induced necrosis in Lowe and its parental lines. To our knowledge, this is the first time this assay has been used to assess mycotoxin resistance in Canadian barley. We demonstrated that this method is effective, as the results similarly showed insensitivity in Lowe and more necrosis in the parental varieties. There were slight discrepancies between the two assays, as AC Oxbow showed more ion leakage than Lowe but not significantly more lesions. This may be explained by the different environment in which the leaves incubate, as the lesion assays are done at ambient humidity while the leakage assay leaf disks are submerged in water. High humidity can influence various aspects of the plant's immune response, including impeding stomatal closure and downregulating salicylic acid and ethylene signalling (Qiu et al., 2022; Yao et al., 2022). This opens the possibility that these aspects of immunity, which were not investigated in the scope of this research, may potentially play a role in mediating gramillin-induced cell death, and may merit further investigation. Nonetheless, we found ion leakage to be an unbiased, quantifiable, and reproducible method for assessing gramillin-induced cell death.

Gramillin insensitivity does not seem to be linked to inducible immunity but may depend on a host protease

Given that Lowe has both uniquely low sensitivity to gramillin and particularly good FHB resistance, we sought to determine if Lowe is unique in its inducible defense responses, as MAMP response has been linked to *Fgr* resistance (Manes et al., 2021). We found that the early immune responses, such as the ROS burst induced by MAMPs chitin and flg22, as well as basal levels of peroxidase activity, were similar between Lowe and gramillin-sensitive lines. Furthermore, the later immune response of callose deposition in response to gramillin was also identical between Lowe and its most sensitive parent Leo. This indicates that Lowe's insensitivity, as well as its FHB resistance, is unlikely to have a basis in its innate inducible immunity.

Interestingly, we found that some of barley's induced immune responses to gramillin differed from those previously described in *Arabidopsis*. In this dicot species, purified gramillin alone induces a small ROS burst, while it also has the capacity to suppress the ROS burst induced by chitin (Brauer et al., 2023). However, gramillin did not induce a measurable ROS burst from barley leaves. This does not necessarily imply one is not present, as it has been previously observed that monocot ROS bursts are less easily detected than in dicots (Shang-Guan et al., 2018). Oxidative bursts in response to MAMPs do occur in monocots albeit at a smaller amplitude than dicots, but their results are more similar from cell suspensions than leaf disks, suggesting that an aspect of monocot leaf structure may be obstructing ROS measurements (Melcher and Moerschbacher, 2016). Moreover, gramillin did not appear to act to modulate the chitin-induced ROS burst in barley, as there was not a perceptible difference between the burst induced by chitin alone and that when combined with gramillin, in any of the six barley lines assayed. Gramillin may not be able to interact with the barley membrane and immune system the same way it does in

Arabidopsis due to basal physiological differences, as function and phenotype can differ between barley and *Arabidopsis* even when genes are orthologous (Hartmann et al., 2022). For example, the chitin sensing mechanisms differ between *Arabidopsis* and barley. In *Arabidopsis*, chitin sensing is primarily mediated by the receptors AtCERK1, AtLYK5, and AtLYK4 (Cao et al., 2014). Some monocots, including barley, require the plasma membrane glycoprotein CEBiP to interact with CERK1 for chitin-induced signalling (Tanaka et al., 2010). In addition, ionophores have been reported to cause different responses in monocots versus dicots, as surfactin can cause cell death in rice but not dicot species, potentially due to differential recognition at the plasma membrane (Chandler et al., 2015). Recently, the immune elicitation induced by surfactin, which like gramillin is a CLP, was found to be initiated when the ionophore docked into sphingolipid enriched domains of the *Arabidopsis* membrane (Pršić et al., 2023). The membranes of dicots mostly contain sphingolipids with two hexose moieties, while monocot sphingolipids have three hexoses (Cacas et al., 2013). Lenarčič et al. found that necrosis and ethylene-inducing peptide-like 1 proteins (NLP) could only cause cytolysis when bound to sphingolipids with two hexose moieties, rendering monocots insensitive to this toxin (Lenarčič et al., 2017). These differences between the two clades may explain why some aspects of the oxidative burst were not similar between *Arabidopsis* and barley.

There were, however, some parallels between the previously described effects of gramillin and those found to be present in barley. While co-infiltrating DPI into barley affected neither the gramillin-induced cell death as measured by ion leakage in Lowe and Leo, nor gramillin-induced lesion formation in Leo, it did significantly increase lesions in Lowe. Brauer et al. (2023) found that RBOHD was required for the gramillin-induced ROS burst and repressed cell death in *Arabidopsis*. Given that DPI only caused a difference in one line, in only one of two toxicity

measurement methods, our results should be interpreted with caution, but taken together with previously published data, may indicate that RBOH enzymes have a role in reducing gramillin-induced necrosis. Active cell metabolism does not seem to be required for gramillin-induced cell death (Brauer et al., 2023), but it is possible that the presence of ROS in the host tissues may affect gramillin in a metabolism-independent manner, potentially due to ROS oxidating the peptides found in the molecule, which may change their conformation and function (Hu et al., 2020). This is in contrast to surfactin's immunogenic activity, as this CLP induces a ROS burst that does not depend on RBOHD, and DPI has little effect on the induced responses (Jourdan et al., 2009; Pršić et al., 2023). In addition to assessing ROS, we assessed callose deposition in response to gramillin as well as other MAMPs and showed that Lowe responds to gramillin and chitin similarly to Leo. Other virulence factors from *Fgr* have roles in suppressing callose production, including secreted lipase (Blümke et al., 2014), fusaoctaxin A (Jia et al., 2019), and possibly DON (Kang and Buchenauer, 2000). However, gramillin seems to have the opposite effect, as it induced callose formation in barley. It caused a similar effect in *Arabidopsis* (Brauer et al., 2023), though more work is needed to elucidate the signalling pathways involved. This demonstrates that gramillin's immunogenic characteristics that were described in *Arabidopsis* are at least partially present in barley, even though they were not for the ROS aspects. Though a virulence factor inducing immunity may seem counterintuitive, this can be beneficial to the pathogen. For example, *Fgr*'s tricothecene A toxins are also immunogenic, and prompt sustained MAPK signalling that leads to apoptotic cell death (Nishiuchi et al., 2006). ROS can also cause an upregulation in DON production by *Fgr* during infection (Audenaert et al., 2010). Gramillin perception and gramillin sensitivity appear to be independent, as sphingolipid mutants of *Arabidopsis* are less sensitive to the toxin yet deposit as much callose in response to it as the wild-type (Brauer et al., unpublished

data). Similarly, here Lowe and Leo barley deposit similar amounts of callose in response to gramillin though Leo is much more sensitive to it. Furthermore, this demonstrates that gramillin does interact with Lowe's cells, as it is able to cause downstream effects. This suggests that Lowe's resistance is not due to a difference in its cells that prevents gramillin from interacting with membranes, nor to immediate degradation, unless the degradation products are also able to induce callose. This is improbable, however, since linearized gramillin was shown to have strongly reduced immunogenicity and toxicity by Brauer et al. (2023).

We also observed an increase in gramillin sensitivity in Lowe barley in the lesion assay and in Leo barley in the ion leakage assays with protease inhibitor treatment, suggesting the involvement of proteases. It is possible that it increased Leo's sensitivity in the lesion assay as well, but that that effect was non-significant due to the already-high lesion score obtained by gramillin alone. It is uncertain why the increase in sensitivity in Lowe was not apparent in the ion leakage assay, but this may be due to the effect of humidity from submersion, as discussed above. Several roles have been described for secreted apoplastic proteases during immune response to pathogens, notably through activating immune hydrolases, perceiving pathogen effectors, contributing to hypersensitive response, mediating SAR and priming, mediating DAMP release, or direct antimicrobial activity (Godson and Van Der Hoorn, 2021). The inhibition of these may lead to greater sensitivity to gramillin. For example, the aspartic protease CDR1 identified in *Arabidopsis* is proposed to release a peptide elicitor that induces SA-dependent basal defense responses both locally and systematically (Xia et al., 2004). Two other *Arabidopsis* aspartic proteases, SAP1 and SAP2, act to cleave a conserved protein from *Pseudomonas syringae*, thereby inhibiting bacterial growth *in planta* (Wang et al., 2019). The apoplastic papain-like cysteine protease PIP1 confers broad-ranging immunity against various pathogens and can directly

inactivate pathogen proteins or indirectly activate immunity by releasing elicitors (Ilyas et al., 2015). In the apoplast of barley, a constitutively present thiol protease has been identified (Grunwald et al., 2003), as well as putative protease pathogenesis related protein PR17 (Godson and Van Der Hoorn, 2021). Though proteases seem to be involved in nearly every aspect of plant immunity, much remains unknown about them (Balakireva and Zamyatnin, 2018). It is possible that one or more apoplastic protease is degrading the peptide bonds in gramillin, as lipopeptides are sensitive to proteases (Meena and Kanwar, 2015), or otherwise mediating a more robust defense against gramillin-induced damage. This potential protease would have to be present in sensitive varieties as well, since inhibition increases cell death there too, but Lowe may possibly have a polymorphism in either the coding region or the regulatory region that would allow it to be more effective or be present in larger quantities, granting it greater resistance. However, since gramillin is able to induce callose deposition in Lowe, it must trigger this before or despite degradation. It is possible that a protease like CDR1 or PIP1, or one of the many that have not yet been characterized, has a role in promoting gramillin insensitivity by modulating an aspect of the host's physiology to induce immune responses, protect the cell membrane, or prevent cell death.

Gramillin production does not contribute to virulence in FHB infection, but may modulate other fungal genes

In addition to assessing responses in leaf tissue to purified gramillin, we sought to evaluate its contribution to FHB through spray-inoculation of developing grains. When barley heads were inoculated with gramillin-producing (TC) or non-producing (*Δgra1-1*) *Fgr*, assessment of disease suggested that regardless of fungal strain, Lowe presented milder DON accumulation and symptoms than other varieties with the same FHB resistance rating despite similar fungal biomass. Although Lowe and AAC Connect are both classified as moderately resistant (MR) to FHB, during

their respective breeding tests AAC Connect contained 24% less DON that the check (control) cultivar AC Metcalfe, while Lowe had 50% less (Legge et al., 2017; Juskiw et al., 2019). Leo is a Chilean variety that unfortunately does not have an FHB rating (Beratto M., 1990), so the expected resistance and toxin accumulation is unknown. Since Lowe accumulated significantly less DON than AAC Connect and Leo during the pathology assays, our results are consistent with what would be expected. Similarly, visual assessment of symptoms found Lowe to be significantly more resistant to general infection than Leo and AC Oxbow. Leo is shorter and heads early, two traits that are linked to greater FHB susceptibility (Ogrodowicz et al., 2020), meaning it may generally be less resistant than Lowe. Even though AC Oxbow has the same rating as Lowe, the former is a much older variety, registered in 1994, and previously published data shows it has a similar response to FHB as AC Metcalfe, indicating it may actually be more susceptible (Tekauz et al., 2009; Juskiw et al., 2019). This aside, there may be other factors behind Lowe having lesser visual symptoms than varieties rated as similarly resistant. Disease levels by indoor spray inoculation are not always the same as those caused by grain spawn inoculation in the field (which is how disease ratings are determined). Khanal et al. found that FHB severity in spray-inoculated barley did not correlate with FHB incidence under grain spawn, possibly due to a shorter incubation period in the controlled environment and a lessened impact of heading dates (Khanal et al., 2021). It is also possible that the age of the plants at inoculation had an effect on susceptibility levels. Plants commonly exhibit age-related resistance against pathogens, where they are less susceptible to disease at a more mature stage (Hu and Yang, 2019). This has been demonstrated in *Fgr* inoculation of maize silks, where susceptibility to disease declined with time (Reid et al., 2009). Though the plants in this assay were inoculated at the same growth stage (14 days post-heading), Lowe was

particularly late to head and so was inoculated at an age approximately 1-3 weeks greater than AC Oxbow and Leo.

Despite Lowe showing greater resistance to FHB evaluated through visual symptoms and less DON deposition, assessment of fungal biomass by qPCR did not reveal any differences between the resistance of the barley lines. There is precedent for discrepancies between *Fusarium* disease levels assessed visually and the actual fungal load. With FHB caused by *F. poae*, studies have found that visual symptoms only accounted for 40-67% of variation in fungal biomass (Vogelgsang et al., 2008; Stenglein et al., 2012). Our plants were inoculated after anthesis, as barley flowers while still inside the boot (Jordahl et al., 2012). This may explain the difference in observed infection and quantified fungal presence, as infections that occur later in the life cycle can progress without forming visual symptoms (Horevaj et al., 2011) and the pathogen tends to accumulate more in the chaff than in the grain (Siou et al., 2014), which may cause the outside of the kernel to appear more diseased than it truly is. Furthermore, though several studies have found that DON content predicts fungal biomass, there have equally been studies that found no relationship between these two metrics (Paul et al., 2005; Burlakoti et al., 2007; Fabre et al., 2019). In addition, other factors, including the presence of gramillin, can alter regulation of genes involved in the DON biosynthetic pathway, leading to different DON content despite similar quantities of fungus (Brauer et al., 2023). It must be taken into account that the lack of statistical differences found in the qPCR results may be due to high inter-replicate variation, as well as to relatively small sample size (n=4). Future studies could assess more replicates in order to gain a better understanding of gene regulation during *Fgr* infection. Nonetheless, these results suggest that Lowe's noted resistance to FHB may ensue more from low toxin deposition or detoxification within the plant rather than less propagation of the fungus within the tissues. Lowe's FHB

resistance seems unlikely to be linked to its gramillin insensitivity, as a differential infection level in response to this toxin was not detected during these assays.

Bahadoor et al. (2018), as well as Brauer et al. (2023) demonstrated that gramillin can act as a virulence factor and that *Δgra1-1* strains had reduced infection capabilities, so it was unexpected that the visual symptoms here would show the *Δgra1-1* strain to be more virulent. There is evidence for virulence factors incurring fitness costs, leading supposedly virulent pathogens to be less infectious. Reduced fitness of virulent strains has been shown in *Phytophthora infestans* (Montarry et al., 2010), *Leptosphaeria maculans* (Huang et al., 2006), *Xanthomonas oryzae* (Bai et al., 2007), and Turnip mosaic virus (Jenner et al., 2002). It has been proposed that a trade-off between virulence and aggressiveness may be the cause of this phenomenon (Thrall and Burdon, 2003). Notably, one study showed a *ΔNRPS9 Fgr* strain, lacking the fusaoctaxin virulence factor, to cause increased disease in wheat relative to the wild-type, though the mechanism was not determined (Westphal et al., 2019). It is possible that in the context of the spray inoculation methods and environmental conditions provided during this pathology assay, the role of gramillin was redundant with that of the other virulence factors deployed by *Fgr*, and the production of gramillin incurred a greater energy cost than the gain in virulence it provides. This would lead to a reduction in pathogenicity in the TC strain. A similar trend was present in the fungal biomass quantified by qPCR, but was not quite significant, and there was no apparent effect of gramillin on DON deposition. This evidence is not sufficient to suggest that removing gramillin caused an increase in fungal virulence, but nonetheless with the data generated during these pathology assays it is not possible to support a virulence factor role for gramillin in this infection context.

Differences in experimental design may explain the discrepancy between our results and the previously described impaired virulence of *Δgra1-1*. Brauer et al. (2023) infected plants via point-inoculation at anthesis, whereas our plants were inoculated via spray at 14 days post-heading. Geddes et al. found spray to be the most reproducible inoculation method for barley, and the most representative of natural conditions (Geddes et al., 2008). It is also more effective at distinguishing variation in resistance between barley lines (McCallum and Tekauz, 2002). Though our study and that of Brauer et al. used the same concentration of spores, the spray method delivers a larger volume of inoculum and there is greater potential for delivering an unequal amount of spores to each head. It is possible that the high volume of spores delivered by spray and the ideal disease development environment provided allowed the FHB to progress too quickly for gramillin's effect to be necessary or visible. Spray and point inoculation also target different types of host resistance. Spray inoculation evaluates Type I while point evaluates Type II (He et al., 2015). Unlike wheat, barley naturally has strong Type II resistance, so FHB resistance studies should focus on Type I (Martin et al., 2018). It is possible that gramillin has a virulence function that affects an aspect of Type II resistance but not Type I, and therefore *Δgra1-1* showed reduced virulence in the point-inoculation assays but not in the spray inoculation. This may suggest a role for gramillin in bypassing the rachis node during infection, similar to the function of DON in wheat (though DON does not increase virulence in barley or maize) (Maier et al., 2006).

Since gramillin production did not seem to have an effect on induction of the plant defense genes we assessed, we investigated expression of *Fgr* virulence genes in TC or *Δgra1-1* infected heads to explore a role for gramillin in their regulation. Neither the expression of *NRPS9* (which encodes fusaoctaxin A) nor *TRI5* and *TRI6* (which encode DON), were significantly affected by fungal strain or barley line. Brauer et al. (2023) found that *NRPS9* and *TRI6* were dependent on

gramillin production in *Arabidopsis* seedlings. It is possible that *F. graminearum* uses different host-specific infection strategies when infecting a dicot at the seedling stage than the floral and grain tissue of a monocot (Harris et al., 2016). Across the three replicate pathology assays, there was no consistently visible effect on *FGL1* of either fungal treatment or strain. However, a significant positive correlation between *NRPS8* and *FGL1* expression is present in the samples treated with TC *Fgr*. *FGL1* encodes a secreted lipase that acts as a virulence factor (Voigt et al., 2005) by suppressing callose formation at the rachis node (Blümke et al., 2014). Expression of this gene is induced by lipid substrates but repressed by glucose. Voigt et al. were unsure if FGL1 itself secreted the hydrolyzing enzymes needed to provide diacylglycerol or free fatty acid substrates, or whether another enzyme was involved. There is evidence that ionophores can hydrolyze animal cell membranes (Bach and Rifkint, 1990), and sometimes release fatty acids (Nowatzke et al., 1998). Our data suggesting a correlation between gramillin and lipase is limited and preliminary, and is not sufficient to draw concrete conclusions. However, future studies could explore the possibility that the interaction of gramillin with the plant cell membrane may release lipid substrates that induce the expression of lipase. This would fit with the model proposed by Brauer et al. (2023), where the "susceptibility factor" released by gramillin's activity could be free fatty acids, which cause an increase in virulence by upregulating *FGL1*.

Conclusions and Future Directions

We assessed the gramillin sensitivity of Lowe and 18 other Canadian barley varieties that can inform the selection of biparental populations to discover genes associated with gramillin insensitivity. In doing so, we established ion leakage as a reliable quantitative measure of toxin-induced necrosis in barley. Furthermore, we determined that Lowe has similar inducible immune responses to sensitive varieties, suggesting that the basis of insensitivity to gramillin does not lie

in inducible immunity. Rather, we propose that it may be linked to plant protease activity. In addition, our results did not demonstrate a role for gramillin in increasing FHB severity during spray-inoculated infection, as opposed to point-inoculated, implying that gramillin may act to modulate an aspect of Type II immunity rather than Type I. Gramillin production during infection did not seem to regulate the expression of certain plant defense genes, but preliminary evidence points towards a possible role in promoting the expression of other fungal virulence factors.

These findings further the emerging field of microbially produced CLP ionophores and their interactions with plant hosts. Much of the research on this topic has been related to compounds produced by beneficial bacteria that promote inducible systemic resistance, whereas here we have investigated a phytotoxic ionophore produced by a fungus during infection to increase virulence. This opens a new dimension in our understanding of plant-microbe interactions. We also uncovered some differences in CLP response between barley and *Arabidopsis*. Plant immunity is most well studied in dicots, especially the model plant *Arabidopsis*, but is not yet as well characterized in monocots. Our results partially contribute to closing this gap, but highlight the need for more research to be done on biotic stress responses in monocots, particularly crop plants.

Future work should continue to explore the protease inhibitor-meditated sensitivity and refine the pathology assays to reveal gramillin's virulence function. Method development is required to properly assess the degradation of gramillin in extracted barley apoplastic fluid, but this would help identify whether the protease(s) responsible for insensitivity are part of active cell metabolism or constitutively present in the apoplast. In addition, future pathology assays should include cultivar ICB111809, the barley line in which gramillin's virulence was originally demonstrated, and should compare responses to both point and spray inoculation. With an infection

method that adequately shows reduced virulence of Δ*gra1-1 F. graminearum*, it would be valuable to perform RNASeq on infected tissue to reveal which plant and fungal genes are differentially regulated during infection in the presence or absence of gramillin.

References

Abass M, Morris PC (2013) The *Hordeum vulgare* signalling protein MAP kinase 4 is a regulator of biotic and abiotic stress responses. J Plant Physiol **170**: 1353–1359

Alexander NJ, McCormick SP, Waalwijk C, van der Lee T, Proctor RH (2011) The genetic basis for 3-ADON and 15-ADON trichothecene chemotypes in *Fusarium*. Fungal Genet Biol **48**: 485–495

Alexander NJ, Proctor RH, McCormick SP (2009) Genes, gene clusters, and biosynthesis of trichothecenes and fumonisins in *Fusarium*. **28**: 198–215

Alhoraibi H, Bigeard J, Rayapuram N, Colcombet J, Hirt H (2019) The MTI-ETI Model and Beyond. Curr Issues Mol Bio **30**:39-58

Almagro L, Gómez Ros L V., Belchi-Navarro S, Bru R, Ros Barceló A, Pedreño MA (2009) Class III peroxidases in plant defence reactions. J Exp Bot **60**: 377–390

Andersen EJ, Ali S, Byamukama E, Yen Y, Nepal MP (2018) Disease resistance mechanisms in plants. Genes (Basel). doi: 10.3390/GENES9070339

Anderson JP, Gleason CA, Foley RC, Thrall PH, Burdon JB, Singh KB (2010) Plants versus pathogens: an evolutionary arms race. Funct Plant Biol **37**: 499

Andronis EA, Moschou PN, Toumi I, Roubelakis-Angelakis KA (2014) Peroxisomal polyamine oxidase and NADPH-oxidase cross-talk for ROS homeostasis which affects respiration rate in *Arabidopsis thaliana*. Front Plant Sci **5**: 81929

Audenaert K, Callewaert E, Höfte M, De Saeger S, Haesaert G (2010) Hydrogen peroxide induced by the fungicide prothioconazole triggers deoxynivalenol (DON) production by *Fusarium graminearum*. BMC Microbiol **10**: 1–14

Bach R, Rifkint DB (1990) Expression of tissue factor procoagulant activity: Regulation by cytosolic calcium. Cell Biol **87**: 6995–6999

Bahadoor A, Brauer EK, Bosnich W, Schneiderman D, Johnston A, Aubin Y, Blackwell B, Melanson JE, Harris LJ (2018) Gramillin A and B: Cyclic lipopeptides identified as the nonribosomal biosynthetic products of *Fusarium graminearum*. J Am Chem Soc **140**: 16783–16791

Bai G, Shaner G (2004) Management and resistance in wheat and barley to Fusarium head blight. https://doi.org/101146/annurev.phyto42040803140340 **42**: 135–161

Bai J, Choi SH, Ponciano G, Leung H, Leach JE (2007) *Xanthomonas oryzae* pv. *Oryzae*

avirulence genes contribute differently and specifically to pathogen aggressiveness. https://doi.org/101094/MPMI200013121322 **13**: 1322–1329

Balakireva A V., Zamyatnin AA (2018) Indispensable role of proteases in plant innate immunity. Int J Mol Sci. doi: 10.3390/IJMS19020629

Bentham AR, de la Concepcion JC, Mukhi N, Zdrzałek R, Draeger M, Gorenkin D, Hughes RK, Banfield MJ (2020) A molecular roadmap to the plant immune system. J Biol Chem **295**: 14916–14935

Beratto M. E (1990) Leo INIA - CCU, nueva variedad de cebada maltera. Agriculture técnica **50(1)**: 89-90

Bigeard J, Colcombet J, Hirt H (2015) Signaling mechanisms in pattern-triggered immunity (PTI). Mol Plant **8**: 521–539

Blattner FR (2018) Taxonomy of the genus *Hordeum* and barley (*Hordeum vulgare*). *In*: Stein, N. & Muehlbauer, G.J. (eds.) *The barley genome*. Springer International Publishing, Cham, pp. 11–23.

Blume B, Nurnberger T, Nass N, Scheel D (2000) Receptor-mediated increase in cytoplasmic free calcium required for activation of pathogen defense in parsley. Plant Cell **12**: 1425

Blümke A, Falter C, Herrfurth C, Sode B, Bode R, Schäfer W, Feussner I, Voigt CA (2014) Secreted fungal effector lipase releases free fatty acids to inhibit innate immunity-related callose formation during wheat head infection. Plant Physiol **165**: 346–358

Boddu J, Cho S, Kruger WM, Muehlbauer GJ (2006) Transcriptome analysis of the barley-*Fusarium graminearum* interaction. Mol Plant-Microbe Interact **19**: 407–417

Boller T, He SY (2009) Innate immunity in plants: an arms race between pattern recognition receptors in plants and effectors in microbial pathogens. Science (80-) **324**: 742–743

Brauer E, Bosnich W, Holy K, Power M, Syed M, Thapa I, Krishnan S, Bredow M, Johnston A, Cloutier M, et al (2023) A fungal ionophore toxin activates plant inducible immune signaling to promote susceptibility. doi: 10.2139/SSRN.4382769

Brown NA, Urban M, van de Meene AML, Hammond-Kosack KE (2010) The infection biology of *Fusarium graminearum*: Defining the pathways of spikelet to spikelet colonisation in wheat ears. Fungal Biol **114**: 555–571

Buerstmayr M, Wagner C, Nosenko T, Omony J, Steiner B, Nussbaumer T, Mayer KFX, Buerstmayr H (2021) Fusarium head blight resistance in European winter wheat: insights from genome-wide transcriptome analysis. BMC Genomics **22**: 1–17

Burlakoti RR, Estrada R, Rivera V V., Boddeda A, Secor GA, Adhikari TB (2007) Real-time PCR quantification and mycotoxin production of *Fusarium graminearum* in wheat inoculated with isolates collected from potato, sugar beet, and wheat. Phytopathology **97**: 835–841

Cacas JL, Buré C, Furt F, Maalouf JP, Badoc A, Cluzet S, Schmitter JM, Antajan E, Mongrand S (2013) Biochemical survey of the polar head of plant glycosylinositolphosphoceramides unravels broad diversity. Phytochemistry **96**: 191–200

Cao Y, Liang Y, Tanaka K, Nguyen CT, Jedrzejczak RP, Joachimiak A, Stacey G (2014) The kinase LYK5 is a major chitin receptor in *Arabidopsis* and forms a chitin-induced complex with related kinase CERK1. Elife. doi: 10.7554/ELIFE.03766

Castro MJ;, Lima-Cabello AJ;, Alché E;, Cell JDD, José Jiménez-Quesada M, Castro AJ, Lima-Cabello E, De Dios Alché J (2022) Cell localization of DPI-dependent production of superoxide in reproductive tissues of the olive tree (*Olea europaea* L.). Oxyg 2022, Vol 2, Pages 79-90 **2**: 79–90

CFIA (2015) Registered Variety: AC OXBOW - Canadian Food Inspection Agency. https://inspection.canada.ca/active/netapp/regvar/regvare.aspx?id=1550

Chamarthi SK, Kumar K, Gunnaiah R, Kushalappa AC, Dion Y, Choo TM (2014) Identification of Fusarium head blight resistance related metabolites specific to doubled-haploid lines in barley. Eur J Plant Pathol **138**: 67–78

Chandler S, Van Hese N, Coutte F, Jacques P, Höfte M, De Vleesschauwer D (2015) Role of cyclic lipopeptides produced by *Bacillus subtilis* in mounting induced immunity in rice (Oryza sativa L.). Physiol Mol Plant Pathol **91**: 20–30

Charmley LL, Treholm HL (2017) Section 1 - RG-8 Regulatory Guidance:Contaminants in Feed (formerly RG-1, Chapter 7) - Animal health - Canadian Food Inspection Agency. https://inspection.canada.ca/animal-health/livestock-feeds/regulatory-guidance/rg-8/eng/1347383943203/1347384015909?chap=1

Chaudhary P, Agri U, Chaudhary A, Kumar A, Kumar G (2022) Endophytes and their potential in biotic stress management and crop production. Front Microbiol **13**: 933017

Chen Y, Kistler HC, Ma Z (2019) *Fusarium graminearum* trichothecene mycotoxins: biosynthesis, regulation, and management. https://doi.org/101146/annurev-phyto-082718-100318 **57**: 15–39

Cross AS (2008) What is a virulence factor? Crit Care **12**: 196

Cui H, Tsuda K, Parker JE (2015) Effector-triggered immunity: from pathogen perception to robust defense. https://doi.org/101146/annurev-arplant-050213-040012 **66**: 487–511

Cui L, Yang G, Yan J, Pan Y, Nie X (2019) Genome-wide identification, expression profiles and regulatory network of MAPK cascade gene family in barley. BMC Genomics **20**: 1–20

Dinakar C, Vishwakarma A, Raghavendra AS, Padmasree K (2016) Alternative oxidase pathway optimizes photosynthesis during osmotic and temperature stress by regulating cellular ros, malate valve and antioxidative systems. Front Plant Sci **7**: 171347

Van Doorn WG, Beers EP, Dangl JL, Franklin-Tong VE, Gallois P, Hara-Nishimura I, Jones AM, Kawai-Yamada M, Lam E, Mundy J, et al (2011) Morphological classification of plant cell deaths. Cell Death Differ 2011 188 **18**: 1241–1246

Dweba CC, Figlan S, Shimelis HA, Motaung TE, Sydenham S, Mwadzingeni L, Tsilo TJ (2017) Fusarium head blight of wheat: Pathogenesis and control strategies. Crop Prot **91**: 114–122

Eckey C, Korell M, Leib K, Biedenkopf D, Jansen C, Langen G, Kogel KH (2004) Identification of powdery mildew-induced barley genes by cDNA-AFLP: Functional assessment of an early expressed MAP kinase. Plant Mol Biol **55**: 1–15

Ellinger D, Voigt CA (2014) Callose biosynthesis in *Arabidopsis* with a focus on pathogen response: what we have learned within the last decade. Ann Bot **114**: 1349–1358

European Commission (2006) Setting maximum levels for certain contaminants in foodstuffs (Text with EEA relevance).

Fabre F, Bormann J, Urbach S, Roche S, Langin T, Bonhomme L (2019) Unbalanced roles of fungal aggressiveness and host cultivars in the establishment of the Fusarium Head Blight in bread wheat. Front Microbiol. doi: 10.3389/FMICB.2019.02857/FULL

Farvardin A, González-hernández AI, Llorens E, García-agustín P, Scalschi L, Vicedo B (2020) The apoplast: a key player in plant survival. Antioxidants 2020, Vol 9, Page 604 **9**: 604

Felle HH, Herrmann A, Hanstein S, Hückelhoven R, Kogel KH (2004) Apoplastic pH signaling in barley leaves attacked by the powdery mildew fungus *Blumeria graminis* f. sp. *hordei*. Mol Plant-Microbe Interact **17**: 118–123

Ferrari S, Sella L, Janni M, De Lorenzo G, Favaron F, D'Ovidio R (2012) Transgenic expression of polygalacturonase-inhibiting proteins in *Arabidopsis* and wheat increases resistance to the flower pathogen *Fusarium graminearum*. Plant Biol **14**: 31–38

Foroud NA, Baines D, Gagkaeva TY, Thakor N, Badea A, Steiner B, Bürstmayr M, Bürstmayr H (2019) Trichothecenes in cereal grains – an update. Toxins 2019, Vol 11, Page 634 **11**: 634

Fraser CM, Chapple C (2011) The phenylpropanoid pathway in *Arabidopsis*. *Arabidopsis* Book **9**: e0152

Freedman JC (2012) Ionophores in planar lipid bilayers. Cell Physiol Source B Essentials Membr Biophys 61–66

Geddes J, Eudes F, Tucker JR, Legge WG, Selinger LB (2008) Evaluation of inoculation methods on infection and deoxynivalenol production by *Fusarium graminearum* on barley. Can J Plant Pathol **30**: 66–73

Girard L, Höfte M, Mot R De (2020) Lipopeptide families at the interface between pathogenic and beneficial *Pseudomonas*-plant interactions. Crit Rev Microbiol **46**: 397–419

Godson A, Van Der Hoorn RAL (2021) The front line of defence: a meta-analysis of apoplastic proteases in plant immunity. J Exp Bot **72**: 3381–3394

Grunwald I, Rupprecht I, Schuster G, Kloppstech K (2003) Identification of guttation fluid proteins: the presence of pathogenesis-related proteins in non-infected barley plants. Physiol Plant **119**: 192–202

Guo J, Cheng Y (2022) Advances in fungal elicitor-triggered plant immunity. Int J Mol Sci 2022, Vol 23, Page 12003 **23**: 12003

Hajam IA, Dar PA, Shahnawaz I, Jaume JC, Lee JH (2017) Bacterial flagellin—a potent immunomodulatory agent. Exp Mol Med **49**: e373

Hales B, Steed A, Giovannelli V, Burt C, Lemmens M, Molnár-Láng M, Nicholson P (2020) Type II Fusarium head blight susceptibility conferred by a region on wheat chromosome 4D. J Exp Bot **71**: 4703–4714

Hao G, McCormick S, Tiley H, Gutiérrez S, Yulfo-Soto G, Vaughan MM, Ward TJ (2023a) NX trichothecenes are required for *Fusarium graminearum* infection of wheat. Mol Plant Microbe Interact **36**: 294–304

Hao G, Naumann TA, Chen H, Bai G, McCormick S, Kim H, Tian B, Trick HN, Naldrett MJ, Proctor R (2023b) *Fusarium graminearum* effector FgNls1 targets plant nuclei to induce wheat head blight. Mol Plant-Microbe Interact. doi: 10.1094/MPMI-12-22-0254-R

Hao G, Tiley H, McCormick S (2022) Chitin triggers tissue-specific immunity in wheat associated with Fusarium Head Blight. Front Plant Sci **13**: 832502

Harris LJ, Balcerzak M, Johnston A, Schneiderman D, Ouellet T (2016) Host-preferential *Fusarium graminearum* gene expression during infection of wheat, barley, and maize. Fungal Biol **120**: 111–123

Hartmann A, Berkowitz O, Whelan J, Narsai R (2022) Cross-species transcriptomic analyses reveals common and opposite responses in *Arabidopsis*, rice and barley following oxidative stress and hormone treatment. BMC Plant Biol 2022 221 **22**: 1–24

Harvey KL, Jarocki VM, Charles IG, Djordjevic SP (2019) The diverse functional roles of elongation factor tu (Ef-tu) in microbial pathogenesis. Front Microbiol **10**: 485697

He X, Osman M, Helm J, Capettini F, Singh PK (2015) Évaluation de la résistance des lignées généalogiques canadiennes d'orge à la brûlure de l'épi causée par *Fusarium*. Can J Plant Sci **95**: 923–929

Hoque TS, Uraji M, Ye W, Hossain MA, Nakamura Y, Murata Y (2012) Methylglyoxal-induced stomatal closure accompanied by peroxidase-mediated ROS production in *Arabidopsis*. J Plant Physiol **169**: 979–986

Horevaj P, Milus EA, Bluhm BH (2011) A real-time qPCR assay to quantify *Fusarium graminearum* biomass in wheat kernels. J Appl Microbiol **111**: 396–406

Hou S, Liu Z, Shen H, Wu D (2019) Damage-associated molecular pattern-triggered immunity in plants. Front Plant Sci **10**: 453679

Hu B, Lian Z, Zhou Z, Shi L, Yu Z (2020) Reactive oxygen species-responsive adaptable self-assembly of peptides toward advanced biomaterials. ACS Appl Bio Mater **3**: 5529–5551

Hu L, Yang L (2019) Time to fight: Molecular mechanisms of age-related resistance. Phytopathology **109**: 1500–1508

Huang K, Czymmek KJ, Caplan JL, Sweigard JA, Donofrio NM (2011) HYR1-mediated detoxification of reactive oxygen species is required for full virulence in the rice blast fungus. PLOS Pathog **7**: e1001335

Huang Y, Li L, Smith KP, Muehlbauer GJ (2016) Differential transcriptomic responses to *Fusarium graminearum* infection in two barley quantitative trait loci associated with Fusarium head blight resistance. BMC Genomics **17**: 1–16

Huang YJ, Li ZQ, Evans N, Rouxel T, Fitt BDL, Balesdent MH (2006) Fitness cost associated with loss of the AvrLm4 avirulence function in *Leptosphaeria maculans* (phoma stem canker of oilseed rape). Eur J Plant Pathol **114**: 77–89

Hückelhoven R, Seidl A (2016) PAMP-triggered immune responses in barley and susceptibility to powdery mildew. https://doi.org/101080/1559232420161197465 **11**: e1197465

Hudson K (2023) The interaction of *Fusarium graminearum* and *Fusarium poae* inoculation in barley (*Hordeum vulgare* L.). doi: 10.20381/RUOR-28675

Ilyas M, Hörger AC, Bozkurt TO, Van Den Burg HA, Kaschani F, Kaiser M, Belhaj K, Smoker M, Joosten MHAJ, Kamoun S, et al (2015) functional divergence of two secreted immune proteases of tomato. Curr Biol **25**: 2300–2306

Jacques P (2011) Surfactin and other lipopeptides from *Bacillus spp*. 57–91

Jenner CE, Wang X, Ponz F, Walsh JA (2002) A fitness cost for Turnip mosaic virus to overcome host resistance. Virus Res **86**: 1–6

Jeworutzki E, Roelfsema MRG, Anschütz U, Krol E, Elzenga JTM, Felix G, Boller T, Hedrich R, Becker D (2010) Early signaling through the *Arabidopsis* pattern recognition receptors FLS2 and EFR involves Ca2+-associated opening of plasma membrane anion channels. Plant J **62**: 367–378

Jia LJ, Tang HY, Wang WQ, Yuan TL, Wei WQ, Pang B, Gong XM, Wang SF, Li YJ, Zhang D, et al (2019) A linear nonribosomal octapeptide from *Fusarium graminearum* facilitates cell-to-cell invasion of wheat. Nat Commun 2019 101 **10**: 1–20

Jiang C, Hei R, Yang Y, Zhang S, Wang Q, Wang W, Zhang Q, Yan M, Zhu G, Huang P, et al (2020) An orphan protein of *Fusarium graminearum* modulates host immunity by mediating proteasomal degradation of TaSnRK1α. Nat Commun 2020 111 **11**: 1–13

Jones JDG, Dangl JL (2006) The plant immune system. Nat 2006 4447117 **444**: 323–329

Jordahl J, Meyer S, McMullen M (2012) Results of the 2010 uniform fungicide trial on barley, Fargo, ND. pp 97–99

Jourdan E, Henry G, Duby F, Dommes J, Barthélemy JP, Thonart P, Ongena M (2009) Insights into the defense-related events occurring in plant cells following perception of surfactin-type lipopeptide from *Bacillus subtilis*. Mol Plant-Microbe Interact **22**: 456–468

Juskiw PE, Helm JH, Nyachiro J, Cortez M, Oro M, Salmon DF (2005) Registration of 'Ponoka' barley. Crop Sci **45**: 787–788

Juskiw PE, Oatway L, Oro M, Nyachiro JM, Anbessa Y, Xi K, Turkington TK, Lohr S, Bowness J, Capettini F, et al (2019) Registration of 'Lowe', a two-rowed malting barley with enhanced resistance to Fusarium Head Blight. J Plant Regist **13**: 301–310

Jwa NS, Hwang BK (2017) Convergent evolution of pathogen effectors toward reactive oxygen

species signaling networks in plants. Front Plant Sci. doi: 10.3389/FPLS.2017.01687

Kalde M, Barth M, Somssich IE, Lippok B (2003) Members of the *Arabidopsis* WRKY Group III transcription factors are part of different plant defense signaling pathways. / 295 MPMI **16**: 295–305

Kang Z, Buchenauer H (2000) Ultrastructural and immunocytochemical investigation of pathogen development and host responses in resistant and susceptible wheat spikes infected by *Fusarium culmorum*. doi: 10.1006/pmpp.2000.0305

Karlsson I, Persson P, Friberg H (2021) Fusarium Head Blight from a microbiome perspective. Front Microbiol **12**: 628373

Kawasaki T, Yamada K, Yoshimura S, Yamaguchi K (2017) Chitin receptor-mediated activation of MAP kinases and ROS production in rice and *Arabidopsis*. Plant Signal Behav **12**: 1361076

Khanal R, Choo TM, Xue AG, Vigier B, Savard ME, Blackwell B, Wang J, Yang J, Martin RA (2021) Response of barley genotypes to Fusarium Head Blight under natural infection and artificial inoculation conditions. Plant Pathol J **37**: 455–464

Khokon MAR, Hossain MA, Munemasa S, Uraji M, Nakamura Y, Mori IC, Murata Y (2010) Yeast elicitor-induced stomatal closure and peroxidase-mediated ros production in *Arabidopsis*. Plant Cell Physiol **51**: 1915–1921

Kluger B, Bueschl C, Lemmens M, Michlmayr H, Malachova A, Koutnik A, Maloku I, Berthiller F, Adam G, Krska R, et al (2015) Biotransformation of the mycotoxin deoxynivalenol in *Fusarium* resistant and susceptible near isogenic wheat lines. PLoS One **10**: e0119656

Köster P, DeFalco TA, Zipfel C (2022) Ca2+ signals in plant immunity. EMBO J. doi: 10.15252/EMBJ.2022110741

Langevin F, Eudes F, Comeau A (2004) Effect of trichothecenes produced by *Fusarium graminearum* during Fusarium head blight development in six cereal species. Eur J Plant Pathol **110**: 735–746

Lassowskat I, Böttcher C, Eschen-Lippold L, Scheel D, Lee J (2014) Sustained mitogen-activated protein kinase activation reprograms defense metabolism and phosphoprotein profile in *Arabidopsis thaliana*. Front Plant Sci **5**: 110384

Lee J, Eschen-Lippold L, Lassowskat I, Böttcher C, Scheel D (2015) Cellular reprogramming through mitogen-activated protein kinases. Front Plant Sci **6**: 167061

Legge WG, Badea A, Tucker JR, Fetch TG, Haber S, Menzies JG, Tekauz A, Turkington TK, Martin RA, Choo TM, et al (2017) AAC Connect barley. Can J Plant Sci **97**: 539–548

Legge WG, Therrien MC, Tucker JR, Banik M, Tekauz A, Somers D, Savard ME, Rossnagel BG, Lefol E, Voth D, et al (2004) Progress in breeding for resistance to Fusarium head blight in barley. Can J Plant Pathol **26**: 436–442

Lenarčič T, Albert I, Böhm H, Hodnik V, Pirc K, Zavec AB, Podobnik M, Pahovnik D, Žagar

E, Pruitt R, et al (2017) Eudicot plant-specific sphingolipids determine host selectivity of microbial NLP cytolysins. Science (80-) **358**: 1431–1434

Leplat J, Friberg H, Abid M, Steinberg C (2013) Survival of *Fusarium graminearum*, the causal agent of Fusarium head blight. A review. Agron Sustain Dev **33**: 97–111

Leslie JF, Summerell BA (2013) An Overview of *Fusarium*. *In:* Fusarium - Genomics, Molecular and Cellular Biology, pp. 1-9

Li B, Meng X, Shan L, He P (2016) Transcriptional regulation of pattern-triggered immunity in plants. Cell Host Microbe **19**: 641–650

Liu S, Kracher B, Ziegler J, Birkenbihl RP, Somssich IE (2015) Negative regulation of ABA signaling By WRKY33 is critical for *Arabidopsis* immunity towards *Botrytis cinerea* 2100. Elife. doi: 10.7554/ELIFE.07295

Liu Y, Yu LL, Peng Y, Geng XX, Xu F (2021) Alternative oxidase inhibition impairs tobacco root development and root hair formation. Front Plant Sci **12**: 664792

Ma LJ, Geiser DM, Proctor RH, Rooney AP, O'Donnell K, Trail F, Gardiner DM, Manners JM, Kazan K (2013) *Fusarium* pathogenomics. https://doi.org/101146/annurev-micro-092412-155650 **67**: 399–416

Maget-Dana R, Peypoux F (1994) Iturins, a special class of pore-forming lipopeptides: biological and physicochemical properties. Toxicology **87**: 151–174

Maier FJ, Miedaner T, Hadeler B, Felk A, Salomon S, Lemmens M, Kassner H, Schäfer W (2006) Involvement of trichothecenes in fusarioses of wheat, barley and maize evaluated by gene disruption of the trichodiene synthase (Tri5) gene in three field isolates of different chemotype and virulence. Mol Plant Pathol **7**: 449–461

Manes N, Brauer EK, Hepworth S, Subramaniam R (2021) MAMP and DAMP signaling contributes resistance to *Fusarium graminearum* in *Arabidopsis*. J Exp Bot **72**: 6628–6639

Mao G, Meng X, Liu Y, Zheng Z, Chen Z, Zhang S (2011) Phosphorylation of a WRKY transcription factor by two pathogen-responsive MAPKs drives phytoalexin biosynthesis in Arabidopsis. Plant Cell **23**: 1639–1653

Martin C, Schöneberg T, Vogelgsang S, Morisoli R, Bertossa M, Mauch-Mani B, Mascher F (2018) Resistance against *Fusarium graminearum* and the relationship to β-glucan content in barley grains. Eur J Plant Pathol **152**: 621–634

McCallum BD, Tekauz A (2002) Influence of inoculation method and growth stage on fusarium head blight in barley. https://doi.org/101080/07060660109506976 **24**: 77–80

McMullen M, Bergstrom G, De Wolf E, Dill-Macky R, Hershman D, Shaner G, Van Sanford D (2012) A unified effort to fight an enemy of wheat and barley: Fusarium head blight. Plant Dis **96**: 1712–1728

McMullen M, Jones R, Gallenberg D (1997) Scab of wheat and barley: A re-emerging disease of devastating impact. Plant Dis **81**: 1340–1348

Meena KR, Kanwar SS (2015) Lipopeptides as the antifungal and antibacterial agents:

applications in food safety and therapeutics. Biomed Res Int. doi: 10.1155/2015/473050

Melcher RLJ, Moerschbacher BM (2016) An improved microtiter plate assay to monitor the oxidative burst in monocot and dicot plant cell suspension cultures. Plant Methods **12**: 5

Meng X, Zhang S (2013) MAPK cascades in plant disease resistance signaling. https://doi-org.proxy.bib.uottawa.ca/101146/annurev-phyto-082712-102314 **51**: 245–266

Mesterházy A (1995) Types and components of resistance to Fusarium head blight of wheat. Plant Breed **114**: 377–386

Montarry J, Hamelin FM, Glais I, Corbi R, Andrivon D (2010) Fitness costs associated with unnecessary virulence factors and life history traits: Evolutionary insights from the potato late blight pathogen *Phytophthora infestans*. BMC Evol Biol **10**: 1–9

Mott AG, Desveaux D, Guttman DS (2018) A high-sensitivity, microtiter-based plate assay for plant pattern-triggered immunity. Mol Plant Microbe Interact **31**: 499–504

Muthamilarasan M, Prasad M (2013) Plant innate immunity: An updated insight into defense mechanism. J Biosci 2013 382 **38**: 433–449

Nadarajah K (2016) Induced systemic resistance in rice. Microbial-Mediated Induc Syst Resist Plants 103–124

Nishiuchi T (2013) Plant responses to *Fusarium* metabolites. *In:* Fusarium - Genomics, Molecular and Cellular Biology, pp. 165-175

Nishiuchi T, Masuda D, Nakashita H, Ichimura K, Shinozaki K, Yoshida S, Kimura M, Yamaguchi I, Yamaguchi K (2006) *Fusarium* phytotoxin trichothecenes have an elicitor-like activity in *Arabidopsis thaliana*, but the activity differed significantly among their molecular species. Mol Plant-Microbe Interact **19**: 512–520

Nowatzke W, Ramanadham S, Ma Z, Hsu FF, Bohrer A, Turk J (1998) mass spectrometric evidence that agents that cause loss of ca2+ from intracellular compartments induce hydrolysis of arachidonic acid from pancreatic islet membrane phospholipids by a mechanism that does not require a rise in cytosolic ca2+ concentration. Endocrinology **139**: 4073–4085

O'Brien JA, Daudi A, Finch P, Butt VS, Whitelegge JP, Souda P, Ausubel FM, Bolwell GP (2012) A peroxidase-dependent apoplastic oxidative burst in cultured *Arabidopsis* cells functions in MAMP-elicited defense. Plant Physiol **158**: 2013–2027

Ogrodowicz P, Kuczynska A, Mikolajczak K, Adamski T, Surma M, Krajewski P, Ćwiek-Kupczynska H, Kempa M, Rokicki M, Jasinska D (2020) Mapping of quantitative trait loci for traits linked to Fusarium head blight in barley. PLoS One **15**: e0222375

Omoboye OO, Oni FE, Batool H, Yimer HZ, De Mot R, Höfte M (2019) *Pseudomonas* cyclic lipopeptides suppress the rice blast fungus *Magnaporthe oryzae* by induced resistance and direct antagonism. Front Plant Sci **10**: 468338

Osborne LE, Stein JM (2007) Epidemiology of Fusarium head blight on small-grain cereals. Int J Food Microbiol **119**: 103–108

Panstruga R, Moscou MJ (2020) What is the molecular basis of nonhost resistance? Mol Plant-

Microbe Interact **33**: 1253–1264

Paul PA, Lipps PE, Madden L V. (2005) Relationship between visual estimates of Fusarium head blight intensity and deoxynivalenol accumulation in harvested wheat grain: A meta-analysis. Phytopathology **95**: 1225–1236

Perfect SE, Green JR (2001) Infection structures of biotrophic and hemibiotrophic fungal plant pathogens. Mol Plant Pathol **2**: 101–108

Pfaffl MW (2001) A new mathematical model for relative quantification in real-time RT–PCR. Nucleic Acids Res **29**: e45

Piacentini KC, Savi GD, Olivo G, Scussel VM (2015) Quality and occurrence of deoxynivalenol and fumonisins in craft beer. Food Control **50**: 925–929

Pieterse CMJ, Zamioudis C, Berendsen RL, Weller DM, Van Wees SCM, Bakker PAHM, Nl CMJP, Nl CZ, Nl RLB, Nl SV, et al (2014) Induced systemic resistance by beneficial microbes. https://doi.org/101146/annurev-phyto-082712-102340 **52**: 347–375

Pršić J, Gilliard G, Ibrahim H, Argüelles-Arias A, Rondelli V, Crowet J-M, Genva M, Luzuriaga-Loaiza WP, Deboever E, Nasir MN, et al (2023) Mechanosensing and sphingolipid-docking mediate lipopeptide-induced immunity in *Arabidopsis*. bioRxiv 2023.07.04.547613

Qi PF, Zhang YZ, Liu CH, Chen Q, Guo ZR, Wang Y, Xu BJ, Jiang YF, Zheng T, Gong X, et al (2019) Functional analysis of FgNahG clarifies the contribution of salicylic acid to wheat (*Triticum aestivum*) resistance against Fusarium Head Blight. Toxins 2019, Vol 11, Page 59 **11**: 59

Qiu J, Liu Z, Xie J, Lan B, Shen Z, Shi H, Lin F, Shen X, Kou Y (2022) Dual impact of ambient humidity on the virulence of *Magnaporthe oryzae* and basal resistance in rice. Plant Cell Environ **45**: 3399–3411

Raaijmakers JM, De Bruijn I, De Kock MJD (2006) Cyclic lipopeptide production by plant-associated *Pseudomonas spp.*: Diversity, activity, biosynthesis, and regulation. Mol Plant-Microbe Interact **19**: 699–710

Ranf S, Eschen-Lippold L, Frhlich K, Westphal L, Scheel D, Lee J (2014) Microbe-associated molecular pattern-induced calcium signaling requires the receptor-like cytoplasmic kinases, PBL1 and BIK1. Ann Bot **14**: 1–15

Ranf S, Eschen-Lippold L, Pecher P, Lee J, Scheel D (2011) Interplay between calcium signalling and early signalling elements during defence responses to microbe- or damage-associated molecular patterns. Plant J **68**: 100–113

Rao S, Zhou Z, Miao P, Bi G, Hu M, Wu Y, Feng F, Zhang X, Zhou JM (2018) Roles of receptor-like cytoplasmic kinase VII members in pattern-triggered immune signaling. Plant Physiol **177**: 1679

Reid LM, Bolton AT, Hamilton RI, Woldemariam T, Mather DE (2009) Effect of silk age on resistance of maize to *Fusarium graminearum*. https://doi.org/101080/07060669209500867 **14**: 293–298

Rimbaud L, Papaïx J, Rey JF, Barrett LG, Thrall PH (2018) Assessing the durability and efficiency of landscape-based strategies to deploy plant resistance to pathogens. PLOS Comput Biol **14**: e1006067

Scheler B, Schnepf V, Galgenmüller C, Ranf S, Hückelhoven R (2016) Barley disease susceptibility factor RACB acts in epidermal cell polarity and positioning of the nucleus. J Exp Bot **67**: 3263–3275

Schenk ST, Schikora A (2015) Staining of callose depositions in root and leaf tissues. Iss. doi: 10.21769/BioProtoc.1429

Schmale DG, Leslie JF, Zeller KA, Saleh AA, Shields EJ, Bergstrom GC (2006) Genetic structure of atmospheric populations of *Gibberella zeae*. Phytopathology **96**: 1021–1026

Schneider T, Müller A, Miess H, Gross H (2014) Cyclic lipopeptides as antibacterial agents – Potent antibiotic activity mediated by intriguing mode of actions. Int J Med Microbiol **304**: 37–43

Schroeder HW, Christensen JJ (1963) Factors affecting resistance of wheat to scab caused by *Gibberella zeae*. Phytopathology **53**: 831–838

Selosse MA, Strullu-Derrien C, Martin FM, Kamoun S, Kenrick P (2015) Plants, fungi and oomycetes: a 400-million year affair that shapes the biosphere. New Phytol **206**: 501–506

Seong KY, Pasquali M, Zhou X, Song J, Hilburn K, McCormick S, Dong Y, Xu JR, Kistler HC (2009) Global gene regulation by *Fusarium* transcription factors Tri6 and Tri10 reveals adaptations for toxin biosynthesis. Mol Microbiol **72**: 354–367

Shang-Guan K, Wang M, Htwe NMPS, Li P, Li Y, Qi F, Zhang D, Cao M, Kim C, Weng H, et al (2018) Lipopolysaccharides trigger two successive bursts of reactive oxygen species at distinct cellular locations. Plant Physiol **176**: 2543–2556

Shine MB, Xiao X, Kachroo P, Kachroo A (2019) Signaling mechanisms underlying systemic acquired resistance to microbial pathogens. Plant Sci **279**: 81–86

Sieber CMK, Lee W, Wong P, Münsterkötter M, Mewes HW, Schmeitzl C, Varga E, Berthiller F, Adam G, Güldener U (2014) The *Fusarium graminearum* genome reveals more secondary metabolite gene clusters and hints of horizontal gene transfer. PLoS One **9**: 110311

Singh R, Parihar P, Singh S, Mishra RK, Singh VP, Prasad SM (2017) Reactive oxygen species signaling and stomatal movement: Current updates and future perspectives. Redox Biol **11**: 213–218

Sinha RC, Savard ME, Lau R (1995) production of monoclonal antibodies for the specific detection of deoxynivalenol and 15-acetyldeoxynivalenol by ELISA. J Agric Food Chem **43**: 1740–1744

Siou D, Gélisse S, Laval V, Repinçay C, Canalès R, Suffert F, Lannou C (2014) Effect of wheat spike infection timing on Fusarium head blight development and mycotoxin accumulation. Plant Pathol **63**: 390–399

Steinberg G, Gurr SJ (2020) Fungi, fungicide discovery and global food security. Fungal Genet Biol **144**: 103476

Stenglein SA, Dinolfo MI, Bongiorno F, Moreno MV (2012) Response of wheat (*Triticum spp.*) and barley (*Hordeum vulgare*) to *Fusarium poae* Respuesta del trigo (*Triticum spp.*) y la cebada (*Hordeum vulgare*) a *Fusarium poae*. Agrociencia 46:

Stukenbrock E, Gurr S (2023) Address the growing urgency of fungal disease in crops. Nat 2023 6177959 **617**: 31–34

Summerell BA (2019) Resolving *Fusarium*: Current status of the genus. https://doi-org.proxy.bib.uottawa.ca/101146/annurev-phyto-082718-100204 **57**: 323–339

Tanaka S, Ichikawa A, Yamada K, Tsuji G, Nishiuchi T, Mori M, Koga H, Nishizawa Y, O'Connell R, Kubo Y (2010) HvCEBiP, a gene homologous to rice chitin receptor CEBiP, contributes to basal resistance of barley to *Magnaporthe oryzae*. BMC Plant Biol **10**: 1–11

Tang Z, Tang H, Wang W, Xue Y, Chen D, Tang W, Liu W (2021) Biosynthesis of a new fusaoctaxin virulence factor in *Fusarium graminearum* relies on a distinct path to form a guanidinoacetyl starter unit priming nonribosomal octapeptidyl assembly. J Am Chem Soc **143**: 19719–19730

Tekauz A, McCallum B, Gilbert J (2009) Review: Fusarium head blight of barley in western Canada. https://doi.org/101080/07060660009501156 **22**: 9–16

Thimon L, Peypoux F, Wallach J, Michel G (1993) Ionophorous and sequestering properties of surfactin, a biosurfactant from *Bacillus subtilis*. Colloids Surfaces B Biointerfaces **1**: 57–62

Thrall PH, Burdon JJ (2003) Evolution of virulence in a plant host-pathogen metapopulation. Science (80) **299**: 1735–1737

De Torres M, Sanchez P, Fernandez-Delmond I, Grant M (2003) Expression profiling of the host response to bacterial infection: the transition from basal to induced defence responses in RPM1-mediated resistance. Plant J **33**: 665–676

Tricase C, Amicarelli V, Lamonaca E, Rana RL, Tricase C, Amicarelli V, Lamonaca E, Rana RL (2018) Economic analysis of the barley market and related uses. Grasses as food feed. doi: 10.5772/INTECHOPEN.78967

Tripathy BC, Oelmüller R (2012) Reactive oxygen species generation and signaling in plants. Plant Signal Behav **7**: 1621

Tundo S, Kalunke R, Janni M, Volpi C, Lionetti V, Bellincampi D, Favaron F, D'Ovidio R (2016) Pyramiding PvPGIP2 and TAXI-III But Not PvPGIP2 and PMEI enhances resistance against *Fusarium graminearum*. Mol Plant-Microbe Interact **29**: 629–639

USDA (2023) Barley Explorer. https://ipad.fas.usda.gov/cropexplorer/cropview/commodityView.aspx?cropid=0430000

Valverde-Bogantes E, Bianchini A, Herr JR, Rose DJ, Wegulo SN, Hallen-Adams HE (2019) Recent population changes of Fusarium head blight pathogens: drivers and implications. https://doi.org/101080/0706066120191680442 **42**: 315–329

Vellosillo T, Aguilera V, Marcos R, Bartsch M, Vicente J, Cascón T, Hamberg M, Castresana C (2013) Defense activated by 9-lipoxygenase-derived oxylipins requires specific mitochondrial proteins. Plant Physiol **161**: 617

Vogelgsang S, Sulyok M, Hecker A, Jenny E, Krska R, Schuhmacher R, Forrer HR (2008) Toxigenicity and pathogenicity of *Fusarium poae* and *Fusarium avenaceum* on wheat. Eur J Plant Pathol **122**: 265–276

Voigt CA (2014) Callose-mediated resistance to pathogenic intruders in plant defense-related papillae. Front Plant Sci **5**: 86993

Voigt CA, Schäfer W, Salomon S (2005) A secreted lipase of *Fusarium graminearum* is a virulence factor required for infection of cereals. Plant J **42**: 364–375

Wang S, Yang S, Dai K, Zheng W, Zhang X, Yang B, Ye W, Zheng X, Wang Y (2023) The effector Fg62 contributes to *Fusarium graminearum* virulence and induces plant cell death. Phytopathol Res **5**: 1–13

Wang Y, Garrido-Oter R, Wu J, Winkelmüller TM, Agler M, Colby T, Nobori T, Kemen E, Tsuda K (2019) Site-specific cleavage of bacterial MucD by secreted proteases mediates antibacterial resistance in *Arabidopsis*. Nat Commun 2019 101 **10**: 1–12

Wang Y, Li X, Fan B, Zhu C, Chen Z (2021) Regulation and function of defense-related callose deposition in plants. Int J Mol Sci 2021, Vol 22, Page 2393 **22**: 2393

Wegulo SN, Baenziger PS, Hernandez Nopsa J, Bockus WW, Hallen-Adams H (2015) Management of Fusarium head blight of wheat and barley. Crop Prot **73**: 100–107

Westphal KR, Nielsen KAH, Wollenberg RD, Møllehøj MB, Bachleitner S, Studt L, Lysøe E, Giese H, Wimmer R, Sørensen JL, et al (2019) Fusaoctaxin A, an example of a two-step mechanism for non-ribosomal peptide assembly and maturation in fungi. Toxins 2019, Vol 11, Page 277 **11**: 277

Wildermuth MC, Dewdney J, Wu G, Ausubel FM (2001) Isochorismate synthase is required to synthesize salicylic acid for plant defence. Nat 2001 4146863 **414**: 562–565

Windels CE (2000) Economic and social impacts of Fusarium head blight: Changing farms and rural communities in the Northern Great Plains. Phytopathology **90**: 17–21

Wu CH, Bernard SM, Andersen GL, Chen W (2009) Developing microbe–plant interactions for applications in plant-growth promotion and disease control, production of useful compounds, remediation and carbon sequestration. Microb Biotechnol **2**: 428

Wu S, Shi Z, Chen X, Gao J, Wang X (2022) Arbuscular mycorrhizal fungi increase crop yields by improving biomass under rainfed condition: A meta-analysis. PeerJ **10**: e12861

Xia Y, Suzuki H, Borevitz J, Blount J, Guo Z, Patel K, Dixon RA, Lamb C (2004) An extracellular aspartic protease functions in *Arabidopsis* disease resistance signaling. EMBO J **23**: 980–988

Xu M, Wang Q, Wang G, Zhang X, Liu H, Jiang C (2022a) Combatting Fusarium head blight: advances in molecular interactions between *Fusarium graminearum* and wheat. Phytopathol

Res 2022 41 **4**: 1–16

Xu Q, Hu S, Jin M, Xu Y, Jiang Q, Ma J, Zhang Y, Qi P, Chen G, Jiang Y, et al (2022b) The N-terminus of a *Fusarium graminearum*-secreted protein enhances broad-spectrum disease resistance in plants. Mol Plant Pathol **23**: 1751–1764

Yamada K, Yamaguchi K, Shirakawa T, Nakagami H, Mine A, Ishikawa K, Fujiwara M, Narusaka M, Narusaka Y, Ichimura K, et al (2016) The *Arabidopsis* CERK1-associated kinase PBL27 connects chitin perception to MAPK activation. EMBO J **35**: 2468–2483

Yamaguchi K, Yamada K, Ishikawa K, Yoshimura S, Hayashi N, Uchihashi K, Ishihama N, Kishi-Kaboshi M, Takahashi A, Tsuge S, et al (2013) A receptor-like cytoplasmic kinase targeted by a plant pathogen effector is directly phosphorylated by the chitin receptor and mediates rice immunity. Cell Host Microbe **13**: 347–357

Yang B, Wang Y, Tian M, Dai K, Zheng W, Liu Z, Yang S, Liu X, Shi D, Zhang H, et al (2021) Fg12 ribonuclease secretion contributes to *Fusarium graminearum* virulence and induces plant cell death. J Integr Plant Biol **63**: 365–377

Yao L, Jiang Z, Wang Y, Wan S, Xin X-F (2022) High air humidity dampens salicylic acid pathway and plant resistance via targeting of NPR1. bioRxiv 2022.10.28.514180

Yuan M, Ngou BPM, Ding P, Xin XF (2021) PTI-ETI crosstalk: an integrative view of plant immunity. Curr Opin Plant Biol **62**: 102030

Zadoks JC, Chang TT, Konzak CF (1974) A decimal code for the growth stages of cereals. Weed Res **14**: 415–421

Zhang LT, Zhang ZS, Gao HY, Xue ZC, Yang C, Meng XL, Meng QW (2011) Mitochondrial alternative oxidase pathway protects plants against photoinhibition by alleviating inhibition of the repair of photodamaged PSII through preventing formation of reactive oxygen species in Rumex K-1 leaves. Physiol Plant **143**: 396–407

Zhang S, Li C, Si J, Han Z, Chen D (2022) Action mechanisms of effectors in plant-pathogen interaction. Int J Mol Sci. doi: 10.3390/IJMS23126758

Zhang Y, Li X (2019) Salicylic acid: biosynthesis, perception, and contributions to plant immunity. Curr Opin Plant Biol **50**: 29–36

Supplemental data

Table S 1: Description of barley varieties named in this thesis. List of barley lines for which biparental mapping populations with Lowe are being developed at Olds College (Alberta) in order to determine molecular markers associated with gramillin resistance. The documented susceptibility to FHB is noted in addition to some physiological traits.

Line	FHB susceptibility	Parental lines	Spring or winter	Purpose	Row type	Short form reference
AAC Connect	Moderately resistant to FHB	TR04282 (from Harbin, Manley, AC Oxbow, Metcalfe 1987) / BM9831D-229 (from Newdale, AC Oxbow, Manley)	Spring	Malt	2	Legge et al 2017
AAC Synergy	Moderately susceptible to FHB	TR02267 (from AC Metcalfe, AC Oxbow, Manley, Ellice, Metcalfe 1987) / Newdale	Spring	Malt	2	Legge et al 2013
AB Advantage	Data unavailable	H97098003 / Sundre	Spring	Feed	6	Government of Alberta Field Crop Develeopment Centre, n.d.
AC Oxbow	Moderately resistant to FHB	TR233/WPG8020 // WPG823/TR222	Spring	Malt	2	McCallum and Takeuz, 2002 Juskiw et al., 2018
CDC Bow	Moderately susceptible to FHB	SM04261 / TR05285	Spring	Malt	2	Seed Manitoba, 2018 Canadian Malting Barley Technical Centre, n.d.
CDC Fraser	Intermediate resistance to FHB	TR04280 / SM04261	Spring	Malt	2	Seed Manitoba, 2018 Canadian Malting Barley Technical Centre, n.d.
Gadsby	Intermediate resistance to FHB	H92066001 / TR248 (from Harrington/Seebe)	Spring	General	2	Seed Manitoba, 2018 Juskiw et al, 2011

Legacy	Moderately susceptible to FHB	Bumper/Karl // Bumper/Manker/3 /Bumper/Karl/4/E xcel	Spring	Malt	6	Seed Manitoba, 2018 Canadian Food Inspection Agency, 2022
Leo	Data unavailable	Aramir // Pitayo-Cambrinus / Arivat-RM1508	Spring	Malt	2	Beratto, 1990
Lowe	Moderately resistant to FHB	H920172032 / Ponoka	Spring	Malt	2	Seed Manitoba, 2018 Alberta Field Crop Development Centre, n.d. Canadian Food Inspection Agency, 2022
Maris Otter	Not resistant	Proctor / Pioneer	Winter	Malt	2	Hornsey, n.d.
Metcalfe	Intermediate resistance to FHB	AC Oxbow / Manley	Spring	Malt	2	Legge et al., 2003 SeCan, 2015
Oreana	Susceptible to FHB	Champion / YU501-312	Spring	Feed	2	Seed Manitoba, 2018 Canadian Food Inspection Agency, 2022
Ponoka	Intermediate resistance to FHB	H92001F1 (from Harrington/Camel ot) / TR229 (from AC Oxbow/Manley)	Spring	Feed	2	Juskiw et al., 2005
Radegast	Data unavailable	Data unavailable	Spring	Malt		Svacina, 2005
Sirish	Moderately susceptible to FHB	SY409-209 / NFS 4789	Spring	Feed	2	Seed Manitoba, 2018 Canadian Food Inspection Agency, 2022 FP Genetics, n.d.
Stander	Susceptible to FHB	Excel // Robust/Bumper	Spring	Malt	6	Rassmusson et al., 1993
Xena	Intermediate resistance to FHB	Stark / Baronesse	Spring	Feed	2	Legge et al., 2017 Western Plant Breeders, 2000

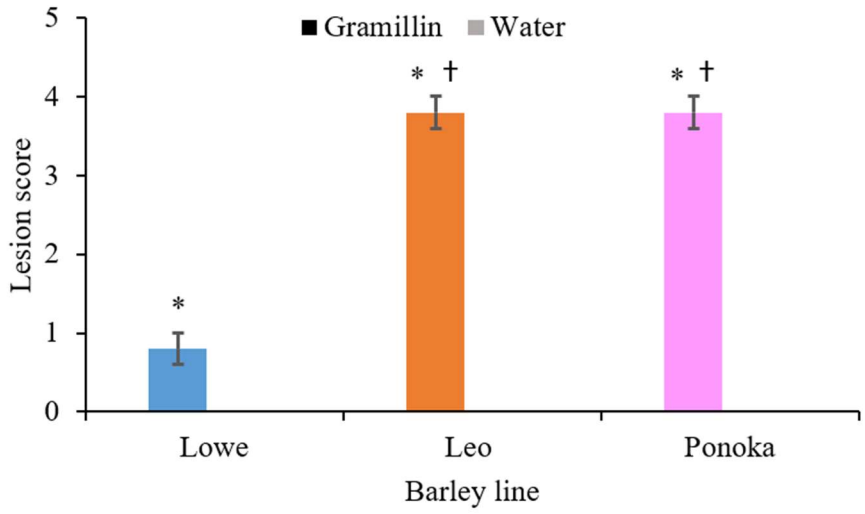

Figure S 1: Lowe is not fully insensitive to gramillin. Gramillin-induced lesion severity in cotyledons infiltrated with 10 µM purified gramillin. Lesions are scored after 24 hours on a 0-4 scale. The average from five samples per line and SEM is presented (n=5) from a single experiment. An asterisk denotes significant difference from the respective water control while a cross denotes significant difference from Lowe for the same treatment. Significance was determined by two-tailed t-test ($p<0.05$). Only one replicate experiment was conducted.

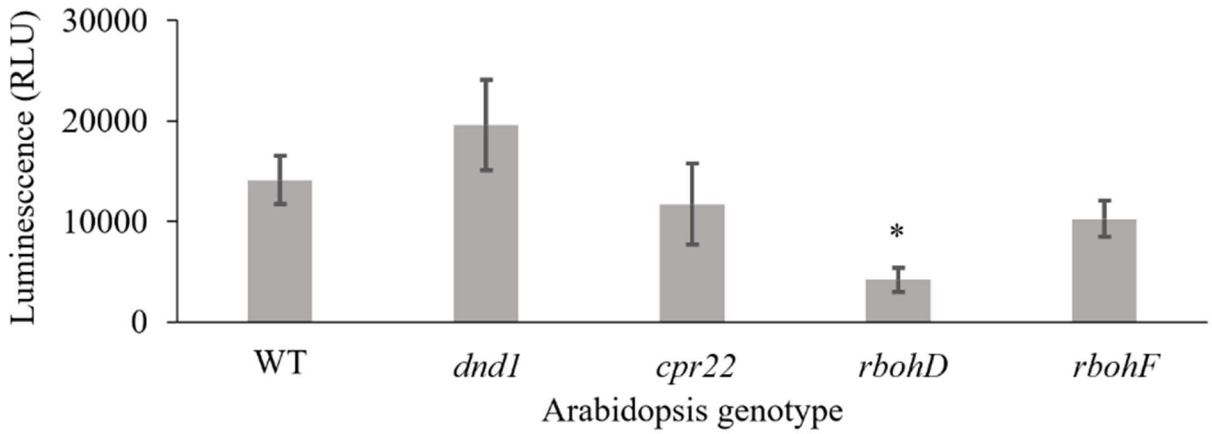

Figure S 2: RBOHD is required for gramillin-induced ROS bursts in *Arabidopsis* leaves. Sum of luminescence values caused by ROS production at all time points during the first 24 minutes after exposure of *Arabidopsis* wild-type (WT) or gene knock-out leaf disks to 10 µM gramillin. Each value represents the average and SEM (n=3-8). An asterisk denotes a line that is significantly different from the wild-type ($p<0.05$). This figure is representative of three replicated assays.

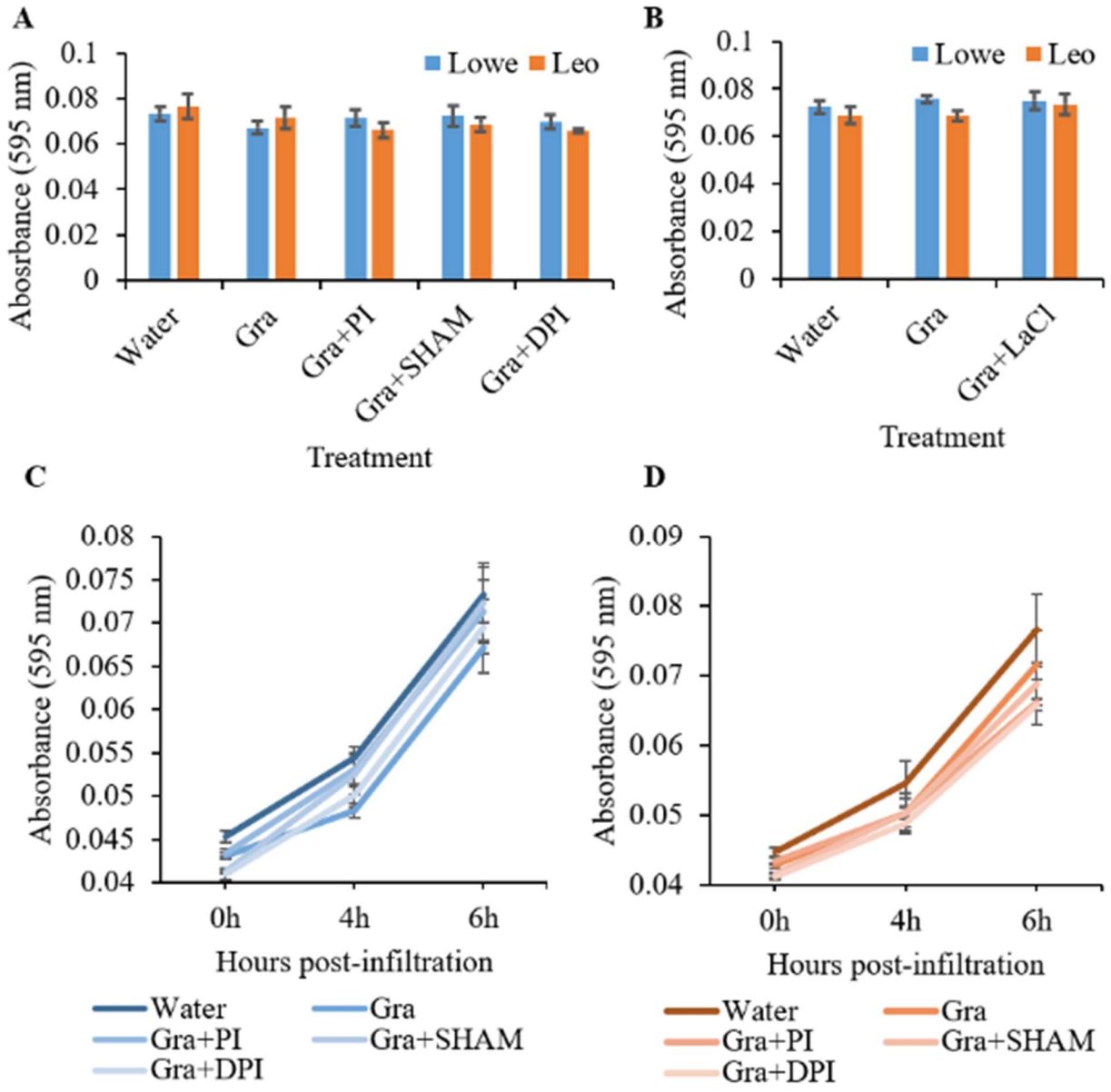

Figure S 3: Gramillin does not induce peroxidase activity in barley. Peroxidase activity from barley cotyledon disks six hours after infiltration with **A)** water, 5 µM purified gramillin (Gra), gramillin combined with a protease inhibitor (PI), 2 mM salicylhydroxamic acid (SHAM), 25 µM diphenyleneiodonium chloride (DPI), or **B)** 1.5 mM lanthanum chloride ($LaCl_3$). No treatments differed significantly from their own water control or gramillin treatment. **C)** Increase in peroxidase activity in Lowe barley over time from the same treatments as in panel A. **D)** Increase in peroxidase activity in Leo barley over time from the same treatments as panel A. In all panels, the average (n=6) and SEM are shown. This data is representative of three replicated experiments. Controls for the PI, SHAM, DPI, and $LaCl_3$ were included and did not differ from the water control (Fig S4).

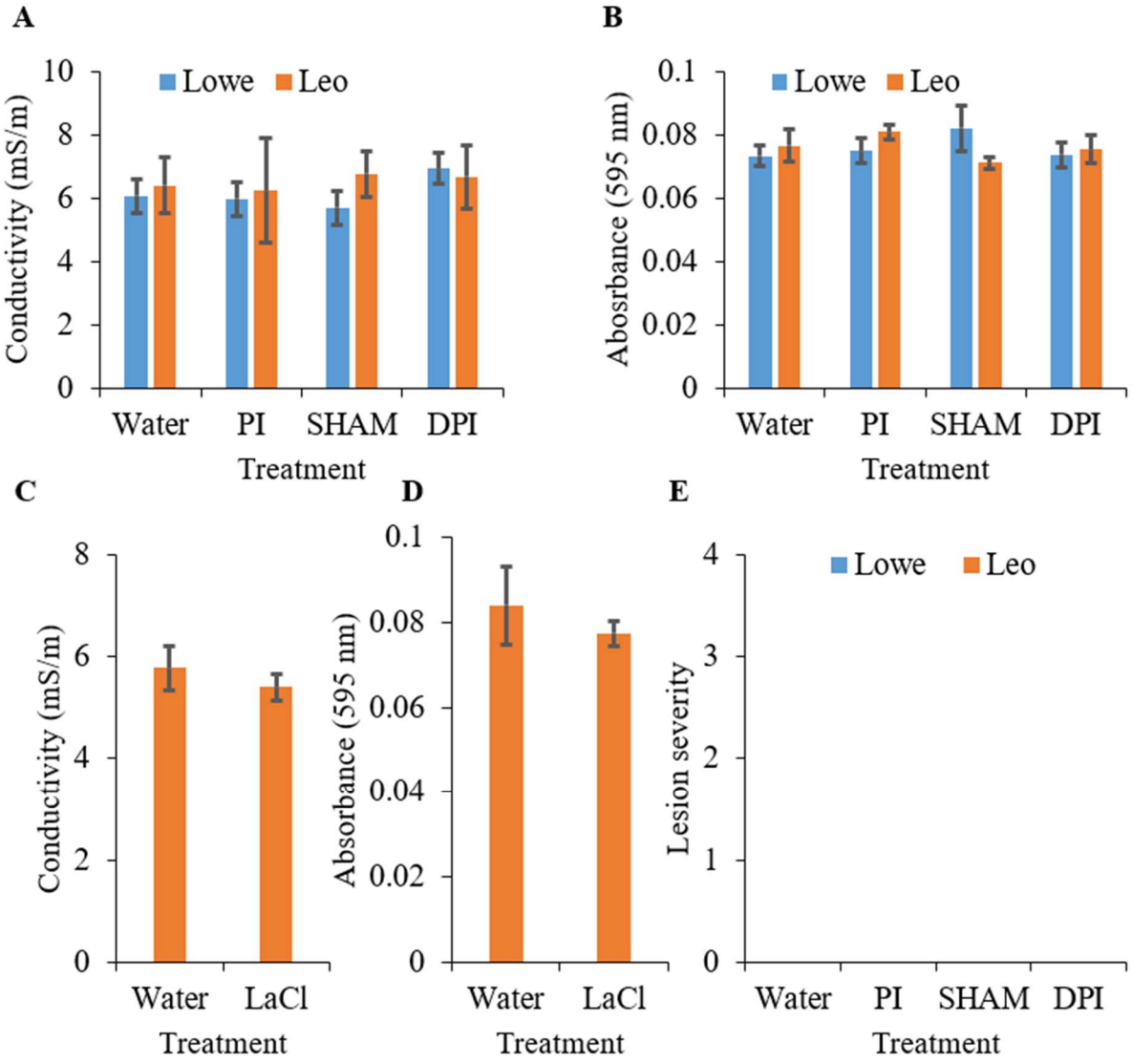

Figure S 4: The negative controls for SHAM, DPI, PI, and $LaCl_3$ do not differ significantly from the water treatment. A) Ion leakage from barley leaf disks six hours after infiltration with water, protease inhibitor (PI), 2 mM salicylhydroxamic acid (SHAM), or 25 µM diphenyleneiodonium chloride (DPI). **B)** Peroxidase activity from barley leaf disks six hours after infiltration with water, PI, 2 mM SHAM, or 25 µM DPI. **C)** Ion leakage from barley leaf disks six hours after infiltration with water or 1.5 mM $LaCl_3$. **D)** Peroxidase activity from barley cotyledon disks six hours after infiltration with water or 1.5 mM $LaCl_3$. **E)** Lesion severity is evaluated by monitoring necrosis in barley cotyledons infiltrated with water, PI, 2 mM SHAM, or 25 µM DPI. Lesions are scored after 24 hours on a 0-4 scale where 4 represents that 75-100% of the infiltrated area has lesioned. For all panels, the average (n=4-6) and SEM are shown. This data is representative of three replicated experiments. In panels C) and D) the treatments were done in Leo barley only. No treatments differed significantly from their water control in any of the panels.

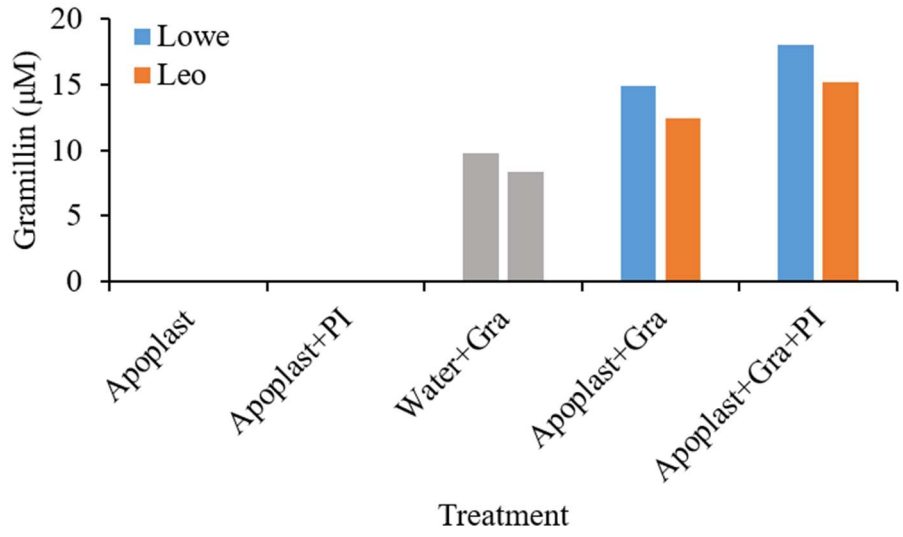

Figure S 5: Gramillin degrades independently of active cell metabolism. Gramillin concentration remaining after 30 minutes from an initial concentration of 20 µM. The gramillin is placed in extracted apoplastic fluid (Apoplast), apoplastic fluid with protease inhibitor (PI), or water. Pure apoplastic fluid and apoplastic fluid combined with PI are included as controls. One value per treatment (n=1) is presented from a single experiment. This experiment was not replicated.

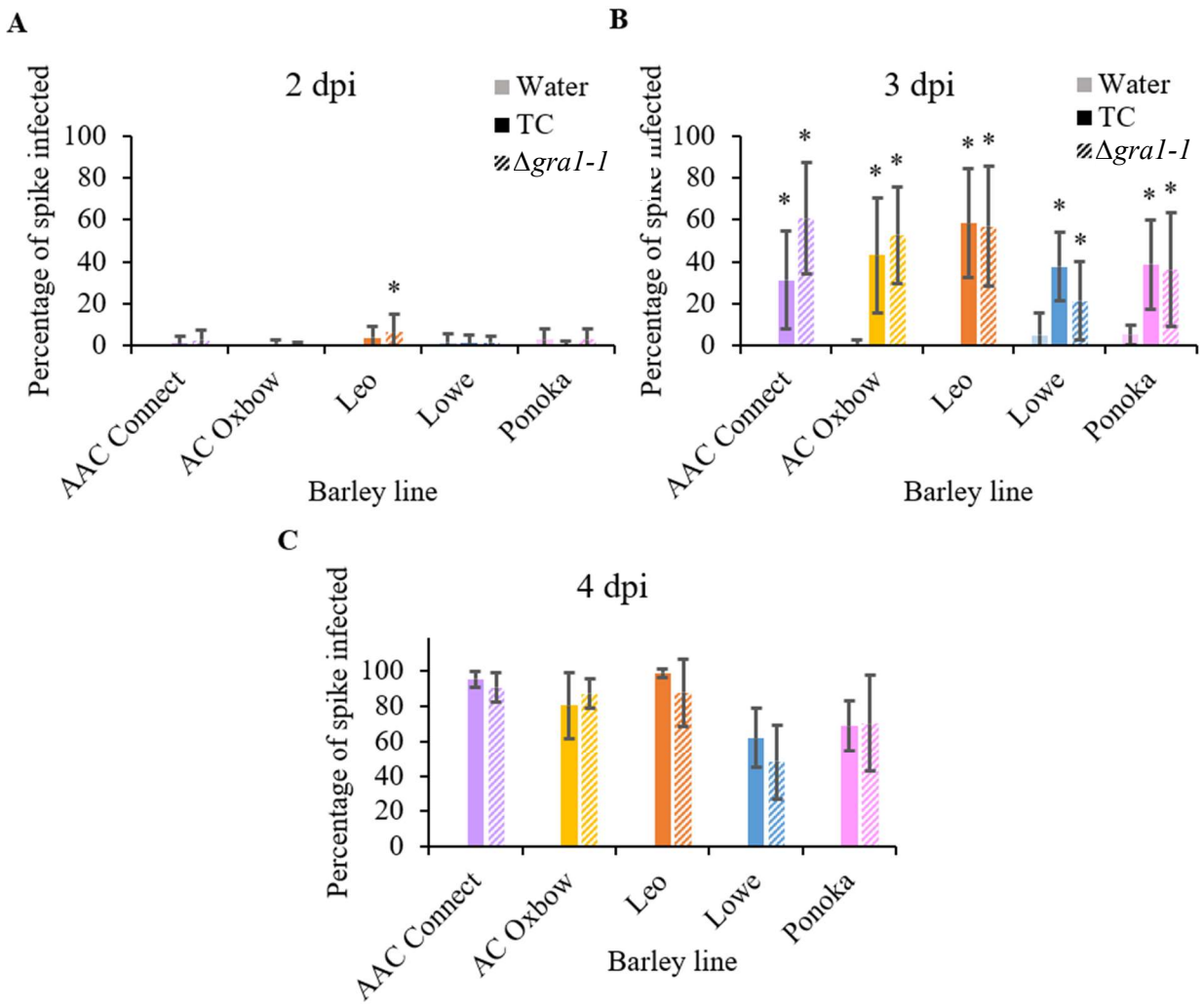

Figure S 6: *F. graminearum* infection shows the most variation between lines at 3 dpi. Percentage of spikelets on a barley spike visually showing symptoms of FHB at **A)** 2 days post-inoculation (dpi), **B)** 3 dpi, and **C)** 4 dpi. Barley heads were spray-inoculated at 14 days post-emergence with gramillin-producing transformation control (TC) *Fgr* spores or gramillin-non-producing (*Δgra1-1*) spores, or a water control. An asterisk denotes a treatment that varied significantly from its own water control; note that water controls were only evaluated up to 3 dpi in this assay. Statistical significance ($p<0.05$) was determined by two-tailed Student's t-tests. The average (n=3-8) and SD are presented here from one experiment. Four replicate experiments were completed with similar trends.

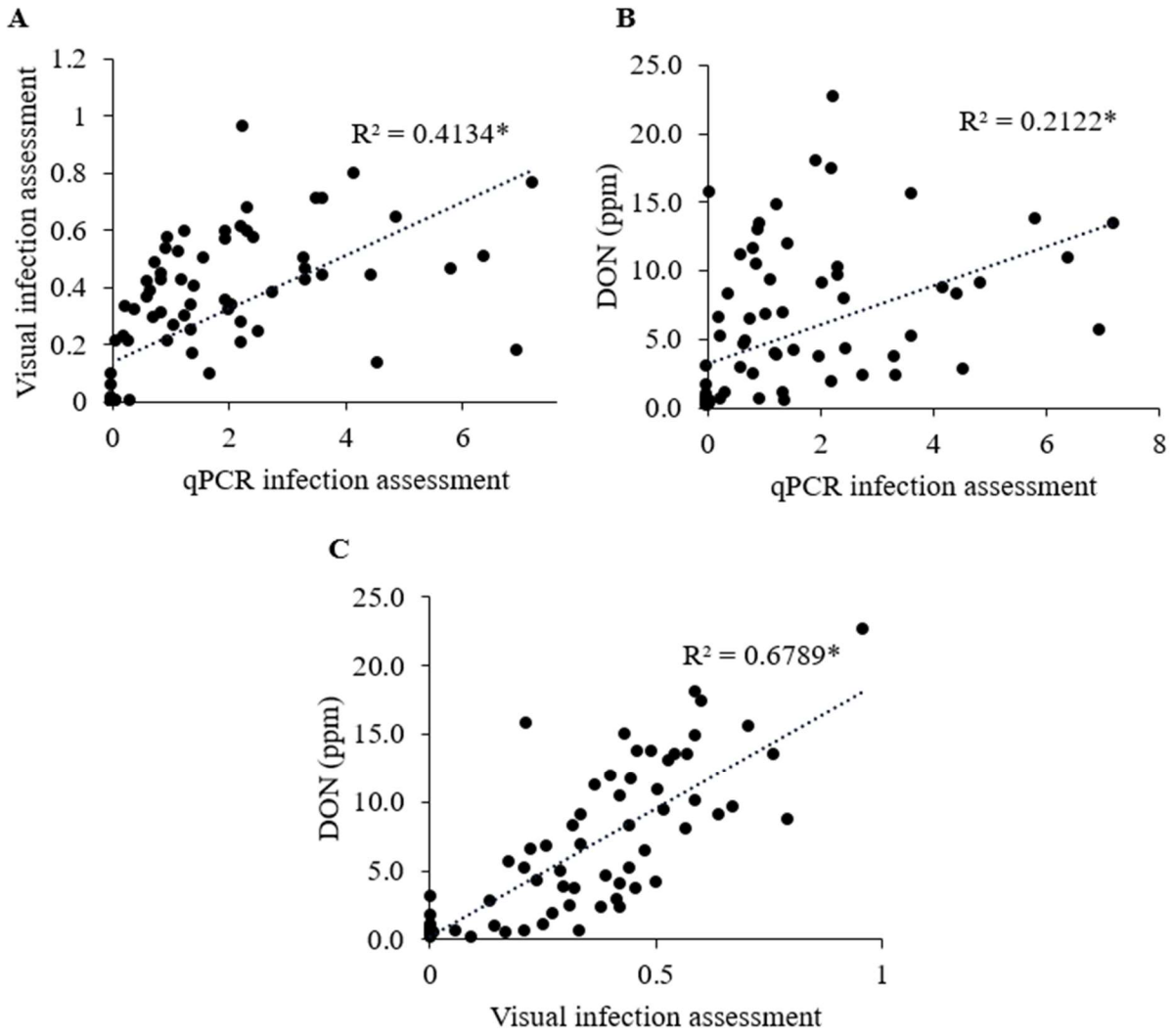

Figure S 7: Assessment of *Fgr* infection by visual symptoms, qPCR, and DON correlate. A) Correlation of the visual infection rating and the fungal colonization as determined by qPCR at 3 days post-infection (dpi) with *Fusarium graminearum* (*Fgr*). **B)** Correlation of the DON content and fungal colonization as determined by qPCR at 3 dpi with *Fgr*. **C)** Correlation of the DON content and visual infection rating at 3 dpi with *Fgr*. In all panels, an asterisk denotes a significant correlation ($p<0.001$), and the figure contains pooled data from three replicate assays. Statistical significance was determined by correlation test.

Table S2: Expression of defense related genes during *F. graminearum* infection. Gene expression is determined by qPCR in barley heads from genotypes AAC Connect, Lowe, or Leo inoculated with water or one of two *Fgr* strains – a transformation control (TC) which produces gramillin or *Δgra1-1* which does not. Expression is normalized to two barley housekeeping genes, *HvCyclophilin* and *HvActin*. The average of four samples is presented with the SD in parentheses. The data is from one experiment; three replicate experiments were performed with similar results. An asterisk denotes a value that differs significantly from the water control of the same line. Statistical significance ($p<0.05$) was determined by ANOVA with post-hoc Tukey's honest significant difference analysis.

Description	AAC Connect; Water	AAC Connect; TC	AAC Connect; *Δgra1-1*	Lowe; Water	Lowe; TC	Lowe; *Δgra1-1*	Leo; Water	Leo; TC	Leo; *Δgra1-1*
BAK1	0.74(0.33)	0.90(0.31)	0.77(0.07)	1.36(0.59)	0.10(0.20)	0.97(0.25)	1.13(0.39)	0.87(0.21)	0.83(0.17)
BIK1	1.04(0.70)	0.81(0.43)	1.76(1.01)	1.43(0.57)	1.04(0.37)	1.38(0.67)	1.58(0.55)	1.89(1.15)	1.27(0.38)
PR2A-2	2.98(4.05)	0.25(0.14)	4.62(8.09)	2.63(3.15)	2.77(1.82)	2.57(2.54)	2.78(4.86)	2.91(3.79)	0.98(0.89)
PUB23-like	0.97(0.87)	0.41(0.26)	1.48(0.57)	0.95(1.12)	1.16(0.74)	1.12(0.66)	0.19(0.14)	0.98(1.15)	0.64(0.32)
SOBIR1	1.60(1.04)	1.72(0.49)	1.32(0.54)	2.17(1.21)	1.16(0.74)	1.16(0.43)	1.91(0.44)	1.88(0.47)	1.73(1.14)
WRKY23	0.87(0.42)	0.89(0.43)	1.45(0.79)	1.44(0.78)	1.05(0.44)	1.14(0.12)	0.74(0.47)	0.89(0.39)	0.91(0.23)
MLOC_3110	2.34(2.09)	0.42(0.29)	3.86(5.52)	2.06(2.08)	1.78(1.89)	2.10(2.45)	3.31(4.58)	3.51(2.39)	2.56(1.25)
MLOC_18474	0.06(0.09)	1.92(1.81)	2.61(1.78)	0.07(0.02)	1.05(0.45)	1.31(0.75)	0.13(0.10)	2.13(1.38)	3.82(2.22)*
MLOC_58734	0(0)	1.88(2.20)	5.45(5.19)	0.08(0.14)	1.17(0.81)	1.79(1.14)	0(0)	1.24(1.39)	4.63(4.53)
MLOC_68201	0.48(0.52)	0.88(0.74)	2.40(0.76)*	0.16(0.08)	1.02(0.34)	0.96(0.07)	0.55(0.86)	1.96(1.13)	1.51(0.73)

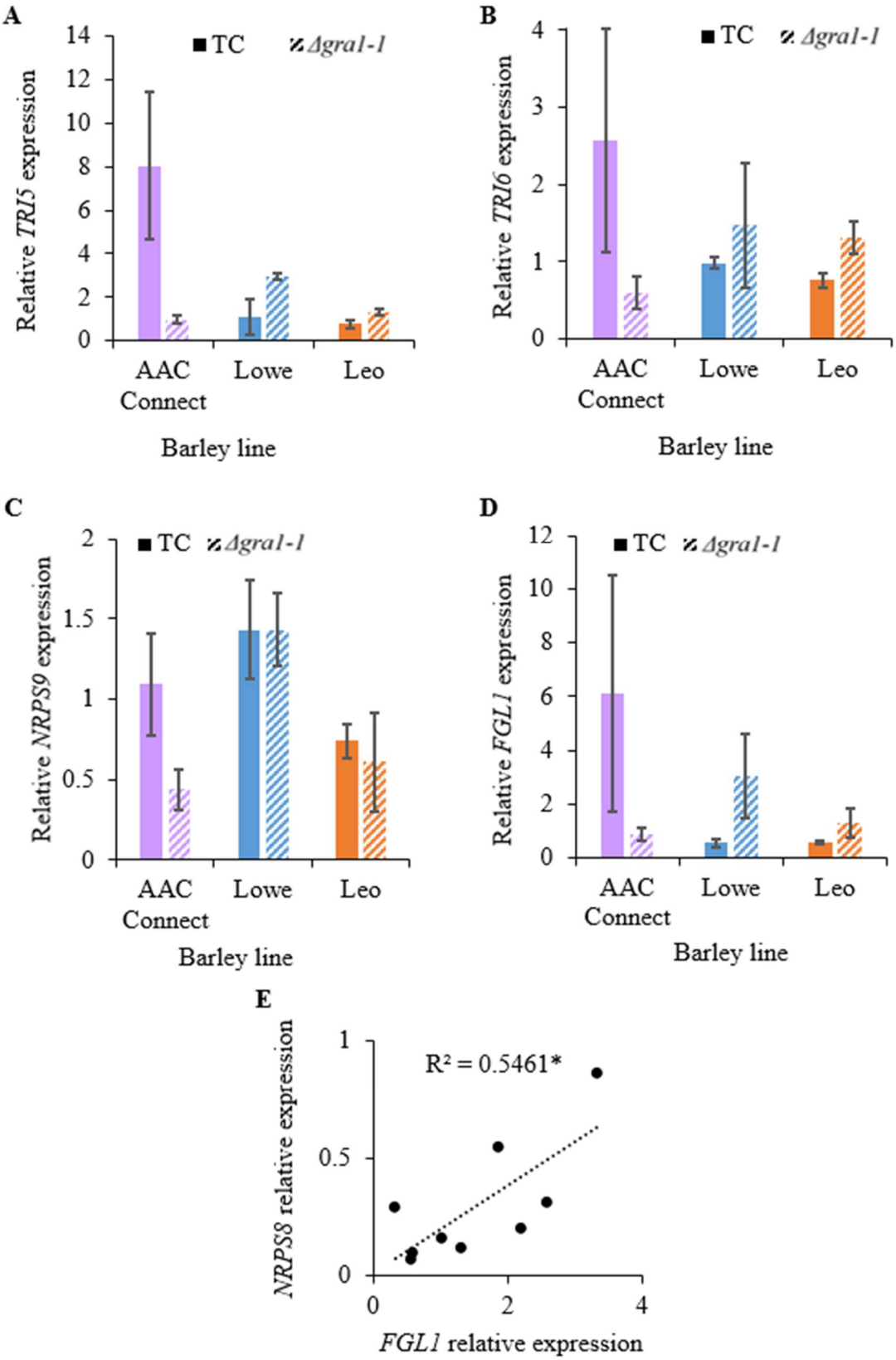
A
Relative TRI5 expression
TC
Δgra1-1
AAC Connect
Lowe
Leo
Barley line
B
Relative TRI6 expression
C
Relative NRPS9 expression
D
Relative FGL1 expression
E
NRPS8 relative expression
R² = 0.5461*
FGL1 relative expression

Figure S 8: Gramillin production does not modulate DON or fusaoctaxin production, but may be linked to lipase production. Barley heads were spray-inoculated at 14 days post-emergence with gramillin-producing transformation control (TC) *Fgr* spores or gramillin-non-producing (*Δgra1-1*) spores, or a water control. Fungal gene expression was quantified by qPCR and normalized to the average expression of two *Fgr* housekeeping genes, *FgGAPDH* and *FgEF1α*. **A)** Relative expression of *TRI5*, a trichodiene synthase involved in DON production. **B)** Relative expression of *TRI6*, a transcription factor involved in DON production. **C)** Relative expression of *NRPS9*, the gene cluster responsible for fusaoctaxin production. **D)** Relative expression of *FGL1*, a secreted lipase. For panels A)-D), the average (n=4) and SEM are presented. Two replicate barley heads from two plants were combined into each sample. This figure is representative of one assay, which was replicated three times with similar trends. There were no significant differences between the TC- and *Δgra1-1*-inoculated lines in panels A, B, C, or D. **E)** Correlation between the average relative expression values of *NRPS8* and *FGL1* in samples inoculated with TC *Fgr*. These are the combined values from three replicated assays (n=11). An asterisk denotes a significant correlation. Statistical significance was determined by ANOVA with post-hoc Tukey's honest significant difference analysis for panels A)-D), while it was determined by correlation test for panel E).

Table S 3: Primer sequences used during qPCR assays.

Gene ID	Description	Primer name and sequence (5'-3')
XM_045106569.1	*BAK1*	BAK1_F: GTGGGGGATTTTGGTTTGGC BAK1_R: CAATTGTTCCACGCACAGCA
XM_045122732.1	*BIK1*	BIK1_F: AGCCACTGTCATGGAACCTG BIK1_R: GATGACCTTGGCATTGTCGC
XM_045117453.1	*PR2A-2*	PR2A-2_F: CATGCTTTGCATGGATGGTGA PR2A-2_R: CCAACCAACCTTACGAACCG
XM_045097780.1	*PUB23-like*	PUB23_F: ACAAACTGTCATCAAACATTGACAC PUB23_R: TGATAACACGGCAATCCAAGAGA
XM_045101391.1	*SOBIR1*	SOBIR1_F: CAGGCAGCAGTTGAACAAGC SOBIR1_R: ACACAGTCACGCATGACACA
XM_045107440.1	*WRKY23*	WRKY23_F: CATAGCTAGCTCCCCGGTTG WRKY23_R: TGACATTCCTGAATTGCACACTG
MLOC_3110	Putative chalcone synthase	3110_F: CCAGTAGTGGACACATTCTATCA 3110_R: ACGTACCTCGTGATTTGTGTCT

MLOC_18474	Putative aromatic amino acid decarboxylase	18474_F: ACACGATTGGCCTCATTGGT 18474_R: TGACGACAGGTTTGAGGTGG
MLOC_58734	Putative germin-like protein 2	58734_F: TGTTTTCCCGCAAGGACTCA 58734_R: GCTGCTAAGTGCAGCAATCG
MLOC_68201	Putative laccase-19	68201_F: GCACCTGAGCATCATCATTTTA 68201_R: AGCTAGGAAGGTCGTGAAGAT
LT222053.1	*NRPS8*	NRPS8_F: CTCGCATAGCATACCTACATCAA NRPS8_R: CGAGATGAGCGAGAAGAAGAAG
LT222055.1	*NRPS9*	NRPS9_F: TTTGGGCCATGTCACTCCTC NRPS9_R: CCGCCACGGCTAATTTGATG
MN313495.1	*TRI5*	TRI5_F: GGCCCAAGGACCTGTTTGAT TRI5_R: CCACGGCTGACGTGATTTCA
LT222054.1	*TRI6*	TRI6_F: CATCGTCGGGACTGTTGGA TRI6_R: AAGGTGGGAAGGGCGATAA
LT222055.1	*FGL1*	FGL1_F: AACGGCTGTCCAACTGTTCA FGL1_R: GTTGGTGATGGGTTTGTGCC
XM_045103936.1	*HvCyclophilin*	Cyclo_F: CTCTGTTTCACAGGGAGGTCT Cyclo_R: CGCACGATGCACAACAAAGA
XM_045114375.1	*HvActin*	Actin_F: GATCAAGGTCGTCGCTCCAC Actin_R: TGGAAAGTGCTGAGTGAGGC
MH572264.1	*FgEF1α*	EF1a_F: CCTGGATCTCGGCGAACTT EF1a_R: CAGGTCGGTGCTGGTTACG
XM_011326605.1	*FgGAPDH*	GAPDH_F: TGACTTGACTGTTCGCCTCGA GAPDH_R: ATGGAGGAGTTGGTGTTGCC

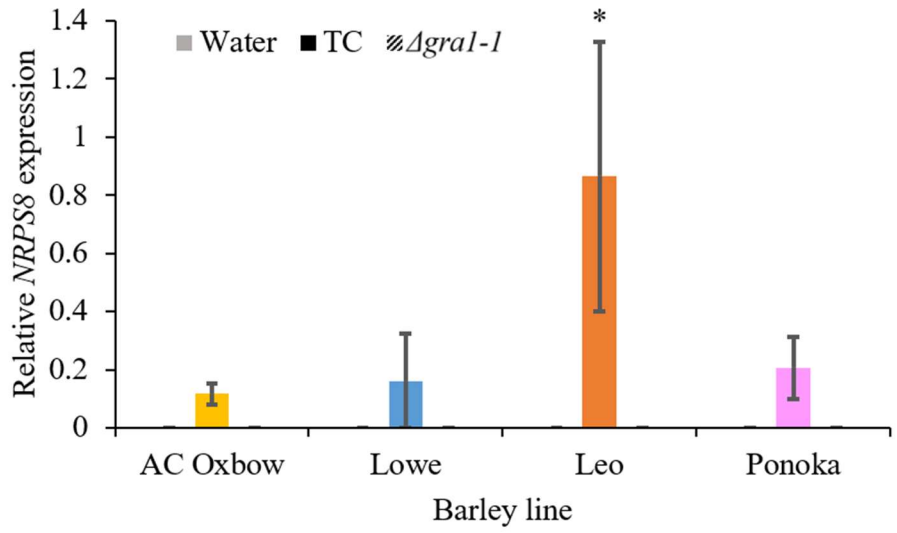

Figure S 9: NRPS8, the gene responsible for gramillin production, is induced during infection and is not expressed in the water or *Δgra1-1* controls. Barley heads were spray-inoculated at 14 days post-emergence with gramillin-producing transformation control (TC) *Fgr* spores or gramillin-non-producing (*Δgra1-1*) spores, or a water control. Fungal gene expression was quantified by qPCR and normalized to the average expression of two *Fgr* housekeeping genes, *FgGAPDH* and *FgEF1α*. An asterisk represents a value that differs significantly from its water control. The average (n=4) and SEM are presented. Three replicate assays were conducted, in all of which there was a significant difference between expression in the TC samples and both the water and *Δgra1-1* samples. Statistical significance ($p<0.05$) was determined by ANOVA with post-hoc Tukey's honest significant difference analysis.

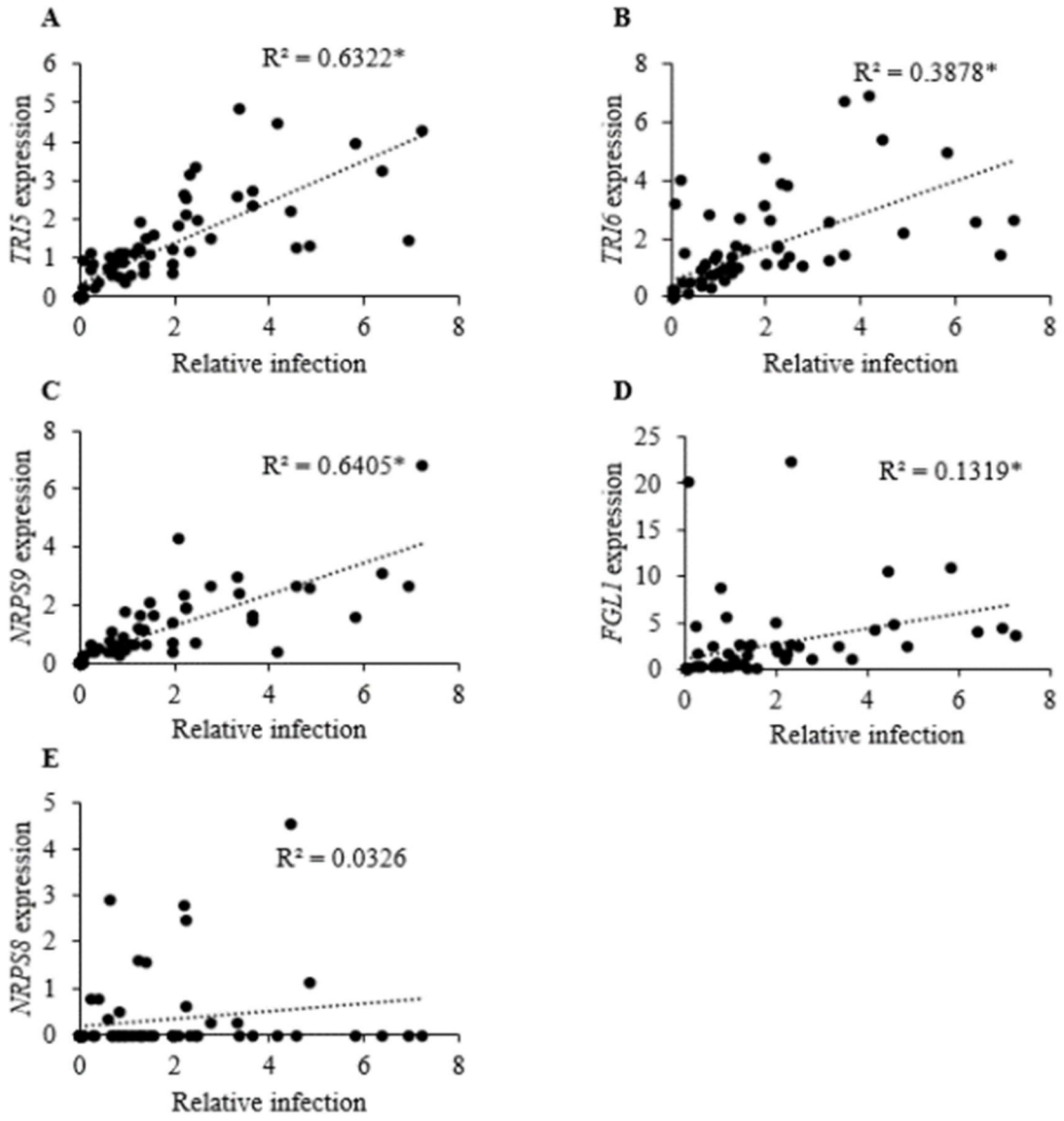

Figure S 10: DON, fusaoctaxin, and lipase expression correlate with the level of infection. Barley heads were spray-inoculated at 14 days post-emergence with gramillin-producing transformation control *Fgr* spores or gramillin-non-producing spores, or a water control. Fungal gene expression was quantified by qPCR and normalized to the average expression of two barley housekeeping genes, *HvCyclophillin* and *HvActin*. The correlation is shown between the relative infection (average expression of two fungal housekeeping genes, *FgGAPDH* and *FgEF1α*) and **A)** Relative expression of *TRI5*, a trichodiene synthase involved in DON production **B)** Relative expression of *TRI6*, a transcription factor involved in DON production **C)** Relative expression of *NRPS9*, the gene cluster responsible for fusaoctaxin production **D)** Relative expression of *FGL1*, a secreted lipase or **E)** Relative expression of *NRPS8*, the gene cluster responsible for gramillin production. An asterisk denotes a significant correlation. Statistical significance ($p<0.001$) was determined by correlation test. This figure shows data pooled from three replicated assays.

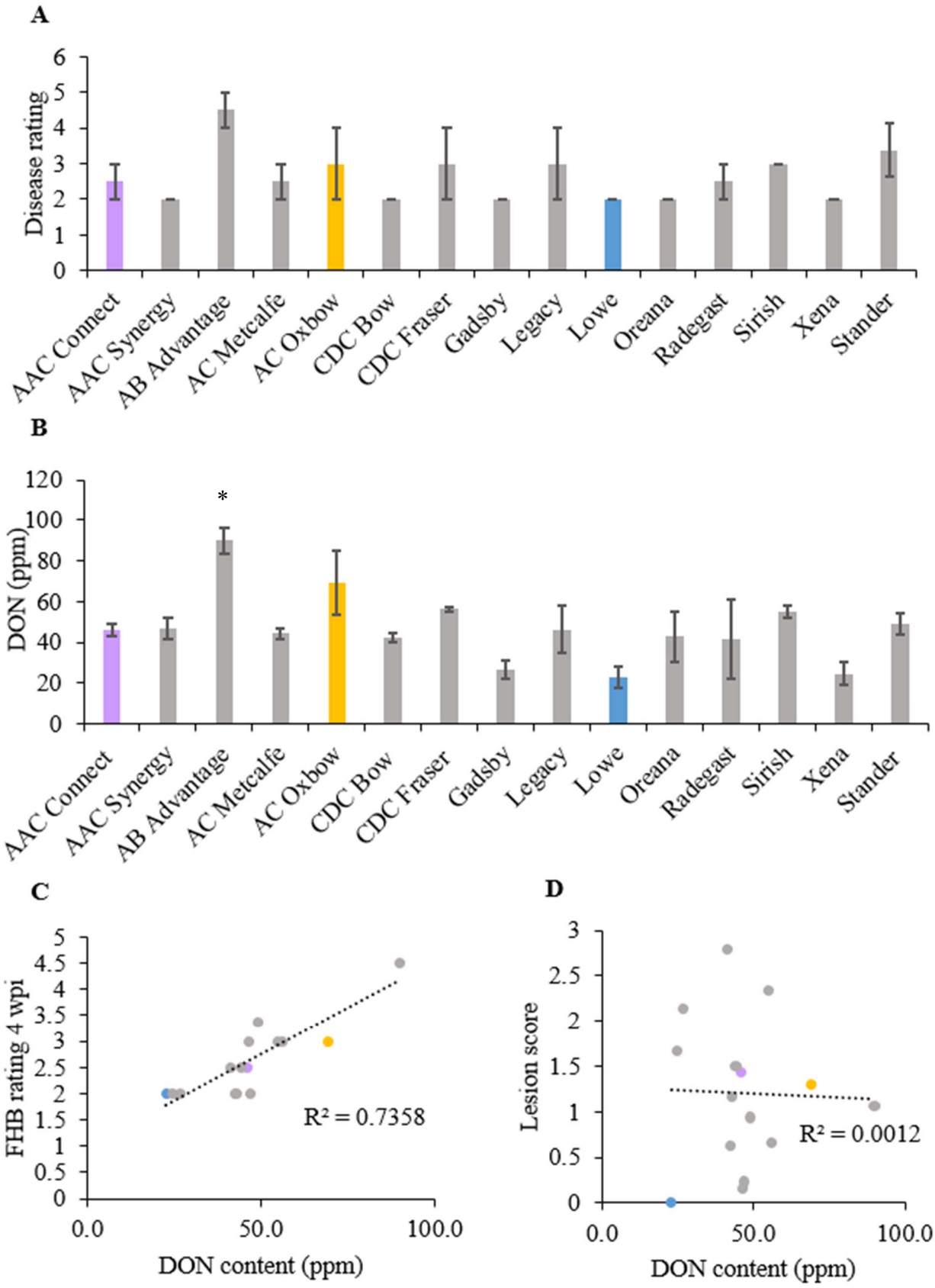
A
Disease rating
0
1
2
3
4
5
6
AAC Connect
AAC Synergy
AB Advantage
AC Metcalfe
AC Oxbow
CDC Bow
CDC Fraser
Gadsby
Legacy
Lowe
Oreana
Radegast
Sirish
Xena
Stander
B
DON (ppm)
0
20
40
60
80
100
120
*
AAC Connect
AAC Synergy
AB Advantage
AC Metcalfe
AC Oxbow
CDC Bow
CDC Fraser
Gadsby
Legacy
Lowe
Oreana
Radegast
Sirish
Xena
Stander
C
FHB rating 4 wpi
0
0.5
1
1.5
2
2.5
3
3.5
4
4.5
5
R² = 0.7358
0.0
50.0
100.0
DON content (ppm)
D
Lesion score
0
0.5
1
1.5
2
2.5
3
R² = 0.0012
0.0
50.0
100.0
DON content (ppm)

Figure S 11: DON content correlates with disease susceptibility in the field but not sensitivity to gramillin. A) Disease ratings of 15 barley lines in a Fusarium head blight nursery four weeks after inoculation. Disease was scored on a 0-5 scale that incorporates incidence and severity. The average of two 2-row plots, with the exception of the check Stander which had eight 2-row plots, and SEM is presented (n=2, n=8 for Stander). There were no statistically significant differences between Lowe and other lines. **B)** DON content (ppm) at harvest of 15 barley lines grown in a Fusarium head blight nursery. The average of samples from two 2-row plots, with the exception of the check Stander which had eight 2-row plots, and SEM is presented (n=2, n=8 for Stander). An asterisk denotes a line that differed significantly from Lowe ($p<0.05$). **C)** Correlation between DON content at harvest and FHB ratings done four weeks post-inoculation (wpi). The average of samples from two 2-row plots, with the exception of the check Stander which had eight 2-row plots, is presented (n=2, n=8 for Stander). **D)** Correlation between DON content at harvest and sensitivity to purified gramillin. Gramillin-induced lesion severity is evaluated by monitoring necrosis in cotyledons infiltrated with 5 μM purified gramillin. Lesions are scored after 24 hours on a 0-4 scale where 4 represents that 75-100% of the infiltrated area has lesioned. The data presented for gramillin sensitivity the combined average from three replicates (n=15). The data presented for DON deposition is the average of samples from two 2-row plots, with the exception of the check Stander which had eight 2-row plots, is presented (n=2, n=8 for Stander).